Numerical approximation of non-isothermal multi-component, multi-phase field systems

Dissertation
zur Erlangung des Grades eines
Doktors der Naturwissenschaften

am Fachbereich der Mathematik und Informatik
der Freien Universität Berlin

vorgelegt von
Max Kahnt

Berlin
2021

Betreuer:	**Prof. Dr. Ralf Kornhuber**	(Freie Universität Berlin)
Erstgutachter:	**Prof. Dr. Ralf Kornhuber**	(Freie Universität Berlin)
Zweitgutachter:	**Prof. Dr. Björn Stinner**	(University of Warwick)

Tag der Disputation: 02.06.2021

Selbstständigkeitserklärung

Ich erkläre gegenüber der Freien Universität Berlin, dass ich die vorliegende Dissertation selbstständig und ohne Benutzung anderer als der angegebenen Quellen und Hilfsmittel angefertigt habe. Die vorliegende Arbeit ist frei von Plagiaten. Alle Ausführungen, die wörtlich oder inhaltlich aus anderen Schriften entnommen sind, habe ich als solche kenntlich gemacht. Diese Dissertation wurde in gleicher oder ähnlicher Form noch in keinem früheren Promotionsverfahren eingereicht. Mit einer Prüfung meiner Arbeit durch ein Plagiatsprüfungsprogramm erkläre ich mich einverstanden.

Datum Unterschrift (Max Kahnt)

Declaration of authorship

I declare to the Freie Universität Berlin that I have completed the submitted dissertation independently and without the use of sources and aids other than those indicated. The present thesis is free of plagiarism. I have marked as such all statements that are taken literally or in content from other writings. This dissertation has not been submitted in the same or similar form in any previous doctoral procedure. I agree to have my thesis examined by a plagiarism examination software.

Date Signature (Max Kahnt)

Contents

1. Introduction

The subject of this thesis is the derivation and analysis of numerical approximations of multi-component, multi-phase field systems. The latter are of importance in a variety of industrial applications. Among these are the production of mechanical workpieces via metal casting as well as semi-conductor devices such as solar cells. In both examples, crucial aspects of the respective elastic, plastic, or electronic quality can be directly correlated with the microscopic structure of the material. Many of these solidified systems of interest exhibit grains at a distinctive scale between molecular level and the typical device size. Depending on the setting, these grains may differ in structure, composition, or mere orientation and one aims to capture their state and evolution in terms of mathematical models in order to assess or predict the desired mechanical or electrical quality.

These grain-like structures are thought of as phases, generalizing the strict physical notion of a phase state in this context. From the microscopic point of view, they are usually assumed to be separated adjacent structures which interact in defined ways, motivating the modeling by sharp interface models comprising free or moving boundary problems, cf. Crank 1987; Kinderlehrer and Stampacchia 2000. The Stefan problem (see Visintin 2012) is considered as a typical model problem in that domain. A direct numerical approach explicitly tracking the interfaces poses intricate numerical challenges, e.g. due to topological changes with vanishing and emerging phases.

Phase field descriptions have emerged as a powerful tool to alternatively model these systems. An order parameter describes the locally present phase and varies strongly across a finite diffuse interface between different neighboring grains. For that, a Ginzburg–Landau type contribution is used to smear out the sharp interface energy over a small length scale ε. Two prototypical approaches are the so-called Allen–Cahn and the Cahn–Hilliard equations. The former describe phase transition processes and is hence considered non-conserving. Caginalp 1989 derived such a system coupled to a temperature variable to assess solidification phenomena. The approach by Cahn and Hilliard 1958 considers conserved masses and is thought of as being interfacially diffuse ab-initio. Here the interface parameter ε can be carefully adapted to fit the numerically accessible scale.

Alongside mechanical properties, thermal boundary/environmental conditions play an important role in the evolution of devices investigated by phase fields motivating mod-

els such as Caginalp 1989; Penrose and Fife 1990; Wheeler, Boettinger, and McFadden 1992. While original models considered binary phase fields, more complex settings were investigated, e.g. eutectic systems, and required the development of multi-phase field systems, cf. Wheeler, McFadden, and Boettinger 1996; Steinbach et al. 1996. Multiple chemical constituents contributing to the emergence of different phases led to the postulation of multi-component, multi-phase field models such as Stinner, Nestler, and Garcke 2004; Eiken, Böttger, and Steinbach 2006. Observations and the consequences drawn in S. G. Kim, W. T. Kim, and Suzuki 1998; Plapp 2011; Choudhury and Nestler 2012 fostered viewpoints favoring formulations in thermodynamic potentials other than those of the conserved variables. Numerical approximations of solutions to such multi-component, multi-phase field models have been obtained in e.g. Nestler, Garcke, and Stinner 2005; Steinbach 2013 and are mostly based on explicit schemes. The increasing scale of the arising problems in terms of variables as well as domain size requires for optimized numerical solution approaches, cf. Nestler and Choudhury 2011.

In this work, we consider a thermodynamically consistent, multi-component, multi-phase field system as proposed by Stinner, Nestler, and Garcke 2004 and analyzed by Stinner 2007. The intent to calibrate such a model to a specific application usually conflicts with the desire to simplify its various input parameters for numerical purposes. In particular, both Ginzburg–Landau energy contributions, i.e. the multi-well potential enforcing pure phase regions as well as the gradient term penalizing large interfaces, exhibit these difficulties. The numerical accessibility of smooth well potentials comes at the price of additional correction terms, cf. Nestler, Garcke, and Stinner 2005, and a more refined numerical framework is necessary to tackle proper obstacle potentials, cf. Kornhuber 1997; Kornhuber and Krause 2006; Gräser and Sander 2014b. Similarly, the gradient term becomes particularly intricate for anisotropic settings and was e.g. investigated by Gräser 2011; Gräser, Kornhuber, and Sack 2013.

Our focus lies on the derivation of numerical approximations within the thermodynamically consistent context with high efficiency and robustness. We aim to exploit the special mathematical structure of the model and the underlying thermodynamics without introducing additional regularizations.

The outline of the thesis is as follows. We introduce the notation for this work as well as the thermodynamic and multi-phase setting in chapter 2 and continue by motivating and presenting the thermodynamically consistent multi-component, multi-phase field model in chapter 3. Based on Rothe's method, we obtain a semi-discretization allowing for adaptive meshes in chapter 4 and the implicit problems are analyzed. In chapter 5, a full discretization with adaptive finite elements based on hierarchical a posteriori error estimation is set up. We transition to a purely algebraic formulation and present the iterative approximation of solutions with a nonsmooth Schur–Newton multigrid approach in chapter 6. Finally, in chapter 7, we perform numerical experiments to underline the thermodynamical consistency and numerical efficiency of our method.

2. Setting for thermodynamically consistent phase field models

Throughout this thesis we consider a bounded domain $\Omega \subset \mathbb{R}^d, d = 1, 2, 3$ with Lipschitz boundary $\partial\Omega$ and a time interval $I = (0, t^*) \subset \mathbb{R}, t^* > 0$.

2.1. Notation

We give a short overview of the notational convention in this work with the goal in mind to foster the focus on the points of interest.

2.1.1. Euclidean spaces

The Euclidean scalar product for two vectors $a, b \in \mathbb{R}^M$ is denoted by $a \cdot b$. The associated norm (and induced operator norm) is denoted by $|\cdot|$. As this work comprises vector-valued parameters of order $M \in \mathbb{N}$ subject to sum constraints, let

$$\Sigma_c^M = \{v = (v_i)_{i=1}^M \in \mathbb{R}^M \mid \textstyle\sum_{i=1}^M v_i = c\}$$

the respective affine subspaces. The tangent space to elements of Σ_c^M usually is identified with Σ_0^M. It is convenient to define the projection

$$\begin{aligned} &P_0^M : \mathbb{R}^M \to \Sigma_0^M, \\ &P_0^M = \mathrm{Id}^M - \mathbb{1}^{M,M}/M \end{aligned}$$

where $\mathbb{1}^{M,N} = (1)_{i,j=1}^{M,N}$ and $\mathrm{Id}^M \in \mathbb{R}^{M\times M}$ the M-dimensional identity. e_i^M denotes the i-th Euclidean basis vector in $\mathbb{R}^M$.

As the functions under consideration will be allowed to take infinite values, we denote by $\overline{\mathbb{R}} = \mathbb{R} \cup \{-\infty, \infty\}$ the extended real line.

2.1.2. Derivatives, integrals, and superposition

For a function f with general domain $\Omega \times I$ all gradients and derivatives shall be understood w.r.t. the spatial domain Ω unless explicitly written differently, e.g. the partial derivative w.r.t. time., i.e. $\partial_t f$.

Integration over Ω or subsets thereof generally is w.r.t. the usual Lebesgue measure of appropriate dimension. We omit the measure for integration w.r.t. the domain Ω for brevity and write $\mathrm{d}\partial\Omega$ in slight abuse of notation to denote integration over $\partial\Omega$ with $(d-1)$-dimensional Lebesgue measure. We write $|\Omega| \coloneqq \int 1$. Integration w.r.t. time is explicitly denoted by $\mathrm{d}t$.

Let $f : \mathbb{R}^M \to \mathbb{R}$ and $x : \Omega \to \mathrm{range}(x) \subset \mathbb{R}^M$. We denote by $\hat{f}(\cdot)$ the *superposition* (or Nemyckii/Nemytskij) operator induced by

$$\hat{f}(x)(\xi) = f(x(\xi))$$

for $x : \Omega \to \mathbb{R}^M$, $\xi \in \Omega$. Generally, we aim to distinguish the operator from its generating function explicitly through this notation in order to clearly separate pointwise and bulk arguments. For legibility we abuse the notation slightly in the case of derivatives, i.e. derivatives w.r.t. superposition shall be understood in the pointwise sense, specifically

$$\nabla \hat{f}(x)(\xi) = \nabla f(x(\xi)).$$

The well-definedness of the operators $\hat{f}, \nabla\hat{f}$ is discussed in place.

2.1.3. Hilbert function spaces

The relevant function spaces in this work are the Hilbert spaces L^2 and H^1 endowed with their usual scalar products denoted by $(\cdot,\cdot)$ and the induced norm written as $\|\cdot\|$. Absent additional indicators imply the use of the respective L^2 scalar product. Using the Riesz representation theorem, many dual operators are identified with their primal counterparts without further notice.

Boundary contributions (on $\partial\Omega$) are denoted by $(\cdot,\cdot)_\partial$ and all bulk quantities (on Ω) occurring as their arguments are to be understood in the sense of their traces. For functions $u, v \in (H^1)^M$, we use a common generalization of the notation for Sobolev scalar products to Cartesian products without introducing another indicator, i.e. let

$$(\nabla u, \nabla v) = \sum_{i=1}^{M} \int \nabla u_i \cdot \nabla v_i.$$

We generally omit the domain if it refers to Ω and explicitly specify it otherwise, i.e.

$$L^2(X) = L^2(\Omega, X), \qquad H^1(X) = H^1(\Omega, X).$$

2.2. Convex analysis setting

We use some common results from convex analysis. We provide a short list of the key properties and consequences here and refer to Ekeland and Témam 1999; Rockafellar 1970a for a detailed discussion. Though most of the concepts have straightforward generalizations to real topological vector spaces and their duals involving the dual pairing, we confine ourselves to the notationally simpler setting with Hilbert space $(H, (\cdot, \cdot))$, where everything can be written in terms of primal variables by virtue of the Riesz representation theorem.

Let $f : H \to \overline{\mathbb{R}}$ for the upcoming definitions. The *effective domain* of f is given by

$$\operatorname{dom} f = \{x \in H \mid f(x) < \infty\}.$$

f is considered *proper*, if $\operatorname{dom} f \neq \emptyset$ and $\{x \in H \mid f(x) > -\infty\} = H$. It is called *convex*, if

$$f(t_1 x_1 + t_2 x_2) \leq t_1 f(x_1) + t_2 f(x_2)$$

for all $0 \leq t_1 \leq 1, t_2 = 1 - t_1$ and $x_1 \neq x_2 \in \operatorname{dom} f$. We call f *strictly convex*, if the inequality is strict for $0 < t_1 < 1$.

f is called *strongly convex*, if

$$f(t_1 x_1 + t_2 x_2) \leq t_1 f(x_1) + t_2 f(x_2) - \tfrac{1}{2} m t_1 t_2 \|x_1 - x_2\|^2$$

with $m > 0$. For a twice continuously differentiable function, positive semi-definiteness (or a strictly positive lower bound) of its Hessian yields strict convexity (or strong convexity, respectively).

Convex functions may still be unbounded from below, like e.g. $-\log : \mathbb{R}^+ \to \mathbb{R}$, which is why one cannot expect related minimization problems to be well defined. A useful trait to capture these cases is coercivity. f is said to be *coercive*, if

$$\|f(x)\| \overset{\|x\| \to \infty}{\longrightarrow} \infty.$$

We use the following result to simplify the deduction of coercivity for composed functions.

Proposition 2.1 (Gräser 2015, Proposition 2)**.** *Let a, b continuous symmetric bilinear forms on H. Let* $\ker a$ *finite dimensional. Let a coercive on* $(\ker a)^\perp$ *and b positive semi-definite on H but positive definite on* $\ker a$*. Then $a + b$ is coercive on H.*

Convexity and coercivity are commonly used to infer the existence of minimizers by being complemented with the property of f being *lower semi-continuous*, i.e.

$$\forall a \in \mathbb{R} : \{x \in H \mid f(x) \leq a\} \text{ is closed.}$$

Proposition 2.2 (Ekeland and Témam 1999, Proposition 1.2)**.** *Let f proper, convex, lower semi-continuous and coercive. Then*

$$\{x \in H \mid f(x) = \inf\{f(x) \mid x \in H\}\} \neq \emptyset,$$

i.e. the inner minimization problem has a solution. The solution is unique if f is strictly convex.

In addition, convexity provides a setting to a specific generalized differentiability. In this work we consider functions incorporating the so-called obstacle potential. To that extent let χ denote the characteristic function as used in convex analysis, i.e.

$$\chi_A(x) = \begin{cases} 0 & \text{if } x \in A, \\ \infty & \text{if } x \notin A. \end{cases}$$

Proposition 2.3. $\chi_A : A \to \overline{\mathbb{R}}$ *is convex if and only if $\emptyset \neq A$ convex.*

χ is generally not differentiable in the classical sense. However, a generalization exists in the form of the convex subdifferential. $y \in H$ is called a subgradient of f at x_0 if

$$f(x) - f(x_0) \geq (y, x - x_0)$$

for all $x \in H$. The *subdifferential* of f at x_0 is then given by the set of all *subgradients*, i.e.

$$\partial f(x_0) = \{y \in H \mid y \text{ is a subgradient of } f \text{ at } x_0\}.$$

In general the subdifferential is set-valued and may be empty. For the case where the subdifferential contains exactly one subgradient, a distinct relation to *ordinary* differentiation can be formulated.

A function f is Gâteaux-differentiable with Gâteaux-derivative ∇f at x, if the directional derivative exists for all directions x' and

$$(\nabla f(x), x') = \lim_{t \searrow 0}(f(x + tx') - f(x))/t.$$

Proposition 2.4 (Ekeland and Témam 1999, Proposition 5.3)**.** *Let f convex. If f is Gâteaux-differentiable, then it is subdifferentiable with only that very subgradient. Conversely, if it is continuous, finite and comprises exactly one subgradient, then that is its Gâteaux-differential.*

We call a function f Fréchet-differentiable with Fréchet-derivative Df at x, if $Df(x)$ is a bounded linear operator such that

$$f(y + \delta y) - f(y) - Df(y)\delta y = o(\delta y).$$

Proposition 2.5 (Zorn 1946)**.** *Let f Gâteaux-differentiable with continuous Gâteaux-derivative. Then f is Fréchet-differentiable.*

The theory of monotone operators pairs nicely with the previous concepts. An operator T is called *monotone*, if

$$(Tx - Ty, x - y) \geq 0$$

for all $x, y \in H$. It is said to be *maximal monotone* if its graph is maximal in the sense of set inclusion among all monotone operators. The subdifferential of a proper, convex and lower semi-continuous function is maximal monotone, cf. Rockafellar 1970b.

Functions can be paired with dual space functions by conjugation. In our Hilbert space setting this simplifies as follows. We call

$$\begin{aligned} f^* &: H \to \overline{\mathbb{R}}, \\ f^*(y) &= \sup\{(y, x) - f(x) \mid x \in H\} \end{aligned}$$

the *polar* of f, also known as the *Legendre–Fenchel transform*. It is convex by construction and, for convex f, we have $f^{**} \equiv f$ which motivates the notion *convex conjugate*. For differentiable f, the convex conjugate coincides with the *Legendre transform* on the interior of its effective domain.

Proposition 2.6. *f^* is convex and lower semi-continuous.*

The subgradients of f can be characterized by the following polar relationship, cf. Ekeland and Témam 1999, Proposition 5.1.

Proposition 2.7. $y \in \partial f(x) \Leftrightarrow f(x) + f^*(y) = (x, y)$.

Proposition 2.8. *Let f proper, strictly convex and continuously differentiable on* $\operatorname{int}\operatorname{dom} f$. *Then $\nabla f^*(y) = (\nabla f)^{-1}(y)$ for all $y \in \operatorname{int}\operatorname{dom} f^*$.*

Proof. f being strictly convex implies that ∇f is strictly monotone and can be inverted single-valuedly. Then the result follows from proposition 2.7. □

In this work, time derivatives of differentiable, strictly convex functions are approximated with finite differences. We prepare the following result that allows to obtain coercivity of the arising (finite dimensional) spatial problems.

Proposition 2.9. *Let H finite-dimensional and f proper, strictly convex and continuously (Fréchet)-differentiable on* $\operatorname{int}\operatorname{dom} f$. *For* $\forall x_0 \in \operatorname{int}\operatorname{dom} f$ *let* $f_0(x) = f(x) - (\nabla f(x_0), x)$. *Then f_0 is coercive.*

Proof. We construct a cone containing graph f with apex over x_0 (but not exactly at $(x_0, f(x_0))$) and use it to show that the difference between the tangent hyperplane at x_0 and the cone boundary grows at least linearly in x.

For fixed x_0, let $\epsilon > 0$ such that $B_\epsilon(x_0) = \{x \in H \mid \|x - x_0\| \leq \epsilon\} \subset \operatorname{int}\operatorname{dom} f$. Consider $x \neq x_0, x_\epsilon \coloneqq x_0 + \epsilon(x - x_0)/x - x_0$. By strict convexity we have

$$0 < m(x_\epsilon) \coloneqq (\nabla f(x_0) - \nabla f(x_\epsilon), x_0 - x_\epsilon).$$

We can express $x = x_0 - \delta(x_0 - x_\epsilon), \delta = \|x - x_0\|/\epsilon$. We estimate using the tangent hyperplane at x_ϵ to obtain

$$f(x) - (\nabla f(x_0), x) \geq f(x_\epsilon) + (\nabla f(x_\epsilon), x_0 - x_\epsilon) - (\nabla f(x_0), x_0) + \tfrac{1}{\epsilon} m(x_\epsilon)\|x - x_0\|.$$

Consequently, we have

$$\begin{aligned} f(x) - (\nabla f(x_0), x) &\geq c_0 + c_1\|x - x_0\|, \\ c_0 &= \inf\{f(x) + (\nabla f(x), x_0 - x) - (\nabla f(x_0), x_0) \mid x \in \partial B_\epsilon(x_0)\}, \\ c_1 &= \inf\{\tfrac{1}{\epsilon} m(x) \mid x \in \partial B_\epsilon(x_0)\}, \end{aligned}$$

for all $x \in \operatorname{int}\operatorname{dom} f$ with constant $c_1 > 0$ by continuity of ∇f and compactness of ∂B_ϵ. □

2.2.1. Linearly parametrized conjugates

We prepare some particular results for linearly parameter dependent convex conjugates. To this extent let now

$$f : \mathbb{R}^M \times \mathbb{R}^N \to \overline{\mathbb{R}}, \qquad \operatorname{dom} f = P \times Y,$$

proper with convex effective domain and $P \subset \mathbb{R}^M$ closed, $Y \subset \mathbb{R}^N$ open. Let furthermore f be linear in P and continuously differentiable as well as strictly convex in Y. Precisely, for all $p \in P$ and $y, y_0 \in Y$ there exists $f_y \in \mathbb{R}^M$ such that

$$\begin{aligned} f(p,y) &= p \cdot f_y, \\ f(p,y) &> f(p,y_0) + \nabla_y f(p,y_0) \cdot (y - y_0). \end{aligned}$$

Convex functions can be characterized by their epigraph being a subset of the intersection of all half spaces constructed from tangent planes to the function. In case of a linearly parametrized f as given here, this reads as follows.

Lemma 2.1. *For all $p, p_0 \in P, y, y_0 \in Y$ we have*

$$f(p,y) \geq f(p_0,y_0) + \nabla_1 f(p,y) \cdot (p - p_0) + \nabla_2 f(p_0,y_0) \cdot (y - y_0).$$

Proof. By linearity in p and convexity in y we have

$$\nabla_1 f(p,y) \cdot (p - p_0) = f(p,y) - f(p_0,y) \leq f(p,y) - f(p_0,y_0) - \nabla_2 f(p_0,y_0) \cdot (y - y_0).$$

□

Let $f^\star$ the convex conjugate of f for every fixed $p \in P$ [1], i.e.

$$f^\star : P \times \mathbb{R}^N \to \overline{\mathbb{R}}, \tag{2.1a}$$

$$f^\star(p,z) = \sup\{z \cdot y - f(p,y) \mid y \in \mathbb{R}^N\}, \tag{2.1b}$$

or equivalently,

$$f^\star(p,z) = (f(p,\cdot))^*(z).$$

The straightforward conclusion from proposition 2.8 reads

$$y^\star(p,z) \coloneqq (\nabla_2 f(p,\cdot))^{-1}(z) = \nabla_2 f^\star(p,z). \tag{2.2}$$

By definition of $f^\star$ and the properties of f we have

$$f^\star(p,z) = z \cdot y^\star - f(p,y^\star), \tag{2.3a}$$

$$f^\star(p, \nabla_2 f(p,y)) = y \cdot \nabla_2 f(p,y) - f(p,y). \tag{2.3b}$$

Additionally, the derivative w.r.t. the parametrization satisfies a helpful relation which allows to avoid analytically determining the parametrized convex conjugate to evaluate its derivatives.

[1] note the difference f^* and $f^\star$

Lemma 2.2.

$$\nabla_1 f^\star(p,z) = -\nabla_1 f(p,y^\star), \tag{2.4a}$$
$$\nabla_1 f^\star(p,\nabla_2 f(p,y)) = -\nabla_1 f(p,y). \tag{2.4b}$$

Proof. $\nabla_1 f^\star(p,z) = \frac{\mathrm{d}}{\mathrm{d}p}(z\cdot y^\star - f(p,y^\star)) = z\cdot\nabla_1 y^\star - \nabla_1 f(p,y^\star) - \nabla_2 f(p,y^\star)\cdot\nabla_1 y^\star$. □

Moreover, the strict convexity is expanded to the entire parameter domain in this specific setting as follows.

Lemma 2.3. *$f^\star$ is strictly convex.*

Proof. For $i=1,2$ let $p_i \in P, z_i \in \mathbb{R}^N, t_i > 0$ where $z_i \in \operatorname{dom} f^\star(p_i,\cdot)$, $y_i^\star$ the solution to $z_i = \nabla_y f(p_i, y_i^\star)$, and $t_1 + t_2 = 1$. Let furthermore $(p_3, z_3) = \sum_{i=1,2} t_i(p_i, z_i)$.

Then, by strict convexity of $f(p_i,\cdot)$ we have with $y \neq y_i$ for $i = 1,2$,

$$f(p_i,y) - f(p_i,y_i) > (y-y_i)\cdot z_i, \tag{2.5}$$

i.e. $f(p_i,\cdot)$ grows quicker than its linear approximation z_i at y_i towards any y. For $y_1 \neq y_2$ we use the linearity of $f(\cdot,y)$ to obtain

$$\begin{aligned}
&\textstyle\sum_{i=1,2} t_i(f(p_i,y) - f(p_i,y_i^\star)) > \sum_{i=1,2} t_i(y-y_i^\star)\cdot z_i \\
\Leftrightarrow\ & f(p_3,y) - \textstyle\sum_{i=1,2} t_i f(p_i,y_i^\star) > y\cdot z_3 - \sum_{i=1,2} t_i y_i^\star \cdot z_i \\
\Leftrightarrow\ & \textstyle\sum_{i=1,2} t_i(y_i\cdot z_i - f(p_i,y_i^\star)) > y\cdot z_3 - f(p_3,y)
\end{aligned}$$

which for $y = y_3^\star = (\nabla_y f(p_3,\cdot))^{-1}(z_3)$ is equivalent to

$$\textstyle\sum_{i=1,2} t_i f^\star(p_i,z_i) > f^\star(p_3,z_3)$$

yielding strict convexity of $f^\star$. □

2.3. Diffuse interface models

Problems of phase transitions can be formulated as free boundary problems for the boundaries of the phases of interest. Particular attention was paid historically to the description of the evolution of a given boundary through problems of Stefan-type, cf. Visintin 2012, implicitly tracking the velocity of the sharp boundary.

Sharp interface models that explicitly describe the evolution of boundaries are cumbersome to deal with when topological changes occur, e.g. when boundaries collapse due to the inscribed region vanishing, or split when an a connected region is becoming disconnected. One way to look at phase field models is that they approximate or replace the sharp interface representation of the boundary by a diffuse interface of finite width proportional to some custom variable $\varepsilon > 0$, cf. Brokate and Sprekels 1996. This approach allows to circumvent the topological issues described above at the expense of a higher dimensional problems whose computational overhead can be minimized with appropriate numerical frameworks, e.g. adaptive grids. Through methods such as matched asymptotic expansions, cf. Lagerstrom 1988, these diffuse models can be led back to sharp interface models.

The underlying functional governing the phase separation and transition processes is often referred to as *Ginzburg–Landau* energy where the lower-dimensional interface integral from the sharp model is replaced by an integral with nonzero contribution in close proximity. In models with thermodynamic background, phase field models often occur naturally in the sense that the sharp interfaces are not the original motivation. Two prototypical phase-field models are the so-called Allen–Cahn-model and the Cahn–Hilliard-model. They arise from gradient flows for the Ginzburg–Landau energies w.r.t. a L^2- or H^{-1}-like scalar product, respectively. The model to be considered in this work exhibits strong relations to both approaches. These basic phase field models comprise a bulk parameter that captures the relative local fraction of the respective quantity of interest.

2.3.1. Vector-valued order parameters and obstacles

Basic models tackle binary problems in the sense that the scalar order parameter models the presence of a single phase $p \in [0, 1]$. Simultaneously, regions of absence of the model parameter phase implicitly represent the presence of a second, counteracting *disorder* phase $1-p \in [0, 1]$. As the latter phase is implicitly defined by a scalar p anyway, many binary models are symmetrized and rescaled to an order parameter $p \in [-1, 1]$ for computational convenience.

For models that take into account a third phase or more, one usually represents each phase explicitly by a separate order parameter. In this work we consider problems with $M \in \mathbb{N}$ order parameters. Points where a single phase is present are characterized by only the respective order parameter being one while all others are zero. Diffuse interface regions where one phase transitions to another exhibit more than a single non-zero order parameter. Here we interpret the order parameters as relative fractions of the presence of each phase. Consequently, they should be non-negative and add up to one. This is accounted for formally by introducing the $M-1$-simplex or Gibbs

simplex G^M, and its function space *relative* imposing the constraint pointwise

$$G^M = \{v = (v_i)_{i=1}^M \in \Sigma_1^M \mid v_i \geq 0, i = 1, \ldots, M\},$$
$$\mathcal{G}^M = \{v \in L^2(\Omega, \mathbb{R}^M) \mid v(x) \in G^M \text{ a.e.}\}.$$

We consider an order parameter

$$p : \Omega \times I \to G^M \subset \mathbb{R}^M$$

where the positivity and sum constraint are built into an optimization functional in terms of χ_{G^M} leading to models of so-called *obstacle potential* type.

2.3.2. Ginzburg–Landau energy

A pivotal modeling factor for phase field models usually ensues from the Ginzburg–Landau contribution $\int g$ to the underlying energy functional. Its generating function g comprises two basically counteracting terms. On one hand there is the local contribution $g^{\text{local}}(p)$ that drives the system towards *pure* phases. It is commonly modeled as a multi-well potential with M distinct global minima in G^M. In this work, we consider multi-well potentials of obstacle type, i.e. with contribution χ_{G^M}. On the other hand there is a gradient contribution $g^{\text{grad}}(p, \nabla p)$ which usually is assumed to be homogeneous of degree two in the second variable, i.e.

$$g^{\text{grad}}(p, \alpha\nabla p) = \alpha^2 g^{\text{grad}}(p, \nabla p)$$

for all $\alpha \in \mathbb{R}^+, p \in \mathbb{R}^M, \nabla p \in \mathbb{R}^{M\times d}$. It punishes steep gradients and allows to account for multi-phase anisotropy (that is in the sense of equilibrium shapes - anisotropic velocities are usually incorporated via a relaxation parameter in the ensuing partial differential equation). We have

$$g(p, \nabla p) = \chi_{G^M}(p) + \tfrac{1}{\varepsilon} g^{\text{local}}(p) + \varepsilon g^{\text{grad}}(p, \nabla p)$$

with $\varepsilon > 0$ scaling the diffuse interface width.

In this work we incorporate a well-known simple instance of such a Ginzburg–Landau contribution, namely the isotropic, quadratic multi-well obstacle potential with a purely concave smooth local contribution, i.e.

$$g^{\text{local}}(p) = -\tfrac{1}{2}\|p\|^2, \tag{2.6a}$$
$$g^{\text{grad}}(p, \nabla p) = \tfrac{1}{2}\|\nabla p\|^2. \tag{2.6b}$$

The corresponding Ginzburg–Landau functional in this work occurs in the form

$$\mathrm{G} : H^1(\mathbb{R}^M) \to \overline{\mathbb{R}}, \tag{2.7a}$$
$$p \mapsto \int \hat{g}(p, \nabla p) \tag{2.7b}$$

by means of superposition and exhibits the splitting

$$\mathrm{G}(p) = \mathrm{G}_\varepsilon(p) + \chi_{\mathcal{G}^M}(p)$$

with smooth contribution G_ε and $\chi_{\mathcal{G}^M}$ the functional simplex obstacle. We assume that G_ε is Fréchet-differentiable with Gâteaux derivative $\nabla \mathrm{G}_\varepsilon$, see Gräser 2011.

2.4. Thermodynamic potentials and free entropies

Classical thermodynamics captivates by its *state functions*, in particular the *thermodynamic potentials*. These are formulated in terms of so-called *natural variables* allowing to obtain other state functions by partial differentiation. This section shall serve as a short introduction to thermodynamic potentials while already adhering to a notation that allows a smooth transition to the forthcoming chapters.

The thermodynamics of irreversible processes considered in this work is based on the *local thermodynamic equilibrium assumption*. Hereby *local* refers to the meso-scale of the respective system of interest, i.e. it resolves the so-called *microstructure* but abstracts from the atomic scale through the meaningful incorporation of temperature, composition, energy and entropy density, etc.

Thermodynamic variables are commonly categorized into *extensive variables* that scale with the size of the system and their *intensive* counterparts. We use latin letters to denote extensive variables. These are e.g. the total mass of the chemical composition, but also include in particular the common thermodynamic potential densities for entropy and the internal energy. Intensive variables like the chemical potentials, but also temperature, are denoted by greek letters in this work.

To this extent let e the internal energy density, s the entropy density and θ the temperature. From the first and second law of thermodynamics, one can derive the *fundamental thermodynamic relation*

$$\mathrm{d}e = \theta \, \mathrm{d}s + \sum_{i=1}^{i_{\max}} \rho_i \, \mathrm{d}p_i \tag{2.8}$$

in terms of e. Here $\{\theta, s\}$ is the conjugate pair of (extensive) absolute temperature θ and (intensive) entropy s. For finitely many further external variables p_i that are necessary to characterize the system, their (intensive) conjugates ρ_i denote the respective generalized forces. Equation (2.8) provides a description of the potential's differential in terms of the differentials of its variables and motivates the interpretation of e as a function of the *natural variables* $(s, p_1, \ldots, p_{i_{\max}})$.

The definition suggests that there is no single thermodynamic potential for a system. The specific choice relies on the applied constraints (in physical context when considering small volumes sometimes referred to as boundary conditions) and henceforth the variables of interest. While the term internal energy is coined for all natural variables being extensive, other combinations of natural variables are reasonable as long as either the extensive or the intensive representation of each pair of conjugates is chosen. An appropriate tool to explore the set of thermodynamic potentials is the Legendre transform as it allows to consecutively swap between both representations of each pair until a suitable representation is obtained. Classical thermodynamics for gases considers the conjugate pairs $\{\theta, s\}$, $\{\text{pressure}, \text{volume}\}$, $\{\mu_j, c_j\}$, where the latter denote the chemical potentials or the relative concentrations of particles of a certain specimen, respectively. The corresponding classical thermodynamic potentials have dedicated names, such as the internal energy $e(s, \text{volume}, c)$, Helmholtz free energy $f(\theta, \text{volume}, c)$, the enthalpy $h(s, \text{pressure}, c)$, the Gibbs enthalpy or Gibbs free energy $g(\theta, \text{pressure}, c)$, and the grand canonical potential $\omega(\theta, \text{pressure}, \mu)$.

In addition to the thermodynamic potentials obtained as described above, the role of independent variables and describing function may eventually be reversed. A monotone relationship between e and s allows to obtain a state function of entropy $s(e, \text{volume}, c)$. Again, replacing variables by their conjugate counterparts generates more state functions with different natural variables. They are being referred to as free entropies and comprise the Massieu potential $s_{\text{Massieu}}(\beta, \text{volume}, c)$, the Planck potential $s_{\text{Planck}}(\beta, \beta \cdot \text{pressure}, c)$, as well as the reduced grand canonical potential $\psi(\beta, \beta \cdot \text{pressure}, \beta \cdot \mu)$. Here the intensive variable of negative inverse temperature $\beta = -1/\theta$ is the conjugate variable to e.

2.4.1. Thermodynamic bulk entropy densities

The model to be presented in the following chapter is based on thermodynamic principles formulated in free entropy. From an application point of view, the fundamental equation for a thermodynamical potential is generally the most assessable in Helmholtz free energy representation f. This is due to the fact the coefficients for a desired parametrization can be obtained by carefully conducted experiments and measurements due to the extensive nature of its variables with the notable exception of temperature which is an intensive quantity. A Legendre transform leads to an internal energy formulation which, by monotonicity w.r.t. its independent variable s, allows to obtain a parametrization of entropy. A final Legendre transform yields a formula for the reduced grand canonical potential ψ. In this section we obtain an explicit fundamental equation for the reduced grand canonical potential according to these relationships.

This section concentrates on the local derivation of said potentials within a fixed pure

phase (bulk) on the relative meso-scale as introduced previously. The global, multi-phase version is obtained by suitable interpolation in section 3.3.1.

We assume that, regardless of the local composition, the mass density is constant. Furthermore, we assume that the pressure is constant. Hence, its constant contributions to the potentials are neglected. Let a parametrization of the free energy $f : \mathbb{R}^+ \times \operatorname{int} G_1^N \to \mathbb{R}$ be given by

$$f(\theta, c) = (\theta\widetilde{L} - L) \cdot c + c_m \theta c \cdot \log c - c_v \theta(\log \theta - 1), \tag{2.9}$$

with $c_v, c_m \in R^+$, $\widetilde{L}, L \in \mathbb{R}^N$, $N \in \mathbb{N}$, and *log* the natural logarithm applied componentwise. Such parametrizations are obtained e.g. for models of ideal solutions, c.f. Haasen 1994.

$-f$ is a convex function in θ. Its Legendre transform w.r.t. θ is the internal energy and the respective conjugate variable is entropy. We deduce

$$s = -\partial_\theta f(\theta, c) = -\widetilde{L} \cdot c - c_m c \cdot \log c + c_v \log \theta, \tag{2.10a}$$

$$\theta = \exp((s + \widetilde{L} \cdot c + c_m c \cdot \log c)/c_v), \tag{2.10b}$$

$$e = f + \theta s = -L \cdot c + c_v \theta \tag{2.10c}$$

which allows us to express the internal energy $e : \mathbb{R} \times \operatorname{int} G_1^N \to \mathbb{R}$ in its natural variables

$$e(s, c) = -L \cdot c + c_v \exp((s + \widetilde{L} \cdot c + c_m c \cdot \log c)/c_v).$$

Notice that e is convex and, in particular, strictly monotone in s. Hence, we can globally invert $e(\cdot, c)$ for arbitrary fixed c, yielding the entropy density $s : X \to \mathbb{R}$, which then is given by

$$s(e, c) = c_v \log(e + L \cdot c) - \widetilde{L} \cdot c - c_m c \cdot \log c - c_v \log c_v$$

in its natural variables and on the domain $X = \{(e, c) \in \mathbb{R} \times \operatorname{int} G_1^N \mid e + L \cdot c > 0\}$. Its partial derivatives up to second order are

$$\begin{aligned}
\partial_e(-s)(e, c) &= -c_v/(e + L \cdot c), \\
\partial_c(-s)(e, c) &= -c_v/(e + L \cdot c)L + \tilde{L} + c_m(1 + \log c), \\
\partial^2_{e,e}(-s)(e, c) &= c_v/(e + L \cdot c)^2, \\
\partial^2_{e,c}(-s)(e, c) &= c_v/(e + L \cdot c)^2 L, \\
\partial^2_{c,c}(-s)(e, c) &= c_v/(e + L \cdot c)^2 L^T L + c_m \operatorname{diag} \tfrac{1}{c}
\end{aligned}$$

and

$$-(e', c')^T(\nabla^2 s(e, c))(e', c') = c_v(e + L \cdot c)^{-2}(e' + L \cdot c')^2 + c_m c'^T \operatorname{diag} \tfrac{1}{c} c' > 0$$

which shows that $-s$ is strictly convex.

We now compute its Legendre transform explicitly and introduce related notation to use later on. The resulting function is the reduced grand canonical potential $\psi = (-s)^*$ and its natural variables are denoted negative inverse temperature β and reduced chemical potentials η. Formally, we consider the function $-\tilde{s}(e,c) = -s(e,c)$ if $(e,c) \in X$ and ∞ else and obtain a conjugate function $\tilde{\psi} : \mathbb{R} \times \mathbb{R}^N \to \overline{\mathbb{R}}$. However, we restrain our notation to its effective domain $\operatorname{dom} \psi$ which we identify with $\mathbb{R}^- \times \Sigma_0^N$. Then

$$\begin{aligned} \psi(\beta,\eta) &= \sup\{e \cdot \beta + c \cdot \eta + s(e,c) \mid (e,c) \in X\} \\ &= \tilde{e}(\beta,\eta) \cdot \beta + \tilde{c}(\beta,\eta) \cdot \eta + s(\tilde{e},\tilde{c}), \\ \text{with } (\tilde{e},\tilde{c}) &= (-\nabla s)^{-1}(\beta,\eta). \end{aligned}$$

We introduce helper functions to reduce notational clutter in the remainder. These definitions should be considered temporary at this point and are made more rigorous later on in the multi-phase context of section 3.3.1. We omit their arguments wherever it is convenient and unambiguous. Let $\tilde{\eta}, \sigma_k, \zeta : \mathbb{R} \times \mathbb{R}^N \to \mathbb{R}$,

$$\begin{aligned} \tilde{\eta}_j(\beta,\eta) &= \exp((\eta_j - \widetilde{L}_j - \beta L_j)/c_m), && j = 1,\dots,N, \\ \sigma_k(\beta,\eta) &= \textstyle\sum_{j=1}^N L_j^k \tilde{\eta}_j(\beta,\eta), && k \in \mathbb{N}, \\ \zeta(\beta,\eta) &= c_m \log \sigma_0(\beta,\eta), \end{aligned}$$

with *exp* the exponential function applied componentwise and $\tilde{\eta} = (\tilde{\eta})_{j=1}^N$.

By the identification of $T_{(e,c)}(X)$ with $\mathbb{R}^- \times \Sigma_N^0$ we obtain

$$\beta = \nabla_1(-s)(\tilde{e},\tilde{c}), \tag{2.11a}$$
$$\eta = \nabla_2(-s)(\tilde{e},\tilde{c}) - t\mathbb{1}^N \tag{2.11b}$$

with $t = \partial_c(-s)(\tilde{e},\tilde{c}) \cdot \mathbb{1}^N / N^2 \in \mathbb{R}$ by orthogonal projection of the ambient gradient to the relevant subspace which yields

$$\beta = -c_v/(\tilde{e} + L \cdot \tilde{c}) \quad \Leftrightarrow \quad \tilde{e} = -c_v/\beta - L \cdot \tilde{c}, \tag{2.12a}$$
$$\eta + t\mathbb{1}^N = \beta L + \widetilde{L} + c_m(1 + \log \tilde{c}) \quad \Leftrightarrow \quad \tilde{c} = \exp(t/c_m - 1)\tilde{\eta}. \tag{2.12b}$$

The constraint $1 = \sum_{i=1}^N \tilde{c}_i = \sum_{i=1}^N \exp(t/c_m - 1)\tilde{\eta}_i = \exp(t/c_m - 1)\sigma_0$ implies

$$t = c_m - \zeta, \tag{2.13a}$$
$$\tilde{c} = \tilde{\eta}/\sigma_0. \tag{2.13b}$$

We use these expressions for $\tilde{c}$ and consequently $\tilde{e}$ as functions in β, η to get

$$\begin{aligned} s(\tilde{e}, \tilde{c}) &= -c_v \log(-\beta) - \widetilde{L} \cdot \tilde{c} - c_m \tilde{c} \cdot \log \tilde{c} \\ &= -c_v \log(-\beta) - \widetilde{L} \cdot \tilde{c} - c_m/\sigma_0 \tilde{\eta} \cdot \log \tilde{\eta} + \zeta, \\ \psi(\beta, \eta) &= \tilde{e} \cdot \beta + \tilde{c} \cdot \eta + s(\tilde{e}, \tilde{c}) \\ &= -c_v(1 + \log(-\beta)) + \zeta. \end{aligned}$$

The first order partial derivatives of ψ are

$$e = \partial_\beta \psi = -c_v/\beta - \sigma_1/\sigma_0, \tag{2.14a}$$

$$c_j = \partial_{\eta_j} \psi = \tilde{\eta}_j/\sigma_0 \tag{2.14b}$$

which coincides with the relations in equations (2.12) and (2.13). Note that equation (2.14a) implies $e + Lc > 0$ which combined with equation (2.10c) corresponds to the strict positivity of temperature $\theta > 0$. Equation (2.14b) directly yields $c \in \operatorname{int} G_1^N$.

3. Continuous non-isothermal multi-phase field systems

In this chapter, we consider a model that is capable of describing phase transformation processes in non-isothermal multi-component alloys as well as in grain structure evolution. In this setting, phase transformations are not restricted to the physical notion of an aggregate phase but can also represent transitions of different crystal orientation or other distinctive characteristics.

3.1. Motivation of the phase field model

We present the derivation of a phase field model according to the approach in Stinner, Nestler, and Garcke 2004. Therein, the focus lies on the thermodynamical consistency for non-isothermal settings, support for an arbitrary number of phases and components, and the assessability of the required parameters for densities (bulk free energy and surface energy) and coefficients (diffusion and mobility).

We consider the independent variables

$$p : \Omega \times I \to \mathbb{R}^M, \tag{3.1a}$$

$$e : \Omega \times I \to \mathbb{R}, \tag{3.1b}$$

$$\text{and } c : \Omega \times I \to \mathbb{R}^N, \tag{3.1c}$$

where p is the phase field (or order) parameter, e is the internal energy density, and c the chemical (component) concentration with $M, N \in \mathbb{N}$. We interpret p and c as relative fractions of a structural property or a chemical substance respectively. Hence, it is natural to require additionally that

$$p \in G^M \text{ a.e.}, \tag{3.2a}$$

$$c \in \operatorname{int} G^N \text{ a.e.}. \tag{3.2b}$$

While the former is incorporated by the simplex obstacle functional in the Ginzburg–Landau contribution, the latter constraint has to be considered separately. Notice that we exclude the edge cases where $c \in \partial G^N$.

The model is derived from an energy functional *in entropy form*

$$F_S(p, e, c) = S(p, e, c) - \mathrm{G}(p), \tag{3.3}$$

with entropic contributions for the bulk

$$S(p, e, c) = \int s(p, e, c) \tag{3.4}$$

where

$$s(p, e, c) : \Omega \times I \to \mathbb{R} \tag{3.5}$$

and G a Ginzburg–Landau functional as introduced in equation (2.7b). This functional is thought of representing the system's global entropy as the sum of both, the bulk as well as the interfacial entropic contributions.

We include additional energetic source terms in the form

$$e_{src}(p, e, c) : \Omega \times I \to \mathbb{R}. \tag{3.6}$$

The system is postulated as a gradient flow for F_S with the driving forces $\delta_p F_S$, $\delta_e F_S$, and $\delta_c F_S$ and taking into consideration the constraint equation (3.2a) by incorporating the subdifferential of the non-smooth convex functional $\chi_{\mathcal{G}^M}$. More precisely, a weighted L^2 scalar product is chosen for the evolution of p along with a dissipation mechanism characterized by the kinetic coefficient p_{kin} that leads to an Allen–Cahn type phase field problem. A weighted H^{-1} like scalar product is used to postulate the evolution of (e, c) and leads to continuity equations that satisfy conservation principles to be emphasized later.

In formulas, for the non-conserved phase field parameter we postulate

$$p_{\mathrm{kin}}\varepsilon\partial_t p \in \delta_p \tilde{F}_S(p, e, c) - \partial\chi_{\mathcal{G}^M}(p) \tag{3.7}$$

where $\tilde{F}_S = S - G_\varepsilon$ with $p_{\mathrm{kin}} > 0$ complemented by no-flux boundary conditions.

For the conserved parameters of internal energy and component bulks we have the balance equations

$$\partial_t e = -\nabla \cdot J_0(p, e, c) + e_{src} \tag{3.8a}$$

$$\partial_t c_i = -\nabla \cdot J_i(p, e, c), \qquad i = 1, \ldots, N \tag{3.8b}$$

with the fluxes being linear functions of the thermodynamic driving forces, i.e.

$$J_0(p, e, c) = \kappa\nabla\delta_e \tilde{F}_S(p, e, c), \tag{3.9a}$$

$$J_i(p, e, c) = \textstyle\sum_{j=1}^{N} \mathrm{m}_{ij}\nabla\delta_{c_j}\tilde{F}_S(p, e, c), \qquad i = 1, \ldots, N. \tag{3.9b}$$

> A corollary (...) is that the free energy of a mixture (...) is not the interpolation of the free energies of the respective phases at a given concentration, but it is a mixture of the phases at the respective concentrations at which they are at thermodynamic equilibrium, i.e., at the same chemical potential (...)

Figure 3.1.: Choudhury and Nestler 2012

Here, $\mathrm{m} \in \mathbb{R}^{N,N}$ is symmetric and positive semi-definite with

$$\ker \mathrm{m} = \operatorname{span}\{\mathbb{1}^N\}$$

thereby satisfying the *Onsager reciprocal relations*, cf. Onsager 1931, which ensures the conservation of mass. Consequently also $\eta^T \mathrm{m} \eta > 0$ for $\eta \in \Sigma_0^N$.

Decoupling the flows in the sense that we are not incorporating $\nabla \delta_e \tilde{F}_S$ in J_i and no $\nabla \delta_{c_j} \tilde{F}_S$ in J_0 implies that we neglect any cross effects of mass and energy diffusion.

We impose Robin type boundary conditions to complement these fluxes which are specified later.

3.2. Conjugated thermodynamic modeling

The thermodynamic governance of the system is determined by the choice of the thermodynamic potential density s. We now replace it by the reduced grand canonical potential density and formulate our system in its natural variables instead. Such a reformulation of the system related to the work by Stinner, Nestler, and Garcke 2004 was derived and analyzed in Stinner 2007. S. G. Kim, W. T. Kim, and Suzuki 1998 showed that models based on interpolated free energies are prone to generating excess energy in the interfaces. As a consequence the interface thickness related to ε is constrained to avoid altering the system's dynamics. While this alone hampers the numerical approximation significantly, the interfacial energy contributions in g are effectively also functions of the free energy density landscape as explained by Choudhury and Nestler 2012 in the isothermal case. Plapp 2011 discusses how a grand canonical potential approach allows to unify two different approaches to phase field problems modeling alloy solidification. The different viewpoint provides a more benign modeling approach that allows independent modeling of the bulk and interface contributions.

Notably, Choudhury and Nestler 2012 also consider a Ginzburg–Landau contribution of obstacle type, which is also done in this work, and derive an appropriate antitrapping current, which is not considered here.

Consider the reduced grand canonical potential density (the Massieu potential density) ψ as the convex conjugate of $-s$ (as a function of (p, e, c)) w.r.t. (e, c). Its natural variables are the derivatives of $-s(p, \cdot, \cdot)$ which we identify with elements of $\mathbb{R} \times \Sigma_0^N$. We have

$$\begin{aligned} \beta &: \Omega \times I \to \mathbb{R}, \\ \eta &: \Omega \times I \to \Sigma_0^N, \end{aligned}$$

and

$$\psi(p, \beta, \eta) : \Omega \times I \to \mathbb{R}.$$

It bears the inverse relations

$$\nabla_2 \psi(p, \beta, \eta) = e, \tag{3.10a}$$
$$\nabla_3 \psi(p, \beta, \eta) = c. \tag{3.10b}$$

Using these relations we can transform our system (pointwise) and obtain a corresponding evolution in terms of a global entropy functional *in reduced grand canonical potential form* $F_\Psi(p, \beta, \eta) = F_S(p, e(p, \beta, \eta), c(p, \beta, \eta))$ with the representation

$$F_\Psi(p, \beta, \eta) = S_\Psi(p, \beta, \eta) - \mathrm{G}(p)$$

where the contributions for the bulk are given by

$$S_\Psi(p, \beta, \eta) = \int \psi(p, \beta, \eta) - \beta e(p, \beta, \eta) - \eta \cdot c(p, \beta, \eta).$$

This transformation specifically simplifies the representations for the thermodynamical driving forces from the bulk since

$$\begin{aligned} -\delta_e S(p, e(p, \beta, \eta), c(p, \beta, \eta)) &= \beta, \\ -\delta_c S(p, e(p, \beta, \eta), c(p, \beta, \eta)) &= \eta \end{aligned}$$

by convex conjugate duality of $-s(p, \cdot, \cdot)$ and $\psi(p, \cdot, \cdot)$ and

$$\begin{aligned} \delta_p S(p, e, c) &= \nabla_1 s(p, e(p, \beta, \eta), c(p, \beta, \eta)) && \text{(3.11a)} \\ &= \tfrac{d}{dp} s(p, e, c) - \nabla_1 e \beta - \nabla_1 c \cdot \eta && \text{(3.11b)} \\ &= \nabla_1 (\psi - \beta \nabla_2 \psi - \eta \cdot \nabla_3 \psi) - \nabla_1 e \beta - \nabla_1 c \cdot \eta && \text{(3.11c)} \\ &= \nabla_1 \psi(p, \beta, \eta). && \text{(3.11d)} \end{aligned}$$

This results in the effective postulation of the transformed system as

$$p_{\mathrm{kin}} \varepsilon \partial_t p \in \delta_p \widetilde{F}_\Psi(p, \beta, \eta) - \partial \chi_{\mathcal{G}^M}(p) \tag{3.12a}$$

where $\delta_p \widetilde{F}_\Psi = \nabla_1 \psi(p,\beta,\eta) - \nabla_p \mathrm{G}_\varepsilon(p)$ (c.f. equation (3.11)) with natural boundary conditions coupled to

$$\partial_t \nabla_2 \psi(p,\beta,\eta) = -\nabla \cdot J_0(p,\beta,\eta) + \beta_{src}, \tag{3.13a}$$
$$\partial_t \nabla_3 \psi(p,\beta,\eta) = -\nabla \cdot J_i(p,\beta,\eta), \qquad i = 1,\dots,N, \tag{3.13b}$$

with source term $\beta_{src} = e_{src}$ and with fluxes

$$J_0(p,\beta,\eta) = \kappa \nabla(-\beta), \tag{3.14a}$$
$$J_i(p,\beta,\eta) = \textstyle\sum_{j=1}^N \mathrm{m}_{ij} \nabla(-\eta_j), \qquad i = 1,\dots,N. \tag{3.14b}$$

We specify the thermodynamical boundary conditions at this point to be

$$J_0 \cdot n = \beta_{00}(\beta - \beta_\partial), \tag{3.15a}$$
$$J_i \cdot n = 0, \qquad i = 1,\dots,N, \tag{3.15b}$$

with $\beta_{00} \geq 0$ and n the unit outward normal to Ω thereby imposing no mass flux over the boundary and a (negative inverse) temperature regulation given by $0 < \beta_\partial$ a.e. and controlled by β_{00} on $\partial\Omega$.

3.3. Choice of thermodynamic fundamental equation

In the previous section we set up a model based on a reduced grand canonical potential formulation. In section 2.4.1 we constructed explicit expressions for reduced grand canonical potential densities for multiple components in a fixed phase. Consider M of these thermodynamic bulk potentials each w.r.t. a fixed phase i, i.e. we tag them by a respective subscript, i.e. $\psi_i, -s_i$ etc. We now construct multi-phase potentials $\psi(p,\beta,\eta), -s(p,e,c)$ etc. from these pure phase thermodynamic potentials with $\psi(e_i,\beta,\eta) = \psi_i(\beta,\eta), -s(e_i,e,c) = -s_i(e,c)$ etc. for $i = 1,\dots,M$.

3.3.1. Multi-phase reduced grand canonical potential

We choose to linearly interpolate in this work. The good thermodynamic potential to interpolate in this context is the reduced grand canonical potential ψ as emphasized in section 3.2. Only in reduced models this coincides with linearly interpolating the entropy, internal energy, or free energy over the phase transition regions. It is a modeling freedom that yields preferential calibration properties (see Stinner, Nestler, and Garcke 2004; Plapp 2011; Choudhury and Nestler 2012) and leads to linearity and convexity properties that we make use of later in this work. We set

$$\psi_{\text{ideal}}(p,\beta,\eta) = \textstyle\sum_{i=1}^M p_i \psi_i(\beta,\eta),$$
$$\psi_i(\beta,\eta) = -c_v(1 + \log(-\beta)) + c_m \log \textstyle\sum_{j=1}^N \exp((\eta_j - \widetilde{L}_{i,j} - \beta L_{i,j})/c_m)$$

with, again, positive constants c_v, c_m, latent heats resp. latent heats reduced by melting temperature $L, \widetilde{L} \in \mathbb{R}^{M,N}$ for component $j = 1, \dots, N$ in phase $i = 1, \dots, M$. Throughout this work we stick to the convention of phase $i = 1$ representing the liquid phase, i.e. $L_1 = \widetilde{L}_1 = \mathbb{0}^N$.

In light of the sum constraint $p \in \Sigma_1^M$ as of equation (3.2a), we simplify the notation for the logarithmic negative inverse temperature contribution to be independent of p. Also, we drop the constant contributions since we are not interested in absolute values but derivatives of ψ. We denote the addend for the logarithmic negative inverse temperature contribution by

$$\begin{aligned} \pi : \mathbb{R} &\to \overline{\mathbb{R}}, \\ \beta &\mapsto \begin{cases} -c_v \log(-\beta) & \text{if } \beta < 0, \\ \infty & \text{else.} \end{cases} \end{aligned}$$

For the chemical potential contribution, we use

$$\begin{aligned} \zeta_i : \mathbb{R} \times \Sigma_0^N &\to \mathbb{R}, \\ (\beta, \eta) &\mapsto c_m \log \sigma_{0,i}(\beta, \eta) \end{aligned}$$

where

$$\begin{aligned} \sigma_{k,i} : \mathbb{R} \times \Sigma_0^N &\to \mathbb{R}, && k \in \mathbb{N}, \quad i = 1, \dots, M, \\ (\beta, \eta) &\mapsto \textstyle\sum_{j=1}^N L_{i,j}^k \tilde{\eta}_{i,j}, \\ \tilde{\eta}_{i,j} : \mathbb{R} \times \Sigma_0^N &\to \mathbb{R}, && i = 1, \dots, M, \quad j = 1, \dots, N, \\ (\beta, \eta) &= \exp((\eta_j - \widetilde{L}_{i,j} - \beta L_{i,j})/c_m), \end{aligned}$$

and we write $\zeta = (\zeta_i)_{i=1}^M$. For the remainder of this work, we consider a regularized version of ψ_{ideal} by $\frac{\nu}{2}|\eta|^2$ with a fixed but arbitrary $\nu > 0$. To that extent let

$$\begin{aligned} \psi : \mathbb{R}^M \times \mathbb{R} \times \Sigma_0^N &\to \overline{\mathbb{R}}, \\ (p, \beta, \eta) &\mapsto \pi(\beta) + p \cdot \zeta(\beta, \eta) + \tfrac{\nu}{2}|\eta|^2. \end{aligned}$$

Proposition 3.1. *$\psi(p, \beta, \eta)$ is (affine) linear in p and strictly convex in (β, η) for $p \in G^M$.*

Proof. π is strictly convex in β and $\frac{\nu}{2}$ is strictly convex in η. ζ_i is convex as of proposition A.1 and so is $p \cdot \zeta$ by non-negativity of p_i for $i = 1, \dots, M$. □

For $p \in G^M$, ψ is a convex combination of strictly convex functions. This has several consequences which are exploited throughout this work, mostly in terms of properties of functionals incorporating ψ and relying on these properties pointwise almost everywhere.

We have

$$\begin{aligned}
\nabla\pi : \mathbb{R} &\to \overline{\mathbb{R}}, \\
\beta &\mapsto \begin{cases} -c_v/\beta & \text{if } \beta < 0, \\ \infty & \text{else,} \end{cases} \\
\nabla_1\zeta_i : \mathbb{R} \times \Sigma_0^N &\to \mathbb{R}, \\
(\beta, \eta) &\mapsto -\sigma_{1,i}/\sigma_{0,i}, \\
\nabla_2\zeta_i : \mathbb{R} \times \Sigma_0^N &\to \Sigma_1^N, \\
(\beta, \eta) &\mapsto (\tilde{\eta}_{i,j}/\sigma_{0,i})_{j=1}^N
\end{aligned}$$

and we write $\nabla\zeta = (\nabla_1\zeta, \nabla_2\zeta) = (\nabla_1\zeta_i, \nabla_2\zeta_i)_{i=1}^M$. Then

$$\begin{aligned}
\nabla_1\psi(p, \beta, \eta) &= \zeta(\beta, \eta), \\
\nabla_2\psi(p, \beta, \eta) &= \nabla\pi(\beta) + p \cdot \nabla_1\zeta(\beta, \eta), \\
\nabla_3\psi(p, \beta, \eta) &= p \cdot \nabla_2\zeta(\beta, \eta) + \eta.
\end{aligned}$$

3.3.2. Massieu potential for fixed concentrations

Let ρ_i denote the convex conjugate of the pure phase entropy density s_i for fixed c, i.e. $\rho_i(\beta) = (s_i(\cdot, c))^*(\beta)$, where a direct calculation analogous to the one in section 2.4.1 allows to derive an explicit fundamental equation for each $i = 1, \ldots, M$. By linearly interpolating the phase variable in analogy to section 3.3.1, we obtain the potential density

$$\rho(p, \beta) = \begin{cases} -c_v \log(-\beta) - c_m p \cdot (\beta Lc + \tilde{L}c) & \text{if } \beta < 0 \\ \infty & \text{else} \end{cases}. \tag{3.16}$$

Here, $Lc, \tilde{L}c \in \mathbb{R}^M$ are the latent heats resp. latent heats reduced by melting temperatures for each phase $i = 1, \ldots, M$. The notation incorporating c does not allow for it to be variable, but serves as a reminder that this expression allows to deal with the single-component case as well as multiple-fixed-concentrations cases alike and arises as a special case by restriction of the more general ψ_{ideal}. Also, it avoids additional notation and we expect it to be obvious from the context whether c is variable or not. c_v, c_m are positive constants like before. We omitted all additional constant contributions to ρ arising from the deduction process of its fundamental form for brevity.

3.4. Multi-component problem in RGCP form

We now write down a closed weak formulation of the model postulated in equations (3.12) to (3.15a). By definition of the subdifferential inclusion we obtain the following continuous partial differential inequality for a non-isothermal multi-phase multi-component problem in reduced grand canonical potential form.

Problem 3.1. *Find the phase field* $p \in H^1(I, L^2(\mathbb{R}^M)) \cap L^2(I, H^1(\mathbb{R}^M))$*, the negative inverse temperature density* $\beta \in H^1(I, L^2(\mathbb{R}^-)) \cap L^2(I, H^1(\mathbb{R}^-))$*, and the reduced chemical potentials* $\eta \in H^1(I, L^2(\Sigma_0^N)) \cap L^2(I, H^1(\Sigma_0^N))$ *such that*

$$p(0,\cdot) = \overleftarrow{p}, \qquad \beta(0,\cdot) = \overleftarrow{\beta}, \qquad \eta(0,\cdot) = \overleftarrow{\eta} \tag{3.17}$$

holds with given initial conditions $\overleftarrow{p} \in L^2(G^M)$*,* $\overleftarrow{\beta} \in L^2(\mathbb{R}^-)$*,* $\overleftarrow{\eta} \in L^2(\Sigma_0^N)$ *and*

$$0 \leq \chi_{\mathcal{G}^M}(p') - \chi_{\mathcal{G}^M}(p) + (p_{kin}\varepsilon\partial_t p, p' - p) + (\nabla \mathrm{G}_\varepsilon(p), p' - p)_{H^1} - (\nabla_1 \hat{\psi}, p' - p), \tag{3.18a}$$

$$0 = -(\partial_t \nabla_2 \hat{\psi}, \beta') - (\kappa \nabla\beta, \nabla\beta') - (\beta_{00}(\beta - \beta_\partial), \beta')_\partial + (\beta_{src}, \beta'), \tag{3.18b}$$

$$0 = -(\partial_t \nabla_3 \hat{\psi}, \eta') - (\mathrm{m}\nabla\eta, \nabla\eta') \tag{3.18c}$$

for all test functions $p' \in H^1(\mathbb{R}^M), \beta' \in H^1(\mathbb{R}), \eta' \in H^1(\Sigma_0^N)$ *with smooth reduced grand canonical potential density contributions* $\nabla_i \hat{\psi} = \nabla_i \hat{\psi}(p, \beta, \eta)$ *for* $i = 1, 2, 3$*, interface parameter* $\varepsilon > 0$ *, kinetic phase coefficient* $p_{kin} = p_{kin}(p, \nabla p) > 0$*, and Fréchet differentiable interface energy functional* $\mathrm{G}_\varepsilon(p)$*, as well as source term* β_{src}*, boundary negative inverse temperature* β_∂ *with coefficient* $\beta_{00} > 0$*, and diffusivity coefficients* $\kappa(p, \beta, \eta) > 0$ *and* $\mathrm{m} = \mathrm{m}(p, \beta, \eta) \in \mathbb{R}^{n \times n}$ *s.p.s.-d.*

3.4.1. Existence of solutions

Weak solutions to the system of problem 3.1 have been shown to exist with $\beta_{src} = 0$ under additional assumptions and slightly different regularity conditions for p, β, η and the parametrizations of ψ.

Theorem 3.1. *There exist solutions to problem 3.1 if sufficient bounds and regularity conditions are met for the initial data and the coefficient functions.*

We do not present a full proof here and refer to Stinner 2007, Theorem 3.1-3 instead for details, also stating precisely the additional conditions. The proof for the linear growth in η is tackled by approximating it with functions with scaled quadratic regularization in η and letting their scaling go to 0. Quadratic terms are also used to

tackle the logarithmic growth in β by approximating it with functions which continue the logarithm with quadratic tails outside of some interval determined by the slope range $[s, 1/s], s > 0$ and letting $s \to 0$.

Note that the theorem does not include reduced grand canonical bulk densities that are of both, logarithmic growth in β and linear growth in η which is why we shy away from incorporating ψ_{ideal} and consider the regularized ψ instead with $\nu > 0$. Furthermore, the smoothness assumptions on the Ginzburg–Landau contributions exclude the incorporation of obstacle potentials and as such the above existence result does not apply to the more general subdifferential inclusion case ad-hoc.

The work of Stinner 2007 also motivates some other restrictive modeling decisions, like e.g. disallowing mass-related energy transport (equation (3.9a) is independent of $\delta_c \tilde{F}_S$) and enforcing thermal exchange of the system with its surrounding ($\beta_\partial, \kappa > 0$).

Note that in our case of ψ with logarithmic growth in β, existence of a solution to problem 3.1 implies $\beta < 0$ almost everywhere even if not explicitly required.

3.4.2. Thermodynamic consistency

From a modeling point of view, the derivation of the system is such that it is thermodynamically consistent in the sense of adherence to the fundamental laws of thermodynamics, in particular the first and second one as follows. To this extent we consider in addition to F_Ψ the functionals

$$E_\Psi(p, \beta, \eta) = \int e = \int \nabla_2 \hat{\psi}(p, \beta, \eta), \tag{3.19a}$$

$$C_\Psi(p, \beta, \eta) = \int c = \int \nabla_3 \hat{\psi}(p, \beta, \eta) \tag{3.19b}$$

to capture the total internal energy as well as the total chemical masses in terms of the natural variables of the reduced grand canonical potential by equation (3.10). Since our system is not necessarily isolated energetically, we have to account for the interaction with the environment by

$$\Psi_\partial(p, \beta, \eta) = (\beta_{00}(\beta - \beta_\partial), \beta)_\partial. \tag{3.20}$$

Principally, the underlying gradient flow structure of the model provides the thermodynamical consistence (and Lyapunov stability) in terms of F_Ψ, E_Ψ, C_Ψ after pointwise transformation of thermodynamical potential densities $-s$ and ψ. For a more thorough investigation of the implications of gradient flow modeling, we refer to Garcke 2000; Mielke 2011; Peletier 2012. The precise consequences for the system at hand are as follows.

Proposition 3.2 (Nonnegative entropy production)**.** *Let (p, β, η) be a solution to problem 3.1 with $\beta_{src} = 0$ and $p \in C^1([t_0, t_1], H^1(\mathbb{R}^M))$ for $0 < t_0 \leq t_1 \in I$. Then*

$$F_\Psi(p(t), \beta(t), \eta(t)) \geq F_\Psi(p(t_0), \beta(t_0), \eta(t_0)) + \int_{t_0}^{t} \Psi_\partial(p, \beta, \eta) \,\mathrm{d}t \tag{3.21}$$

for all $t \in [t_0, t_1]$.

Proof. We have $p \in \mathcal{G}^M$ almost everywhere in $[t_0, t_1]$. Test equation (3.18a) with $p(t-\tau), \tau \neq 0$, divide by τ and let $\tau \searrow 0$; test equation (3.18b) with β and equation (3.18c) with η to obtain

$$(p_{\mathrm{kin}} \varepsilon \partial_t p, \partial_t p) \leq (\nabla_1 \hat{\psi}(p, \beta, \eta), \partial_t p) - (\nabla \mathrm{G}_\varepsilon(p), \partial_t p)_{H^1} \tag{3.22a}$$

$$(\kappa \nabla \beta, \nabla \beta) = -(\partial_t \nabla_2 \hat{\psi}(p, \beta, \eta), \beta) - (\beta_{00}(\beta - \beta_\partial), \beta)_\partial \tag{3.22b}$$

$$(\mathrm{m} \nabla \eta, \nabla \eta) = -(\partial_t \nabla_3 \hat{\psi}(p, \beta, \eta), \eta) \tag{3.22c}$$

for almost all t. As the left hand side expressions are all quadratics, this implies nonnegativity of the right hand side terms of equation (3.22). On the other hand, the thermodynamical bulk functional as of equation (3.11a) implies

$$\begin{aligned} \partial_t S_\Psi(p, \beta, \eta) &= \partial_t [\textstyle\int \hat{\psi}(p, \beta, \eta) - (\nabla_2 \hat{\psi}(p, \beta, \eta), \beta) - (\nabla_3 \hat{\psi}(p, \beta, \eta), \eta)] \\ &= (\partial_t p, \nabla_1 \hat{\psi}(p, \beta, \eta)) - (\partial_t \nabla_2 \hat{\psi}(p, \beta, \eta), \beta) - (\partial_t \nabla_3 \hat{\psi}(p, \beta, \eta), \eta). \end{aligned}$$

Consequently, adding up equation (3.22) yields

$$\partial_t \tilde{F}_\Psi(p, \beta, \eta) = \delta_t S_\Psi(p, \beta, \eta) - (\nabla \mathrm{G}_\varepsilon(p), \partial_t p)_{H^1} \geq \Psi_\partial(p, \beta, \eta)$$

and integrating over $[t_0, t]$ yields the claim. □

Proposition 3.3 (Conservation of mass and energy)**.** *Let (p, β, η) be a solution to problem 3.1 with $\beta_{src} = 0$. Then*

$$E_\Psi(p(t_1), \beta(t_1), \eta(t_1)) = E_\Psi(p(t_0), \beta(t_0), \eta(t_0)) - \int_{t_0}^{t_1} \Psi_\partial(p, \beta, \eta) \,\mathrm{d}t, \tag{3.23a}$$

$$C_\Psi(p(t_1), \beta(t_1), \eta(t_1)) = C_\Psi(p(t_0), \beta(t_0), \eta(t_0)) \tag{3.23b}$$

for almost all $t_0 \leq t_1 \in I$.

Proof. Test equation (3.18b) with $\beta' = 1$ and equation (3.18c) with the orthogonal projection of the i-the Euclidean basis vector in $\mathbb{R}^N$ to Σ_0^N, i.e. with $\eta' = P_0^N e_i^N = e_i^N - \mathbb{1}^N/N$ for $i = 1, \ldots, N$. The constant nature of the test functions has many

terms vanishing: the H^{-1} contributions due to spatial homogeneity and the projective contributions due to temporal uniformity. We obtain

$$0 = \int -\partial_t \nabla_2 \hat{\psi}(p, \beta, \eta) - \Psi_\partial(z) \tag{3.24a}$$

$$0 = \int -\partial_t \nabla_3 \hat{\psi}(p, \beta, \eta) \cdot e_i^N, \tag{3.24b}$$

for $i = 1, \dots, N$ where integration over $[t_0, t_1]$ yields the claim. □

3.5. Penrose–Fife type model

For the special case $N = 1$ we have $\eta = 0$, $c = 1$. The incorporation of ρ as introduced in section 3.3.2 in lieu of ψ allows to rule out the mass conservation equation. Its partial derivatives are significantly simpler to denote and dealt with than their more general ψ-counterparts. As a consequence we replace their occurrences directly by their respective expressions in the upcoming problem formulation.

The arising partial differential equations coincide with the model considered in Gräser, Kahnt, and Kornhuber 2016. Therein the transition to inverse temperature was made using the same monotone relationships that are inherent to the strictly convex thermodynamical potentials without making the explicit detour over the reduced grand canonical potential formulation and afterwards reducing the complexity by assuming constant concentrations. The temperature θ in that work transfers to this work by $\beta = -\theta^{-1}$.

Problem 3.2. *Find the phase field $p \in H^1(I, L^2(\mathbb{R}^M)) \cap L^2(I, H^1(\mathbb{R}^M))$ and the negative inverse temperature density $\beta \in H^1(I, L^2(\mathbb{R}^-)) \cap L^2(I, H^1(\mathbb{R}^-))$ such that*

$$p(0, \cdot) = \overleftarrow{p}, \qquad \beta(0, \cdot) = \overleftarrow{\beta}$$

holds with given initial conditions $\overleftarrow{p} \in L^2(G^M)$ and $\overleftarrow{\beta} \in L^2(\mathbb{R}^-)$,

$$0 \leq (p_{kin}\varepsilon\partial_t p + c_m(\beta Lc + \widetilde{L}c), p' - p) + (\nabla \mathrm{G}_\varepsilon(p), p' - p)_{H^1} + \chi_{\mathcal{G}^M}(p') - \chi_{\mathcal{G}^M}(p), \tag{3.25a}$$

$$0 = (c_m \partial_t p \cdot Lc - c_v \partial_t \beta/\beta^2, \beta') - (\kappa \nabla \beta, \nabla \beta') - (\beta_{00}(\beta - \beta_\partial), \beta')_\partial - (\beta_{src}, \beta') \tag{3.25b}$$

for all test functions $p' \in H^1(\mathbb{R}^M)$, $\beta \in H^1(\mathbb{R})$, interface parameter $\varepsilon > 0$, kinetic phase coefficient $p_{kin} > 0$, and Fréchet differentiable interface energy functional $\mathrm{G}_\varepsilon(p)$, as well as source term β_{src}, boundary negative inverse temperature β_∂ with coefficient $\beta_{00} > 0$, and diffusivity coefficient $\kappa(p, \beta) > 0$.

The resulting partial differential system is a generalization of the well-established, two-phase Penrose–Fife model (Penrose and Fife 1990; Brokate and Sprekels 1996) to multiple components. The general existence result (theorem 3.1) as well as the thermodynamic consistency properties (propositions 3.2 and 3.3) carry over.

Note that the same approach could also be applied for the case $N > 1$ in a setting where the mass (related) transport can be ignored, e.g. since the dynamics are very slow compared to the time scale of interest ($\mathrm{m} \approx 0$). In this case the concentrations of the chemical components become constant in time ($c(t) = c(t_0)$ a.e.). Then the reduced chemical potentials η are not necessarily constant in time as well as they depend on temperature resp. inverse negative temperature, too. Nevertheless, their variation from the initial reduced chemical potentials as obtained from the initial chemical concentration is a function of the negative inverse temperature. For simplicity of presentation, this reduced setting is not considered explicitly here.

3.6. Problems on thin domains

Additionally we want to consider problems with reduced spatial dimension due to negligible effects in one space direction. This might be motived by a thin domain. To this end consider $\Omega = \Omega' \times [0, H], 0 < H$. We think of the problem to be *thin* in the sense that variations of all quantities normal to Ω' can be neglected and that the boundary conditions on top of the thin domain coincide with their spatial counterparts on the bottom. Aforementioned quantities with negligible normal variation include initial data, boundary conditions on $\partial\Omega' \times [0, H]$, fluxes and all coefficients. Consequently, the solution will inherit this property as well. Precisely, assume that

$$\begin{aligned} \nabla p_i \cdot g = \nabla \overleftarrow{p}_i \cdot g = 0, \quad & i = 1, \dots, M, \\ \nabla \beta \cdot g = \nabla \overleftarrow{\beta} = 0, & \\ \nabla \eta_j \cdot g = \nabla \overleftarrow{\eta}_j = 0, \quad & j = 1, \dots, N, \\ \nabla \beta_{src} \cdot g = 0 & \end{aligned}$$

almost everywhere on $\Omega \times I$ with $g = (\mathbb{0}_{d-1}, 1) \in \Omega' \times [0, H]$. Assume further that

$$\begin{aligned} \tilde{J}_i \cdot n = 0 \quad \text{on } \partial\Omega \times H, \\ \tilde{J}_i((\cdot, 0), t) \cdot n(\cdot, 0) = \tilde{J}_i((\cdot, H), t) \cdot n(\cdot, H) \quad \text{on } \Omega' \end{aligned}$$

almost everywhere and for almost every $t \in I$ where n the outward normal w.r.t. Ω, and $\tilde{J}_i = J_i(p, \beta, \eta) : \partial(\Omega' \times [0, H]) \times I \to \mathbb{R}^d$ for all $i = 0, \dots, N$.

With these assumptions we can collapse the domain *vertically* by its height H, and, since it suffices to test with vertically constant test functions, factor out H from all

bulk integrals. For the boundary integral in negative inverse temperature we have

$$(\beta_{00}(\beta - \beta_\partial), \beta')_{\partial(\Omega)} = (2\beta_{00}(\beta - \beta_\partial, \beta'))_{\Omega'}$$

without any additional boundary contribution and set

$$\begin{aligned}\beta'_{00} &= \tfrac{2}{H}\beta_{00}\\ \beta'_{src} &= \beta_{src} - \tfrac{2}{H}\beta_{00}\beta_\partial\end{aligned}$$

on $\Omega' \times \{0\}$ which we identify with Ω'. As a consequence we can write the following thin-film derivate for this simplified setting w.r.t. the reduced space Ω'.

With the assumptions above, problem 3.1 reduces to the following.

Problem 3.3. *Find the phase field $p \in H^1(I, L^2(\Omega', \mathbb{R}^M)) \cap L^2(I, H^1(\Omega', \mathbb{R}^M))$, negative inverse temperature density $\beta \in H^1(I, L^2(\Omega', \mathbb{R})) \cap L^2(I, H^1(\Omega', \mathbb{R}))$, and reduced chemical potentials $\eta \in H^1(I, L^2(\Omega', \mathbb{R}^N)) \cap L^2(I, H^1(\Omega', \Sigma_0^N))$ such that*

$$p(0, \cdot) = \overleftarrow{p}, \qquad \beta(0, \cdot) = \overleftarrow{\beta}, \qquad \eta(0, \cdot) = \overleftarrow{\eta}$$

holds with given initial conditions $\overleftarrow{p} \in L^2(\Omega', G^M)$, $\overleftarrow{\beta} \in L^2(\Omega', \mathbb{R}^-)$, $\overleftarrow{\eta} \in L^2(\Omega', \Sigma_0^N)$ and

$$0 \leq (p_{kin}\varepsilon\partial_t p, p' - p) - (\nabla_1\hat{\psi}, p' - p) + (\nabla \mathrm{G}_\varepsilon(p), p' - p)_{H^1} + \chi_{\mathcal{G}^M}(p') - \chi_{\mathcal{G}^M}(p), \tag{3.26a}$$

$$0 = (-\partial_t \nabla_2\hat{\psi} - \beta'_{00}\beta, \beta') - (\kappa\nabla\beta, \nabla\beta') + (\beta'_{src}, \beta'), \tag{3.26b}$$

$$0 = (-\partial_t \nabla_3\hat{\psi}, \eta') - (\mathrm{m}\nabla\eta, \nabla\eta') \tag{3.26c}$$

for all test functions $p' \in H^1(\Omega', \mathbb{R}^M), \beta' \in H^1(\Omega', \mathbb{R}), \eta' \in H^1(\Omega', \Sigma_0^N)$.

Similarly, for fixed concentrations, problem 3.2 reduces to the following.

Problem 3.4. *Find the phase field $p \in H^1(I, L^2(\Omega', \mathbb{R}^M)) \cap L^2(I, H^1(\Omega', \mathbb{R}^M))$ and negative inverse temperature density $\beta \in H^1(I, L^2(\Omega', \mathbb{R})) \cap L^2(I, H^1(\Omega', \mathbb{R}))$ such that*

$$p(0, \cdot) = \overleftarrow{p}, \qquad \beta(0, \cdot) = \overleftarrow{\beta}$$

holds with given initial conditions $\overleftarrow{p} \in L^2(\Omega', G^M)$, $\overleftarrow{\beta} \in L^2(\Omega', \mathbb{R}^-)$, and

$$0 \leq (p_{kin}\varepsilon\partial_t p, p' - p) + (\beta L + \widetilde{L}, p' - p) + (\nabla \mathrm{G}_\varepsilon(p), p' - p)_{H^1} + \chi_{\mathcal{G}^M}(p') - \chi_{\mathcal{G}^M}(p), \tag{3.27a}$$

$$0 = (-\partial_t\partial_\beta\psi - \beta_{00'}\beta, \beta') - (\kappa\nabla\beta, \nabla\beta') + (\beta'_{src}, \beta') \tag{3.27b}$$

for all test functions $p' \in H^1(\Omega', \mathbb{R}^M), \beta' \in H^1(\Omega', \mathbb{R}), \eta' \in H^1(\Omega', \Sigma_0^N)$.

All existence statements, conservative laws and entropy increase properties carry over in straightforward fashion. For this reason, the analysis in the remainder of this work is only formulated in terms of problem 3.1 and 3.2.

4. Semi-discrete non-isothermal multi-phase field systems

Rothe's method As our problems incorporate a phase field parameter whose evolution is driven by a Ginzburg–Landau functional of obstacle type, the resulting order parameter are mostly constant in space and exhibit relatively narrow regions of high spatial variance. The fact that these narrow regions move over time motivates the use of time-dependent, locally refined spatial grids. As a result, it is convenient to use Rothe's method, cf. Bornemann 1990; Deuflhard and Weiser 2011. Hence, we discretize in time first. The resulting spatial problems subsequently are discretized in space, independent of each other.

Ginzburg–Landau splitting In light of the well-known stiffness of the non-linear parabolic system of equations, we avoid using a purely explicit time discretization scheme. Equation (3.18a) is an anisotropic multi-phase Allen–Cahn problem. Gräser, Kornhuber, and Sack 2013 showed that unconditional stability cannot be expected for fully implicit time discretizations. Semi-implicit time discretizations based on splittings of the respective Ginzburg–Landau contribution allow to trade unconditional stability for a potential loss of accuracy, cf. Blank et al. 2012 or Bartels 2015, section 6.3.1. We assume a splitting $G_\varepsilon = \mathrm{G}_{\mathrm{im}} + \mathrm{G}_{\mathrm{ex}}$ with Fréchet-differentiable addends and $(\nabla \mathrm{G}_{\mathrm{im}}(\cdot), \cdot)_{H^1}$ a positive semi-definite, symmetric bilinear form that satisfies

$$G_\varepsilon(p') - G_\varepsilon(p) + (\nabla \mathrm{G}_{\mathrm{im}}(p) + \nabla \mathrm{G}_{\mathrm{ex}}(p'), p - p')_{H^1} \geq 0 \tag{A4.1a}$$

for all $p, p' \in \mathcal{G}^M$ to simplify the subsequent analysis. Such splittings usually amount to a convex-concave splitting though additional non-convex contributions to G_{im} can eventually be compensated, e.g. by mass terms originating from the time derivative $\partial_t p$ and involving e.g. a time step constraint for unconditional stability, cf. Gräser, Kornhuber, and Sack 2013.

A corresponding splitting for the isotropic, quadratic interaction potential arising from the choice (2.6) is given by $\mathrm{G}_{\mathrm{im}}(p) = \frac{\varepsilon}{2}\|\nabla p\|^2$, $\mathrm{G}_{\mathrm{ex}}(p) = -\frac{1}{2\varepsilon}\|p\|^2$.

Semi-implicit time-discretization We derive consistent discretizations of the continuous models with Euler-type discretizations in time and finite elements in space. We

aim at inheriting the structure-defining properties as of propositions 3.2 and 3.3 from the continuous modelling.

Let $0 = t_0 < t_1 < \ldots < t_{n_{\max}} = t_{\max}$ a partition of I with uniform step size

$$0 < \tau = t_n - t_{n-1}$$

for $n = 1, \ldots, n_{\max}$ and given $n_{\max} \in \mathbb{N}$.

We approximate the time derivatives by backward finite differences with step size $\tau > 0$ while freezing all coefficients and taking the (concave) Ginzburg–Landau contribution $\mathrm{G}_{\mathrm{ex}}(p)$ explicitly.

4.1. Multi-component problem in RGCP form

From problem 3.1 we obtain the semi-discrete partial differential inequality for a non-isothermal multi-phase multi-component problem in reduced grand canonical potential form.

Problem 4.1. *Find* $(p^n, \beta^n, \eta^n) \in H^1(\mathbb{R}^M) \times H^1(\mathbb{R}^-) \times H^1(\Sigma_0^N)$ *for* $n = 1, \ldots, n_{\max}$ *such that*

$$z^0 = \overleftarrow{z}$$

holds with given initial conditions $\overleftarrow{z} = (\overleftarrow{p}, \overleftarrow{\beta}, \overleftarrow{\eta}) \in L^2(G^M) \times L^2(\mathbb{R}^-) \times L^2(\Sigma_0^N)$ *and*

$$\begin{aligned}
0 &\leq (p_{kin}\tfrac{\varepsilon}{\tau}(p^n - p^{n-1}), p' - p^n) - (\nabla_1\hat{\psi}^n, p' - p^n) + (\mathrm{G}'_\varepsilon, p' - p^n)_{H^1} + \chi(p') - \chi(p^n),\\
0 &= (-\nabla_2\hat{\psi}^n + \nabla_2\hat{\psi}^{n-1}, \beta') - (\tau\kappa\nabla\beta^n, \nabla\beta') + (\tau\beta_{src}, \beta') - (\tau\beta_{00}(\beta^n - \beta_\partial), \beta')_\partial,\\
0 &= (-\nabla_3\hat{\psi}^n + \nabla_3\hat{\psi}^{n-1}, \eta') - (\tau\mathrm{m}\nabla\eta^n, \nabla\eta')
\end{aligned}$$

for all test functions $(p', \beta', \eta') \in H^1(\mathbb{R}^M) \times H^1(\mathbb{R}) \times H^1(\Sigma_0^N)$ *with reduced grand canonical potential densities* $\nabla_i\hat{\psi}^n = \nabla_i\hat{\psi}(p^n, \beta^n, \psi^n)$*, interface parameter* $\varepsilon > 0$ *and step size* $\tau > 0$*, kinetic phase coefficients* $p_{kin} = p_{kin}(p^{n-1}) > 0$*, interface energy contributions* $\mathrm{G}'_\varepsilon = \nabla\mathrm{G}_{\mathrm{im}}(p^n) + \nabla\mathrm{G}_{\mathrm{ex}}(p^{n-1})$*, as well as source term* $\beta_{src} = \beta_{src}(t^n)$*, boundary negative inverse temperature* $\beta_\partial = \beta_\partial(t^n)$ *with coefficient* $\beta_{00} \geq 0$*, and diffusivity coefficients* $\kappa = \kappa(p^{n-1}, \beta^{n-1}, \eta^{n-1}) > 0, \mathrm{m} = \mathrm{m}(p^{n-1}, \beta^{n-1}, \eta^{n-1}) \in \mathbb{R}^{N\times N}$ *with* $\mathbb{1}_N \in \ker \mathrm{m}$ *a.e.*

The semi-discrete problem exhibits a sequence of stationary problems. We look at a single time step at a time and simplify our notation accordingly. We no further explicitly denote the time step for frozen or solution-independent coefficients. For the

variables p, β, η we drop the superscripts for the current time step n and replace the superscripts for the previous time step $n-1$ by $(.)^{\text{old}}$.

As the subsequent analysis makes heavy use of Lagrange duality theory for saddle point problems, we adjust our notation accordingly. The potentials β, η form the dual variable and we write

$$\begin{aligned} y &= (\beta, \eta), \\ Y &= \mathbb{R} \times \Sigma_0^N. \end{aligned}$$

Assumptions We make the following assumptions.

The initial conditions (and the subsequent semi-discrete time iterates, as will be shown) fulfill

$$p^{\text{old}} \in L^2(G^M), \tag{A4.2a}$$
$$y^{\text{old}} \in L^2(Y), \tag{A4.2b}$$
$$1/\beta^{\text{old}} \in L^2(\mathbb{R}), \tag{A4.2c}$$
$$-\beta^{\text{old}} > 0 \text{ a.e.} \tag{A4.2d}$$

and the thermal boundary conditions satisfy the regularity assumptions

$$\beta_{00} \in C^1(\partial\Omega), \tag{A4.3a}$$
$$\beta_{\partial} \in C^1(\partial\Omega), \tag{A4.3b}$$

as well as the bounds

$$\beta_{00,\text{-}} \leq \beta_{00}(\partial\xi) \leq \beta_{00,+}, \tag{A4.4a}$$
$$\beta_{\text{bnd,-}} \leq -\beta_{\partial}(\partial\xi) \leq \beta_{\text{bnd},+}, \tag{A4.4b}$$

for almost all $\partial\xi \in \partial\Omega$ with positive constants $0 < \beta_{00,\text{-}}, \beta_{00,+}, \beta_{\text{bnd,-}}, \beta_{\text{bnd},+}$.

The source term shall also be bounded, i.e.

$$\beta_{\text{src,-}} \leq \beta_{src} \leq \beta_{\text{src},+}. \tag{A4.5a}$$

For the mass terms we assume the bounds (and list ν for completeness)

$$p_{\text{-}}\|p\|^2 \leq (p_{\text{kin}}p, p) \leq p_{+}\|p\|^2, \tag{A4.6a}$$
$$\nu\|\eta\|^2 = (\nu\eta, \eta) \tag{A4.6b}$$

as well as for the Laplace terms

$$\mathrm{G}_{\text{-}}\|\nabla p\|^2 \leq (\nabla \mathrm{G}_{\mathrm{im}}(p), p)_{H^1} \leq \mathrm{G}_{+}\|\nabla p\|^2, \tag{A4.7a}$$
$$\kappa_{\text{-}}\|\nabla \beta\|^2 \leq (\kappa \nabla \beta, \nabla \beta) \leq \kappa_{+}\|\nabla \beta\|^2, \tag{A4.7b}$$
$$\mathrm{m}_{\text{-}}\|\nabla \eta\|^2 \leq (\mathrm{m} \nabla \eta, \nabla \eta) \leq \mathrm{m}_{+}\|\nabla \eta\|^2, \tag{A4.7c}$$

for all $p \in H^1(\mathbb{R}^M), \beta \in H^1(\mathbb{R}), \eta \in H^1(\Sigma_0^N)$ with positive constants

$$0 < p_{\text{-}}, p_{+}, \nu, \mathrm{G}_{\text{-}}, \mathrm{G}_{+}, \kappa_{\text{-}}, \kappa_{+}, \mathrm{m}_{\text{-}}, \mathrm{m}_{+}.$$

We introduce the bilinear and linear forms

$$\begin{aligned}
a_p(p, p') &= (p_{\mathrm{kin}} \tfrac{\varepsilon}{\tau} p, p') + (\nabla \mathrm{G}_{\mathrm{im}}(p), p')_{H^1} \\
c(y, y') &= (\tau \kappa \nabla \beta, \nabla \beta') + (\tau \mathrm{m} \nabla \eta, \nabla \eta') + (\tau \beta_{00} \beta, \beta')_{\partial} + (\nu \eta, \eta'), \\
f_p(p') &= (p_{\mathrm{kin}} \tfrac{\varepsilon}{\tau} p^{\mathrm{old}}, p') - (\nabla \mathrm{G}_{\mathrm{ex}}(p^{\mathrm{old}}), p')_{H^1}, \\
f_y(y') &= (-\nabla_2 \psi(p^{\mathrm{old}}, y^{\mathrm{old}}), y') - (\tau \beta_{src}, \beta') - (\tau \beta_{00} \beta_{\partial}, \beta')_{\partial}
\end{aligned}$$

which allows to equivalently write each stationary subproblem of problem 4.1 as follows.

Problem 4.2. *Find $p \in H^1(\mathbb{R}^M)$, $y \in H^1(Y)$ such that $\beta < 0$ a.e. and*

$$f_p(p' - p) \leq a_p(p, p' - p) + \chi(p') - \chi(p) - (\hat{\zeta}(y), p' - p), \tag{4.8a}$$
$$f_y(y') = -(\nabla \hat{\pi}(y) + p \cdot \nabla \hat{\zeta}(y), y') - c(y, y') \tag{4.8b}$$

for all test functions $p' \in H^1(\mathbb{R}^M)$, $y' \in H^1(Y)$.

As a consequence of the assumptions above the bilinear forms a, c are continuous and coercive on $H^1(\mathbb{R}^M)$ and $H^1(Y)$, respectively, i.e.

$$a_{\mathrm{ell}}\|p\|^2 \leq a_p(p, p) \leq a_{\mathrm{cnt}}\|p\|^2, \tag{4.9a}$$
$$c_{\mathrm{ell}}\|y\|^2 \leq c(y, y) \leq c_{\mathrm{cnt}}\|p\|^2, \tag{4.9b}$$

with positive constants $0 < a_{\mathrm{ell}}, a_{\mathrm{cnt}}, c_{\mathrm{ell}}, c_{\mathrm{cnt}}$ by the trace theorem and where, for the coercivity of c, we use Gräser 2015, Proposition 2. Similarly, the linear forms f_p, f_y are continuous as

$$|f_p(p)| \leq f_{p,+}\|p\|, \tag{4.10a}$$
$$|f_y(y)| \leq f_{y,+}\|y\|, \tag{4.10b}$$

with positive constants $0 < f_{p,+}, f_{y,+}$.

We show that finding a solution to problem 4.2 can equivalently be done by minimizing a functional for the dual variable y and incorporating an associated and uniquely defined primal variable $\hat{p}(y)$. We proceed with the following steps: Show that for a fixed dual variable, the primal variable is uniquely obtained as a minimizer for a functional associated with equation (4.8a). Use this to construct the dual Schur complement and show that the resulting problem associated with equation (4.8b) admits a unique solution.

4.1.1. Existence and uniqueness of the phase field

We have the following property for the superposition operator $\hat{\zeta}$.

Proposition 4.1. *The Nemyckii operator $\hat{\zeta} : L^2(Y) \to L^2(\mathbb{R}^M)$ is bounded.*

Proof. By growth condition A.1a and application of Zeidler 1990, Proposition 26.6. □

As a result of proposition 4.1, it is meaningful to consider the functional

$$\begin{aligned} Z : L^2(\mathbb{R}^M) \times L^2(Y) &\to \mathbb{R}, \\ (p, y) &\mapsto (\hat{\zeta}(y), p). \end{aligned}$$

Let the functional

$$\begin{aligned} \varphi : H^1(\mathbb{R}^M) &\to \overline{\mathbb{R}}, \\ p &\mapsto \tfrac{1}{2} a_p(p, p) + \chi_{\mathcal{G}^M}(p). \end{aligned}$$

The optimization functional associated with equation (4.8a) for arbitrary but fixed $y \in L^2(Y)$ is

$$\begin{aligned} H^1(\mathbb{R}^M) &\to \overline{\mathbb{R}}, \\ p &\mapsto \varphi(p) - f_p(p) - Z(y, p) \end{aligned}$$

and its (to be shown) respective minimizer is denoted by

$$\begin{aligned} \hat{p} : L^2(Y) &\to H^1(G^M), \\ y &\mapsto \operatorname{argmin}\{\varphi(p) - f_p(p) - Z(y, p) \mid p \in H^1(\mathbb{R}^M)\}. \end{aligned}$$

Proposition 4.2. *Let $y \in L^2(Y)$. Then $f_p + Z(y, \cdot) \in L^2(\mathbb{R}^M)' \subset H^1(\mathbb{R}^M)'$.*

Proof. f_p and $Z(y,\cdot)$ are bounded linear functionals on $L^2(\mathbb{R}^M)$. This is implied by assumptions A4.2a and A4.6a as well as Fréchet-differentiability of G_{ex} (see chapter 4) for f_p and by proposition 4.1 for $Z(y,\cdot)$. □

Theorem 4.1. *$\hat{p}$ is well-defined.*

Proof. φ is strictly convex, lower semi-continuous and coercive since $a(\cdot,\cdot)$ is continuous and strongly convex and $\mathcal{G}^M$ is closed and convex. Proposition 4.2 holds. Consequently, the optimization functional is proper, strictly convex, lower semi-continuous and coercive. Existence and uniqueness of the minimizer $\hat{p}(y)$ is then given by proposition 2.2. $\hat{p}(y) \in \mathcal{G}^M$ since the effective domain coincides with $\operatorname{dom} \chi_{\mathcal{G}^M}$. □

By the minimizing property, we have $0 \in \partial(\varphi(\cdot) - f_p - Z(y,\cdot))(\hat{p}(y))$, i.e.

$$\hat{p}(y) = (\partial\varphi)^{-1}(f_p + Z(y,\cdot)) = \partial\varphi^*(f_p + Z(y,\cdot)) \tag{4.11}$$

with $\varphi^* : H^1(\mathbb{R}^M)' \to \overline{\mathbb{R}}$ the convex conjugate of φ. By definition of the convex subdifferential, this is equivalent to $\hat{p}$ solving equation (4.8a).

Proposition 4.3. *$\hat{p}$ is Lipschitz-continuous.*

Proof. $\partial\varphi^*$ is Lipschitz-continuous with constant $1/a_{\mathrm{ell}}$ by Goebel and Rockafellar 2008, Corollary 4.3. $\hat{\zeta}$ is Lipschitz with $c_2 = \sum_{i=1}^{M} c_{2,i}$ the sum of the componentwise Lipschitz-constants for ζ_i from equation (A.1c) such that

$$\begin{aligned}
\|\hat{p}(y') - \hat{p}(y)\|_{H^1(\mathbb{R}^M)} &\leq \tfrac{1}{a_{\mathrm{ell}}} \|f_p + Z(y',\cdot) - f_p - Z(y,\cdot)\|_{H^1(\mathbb{R}^M)'} \\
&\leq \tfrac{1}{a_{\mathrm{ell}}} \|Z(y',\cdot) - Z(y,\cdot)\|_{L^2(\mathbb{R}^M)'} \\
&= \tfrac{1}{a_{\mathrm{ell}}} \|\hat{\zeta}(y') - \hat{\zeta}(y)\|_{L^2(\mathbb{R}^M)} \\
&\leq \tfrac{1}{a_{\mathrm{ell}}} c_2 \|y' - y\|_{L^2(Y)}.
\end{aligned}$$

□

4.1.2. Dual Schur-complement formulation

We now replace occurrences of p in equation (4.8b) by $\hat{p}$ to obtain a problem in y only using the relationship in equation (4.11). To that extent we introduce, formally,

$$\begin{aligned}
\nabla r : L^2(Y) &\to L^2(Y), \\
y &\mapsto \nabla\hat{\zeta}(y)\hat{p}(y),
\end{aligned}$$

which is benign in the following sense.

Proposition 4.4. *∇r is well-defined and continuous.*

Proof. Let $C = \sum_{i=1}^{M} |c_{2i}|$ with c_{2i} the constants from equation (A.1b) for each phase $i = 1, \dots, M$. Since $\hat{p} \in \mathcal{G}^M$ we have that

$$\|\nabla r(y)\|^2 \leq \int \left(\sum_{i=1}^{M} |\nabla \hat{\zeta}_i(y)| \hat{p}_i(y) \right)^2 \leq C^2 |\Omega|,$$

which shows that indeed $\nabla r(y) \in L^2(Y)$ for all $y \in Y$. To show continuity, we can appropriately add and subtract a term $\nabla \hat{\zeta}(y) \hat{p}(y')$, use the triangle inequality, proposition 4.3 with Lipschitz constant L_p, and the fact that $\hat{p} \in \mathcal{G}$ to obtain

$$\|\nabla r(y) - \nabla r(y')\| \leq C^2 |\Omega| L_p \|y - y'\| + |\Omega| \|\nabla \hat{\zeta}(y) - \nabla \hat{\zeta}(y')\|$$

for all $y, y' \in Y$ and by growth equation (A.1b) and Zeidler 1990, Proposition 26.6, $\nabla \hat{\zeta}$ is a continuous and bounded Nemyckii operator as well. This proves the claim. □

Now let

$$h' : H^1(Y) \times H^1(Y) \to \overline{\mathbb{R}},$$
$$(y, y') \mapsto \begin{cases} (\nabla \hat{\pi}(y) + \nabla r(y), y') + c(y, y') + f_y(y') & \text{if } \nabla \hat{\pi}(y) \in L^2(\mathbb{R}), \\ \infty & \text{else,} \end{cases}$$

which by theorem 4.1 allows to formulate the following Schur-complement formulation.

Problem 4.3. *Find $(\beta, \eta) = y \in H^1(Y)$ such that $\beta < 0$ a.e. and*

$$h'(y, y') = 0$$

for all $y' \in H^1(Y)$.

Corollary 4.1. *(p, y) solves problem 4.2 iff y solves problem 4.3 and $p = \hat{p}(y)$.*

4.1.3. Existence and uniqueness of the potentials

First of all, we consider the term coupling the equations (4.8a) and (4.8b). To that extent let

$$r : L^2(Y) \to \mathbb{R},$$
$$y \mapsto \varphi^*(f_p + Z(y, \cdot))$$

which is well-defined by proposition 4.2. By convex conjugation and proposition 4.1 we infer the following.

Corollary 4.2. *r is lower semi-continuous.*

Proposition 4.5. *r is strictly convex.*

Proof. Let $t_1 \in (0,1), t_2 = 1 - t_1$ and $y_1 \neq y_2 \in L^2(Y)$ with $y_3 = t_1 y_2 + t_2 y_2$. Then

$$\begin{aligned} t_1 r(y_1) + t_2 r(y_2) - r(y_3) &= t_1 \varphi^*(f_p + Z(y_1, \cdot)) + t_2 \varphi^*(f_p + Z(y_2, \cdot)) \\ &\quad - \varphi^*(f_p + Z(y_3, \cdot)) \\ &\geq t_1 (f_p(\hat{p}(y_3)) + Z(y_1, \hat{p}(y_3)) - \varphi(\hat{p}(y_3)) \\ &\quad + t_2 (f_p(\hat{p}(y_3) + Z(y_2, \hat{p}(y_3)) - \varphi(\hat{p}(y_3))) \\ &\quad - (f_p(\hat{p}(y_3)) + Z(y_3, \hat{p}(y_3)) - \varphi(\hat{p}(y_3)) \\ &= (t_1 \hat{\zeta}(y_1) + t_2 \hat{\zeta}(y_2) - \hat{\zeta}(y_3), \hat{p}(y_3)) > 0 \end{aligned}$$

since $(\hat{p}(y_3))_i \geq 0$ a.e. and ζ_i strictly convex for all $i = 1, \ldots, M$. □

Proposition 4.6. *r is Gâteaux-differentiable with derivative $\nabla r(y)$.*

Proof. $(\nabla r(y), \cdot)$ is a continuous linear functional by proposition 4.4. Equation (4.11) implies

$$\varphi^*(p') \geq \varphi^*(f_p + Z(y, \cdot)) + p'(\hat{p}(y)) - f_p(\hat{p}(y)) - Z(y, \hat{p}(y))$$

for all $p' \in H^1(\mathbb{R}^M)'$. In particular for all $y' \in Y$ inserting $p' = f_p + Z(y', \cdot)$ yields

$$r(y') \geq r(y) + Z(y', \hat{p}(y)) - Z(y, \hat{p}(y))$$

and by non-negativity of $(\hat{p}(y))_i$ a.e. and convexity of ζ_i, $i = 1, \ldots, M$ also

$$Z(y', \hat{p}(y)) - Z(y, \hat{p}(y)) = (\hat{\zeta}(y') - \hat{\zeta}(y), \hat{p}(y)) \geq (\nabla r(y), y' - y)$$

which implies $\nabla r(y) \in \partial r(y)$. Consequently, ∇r is monotone and

$$\begin{aligned} F : L^2(Y) &\to L^2(Y), \\ y &\mapsto y + \nabla r(y) \end{aligned}$$

is strongly monotone. Continuity of F implies that it is a bijection using Deimling 2010, Theorem 11.2. By Brézis 1971, Theorem 2, we deduce that $\nabla r : L^2(Y) \to L^2(Y)'$ is maximal monotone and hence coincides with ∂r. Since r is continuous and finite the claim follows by proposition 2.4. □

Finally r is bounded from below by

$$r(y) \geq f_p(p^{\text{old}}) - a_p(p^{\text{old}}, p^{\text{old}}) - c_0|\Omega| - c_1|\Omega|^{\frac{1}{2}}\|y\| \tag{4.12}$$

for all $y \in Y$ by the linear lower bound of ζ pointwise. The constants c_0, c_1 can be taken as the respective maximum over the constants in equation (A.1a) per phase.

Now we address the non-coupling contributions in equation (4.8b), while taking special care of the logarithmic barrier for the negative inverse temperature β imposed by $\hat{\pi}$. The results resemble the approach of Klein 1997, Chapter 5, where a related problem was investigated. Nevertheless, in our presentation we adhere to the layout of Schiela 2009, Section 4 and 5 despite the differing contextual objective.

To that extent, let

$$\begin{aligned} q : H^1(Y) &\to \mathbb{R}, \\ y &\mapsto \tfrac{1}{2}c(y,y) + f_y(y). \end{aligned}$$

Proposition 4.7. *q is strictly convex, lower semi-continuous, and coercive.*

Proof. Note that we have the bounds equations (4.9b) and (4.10b). Strict convexity follows directly from the strong convexity of c and the linearity of f_y. Lower semi-continuity is implied by the continuity. q is coercive, since the strongly convex contributions dominate the linear terms for $\|y\| \to \infty$. □

Proposition 4.8. *q is Gâteaux-differentiable with derivative $(\nabla q(y), \cdot) = c(y, \cdot) + f_y$.*

Proof. q is even trivially Fréchet-differentiable by the assumptions implying that c and f_y are continuous quadratic and linear forms, respectively, cf. equations (4.9b) and (4.10b). □

Let

$$\begin{aligned} \Pi : L^2(Y) &\to \overline{\mathbb{R}}, \\ y &\mapsto \begin{cases} \int \hat{\pi}(y) & \text{if } \hat{\pi}(y) \in L^1(\mathbb{R}), \\ \infty & \text{else}, \end{cases} \\ h : H^1(Y) &\to \overline{\mathbb{R}}, \\ y &\mapsto q(y) + r(y) + \Pi(y). \end{aligned}$$

Lemma 4.1. *Π is well-defined, strictly convex, and lower semi-continuous.*

Proof. Follows pointwise from the properties of π, cf. Schiela 2009, Proposition 4.3. □

Its subdifferential is single-valued, wherever not empty.

Proposition 4.9.

$$\partial\Pi(y) = \begin{cases} \{(\nabla\hat{\pi}(y), \mathbb{0}^N)\} & \text{if } 1/\beta \in L^2(\mathbb{R}) \text{ and } \beta < 0 \text{ a.e.,} \\ \emptyset & \text{else.} \end{cases}$$

Proof. C.f. Brézis 1971, p. 115, Klein 1997, Lemma 5.3, and Schiela 2009, p. 1009. □

This property is reasonably close to the Gâteaux-differentiability of the other contributions to h to allow establishing an analogue relationship between potential h and its directional derivative h'.

Also, we have the following lower bound implied by the pointwise definition of $\hat{\pi}$.

$$\Pi(y) \geq -c_v|-\textstyle\int 1+\beta| \geq -c_v(|\int -\beta| - |\Omega|) \geq -c_v|\Omega|^{\frac{1}{2}}\|\beta\| + c_v|\Omega| \tag{4.13}$$

Theorem 4.2. *h admits a unique minimizer $y = (\beta, \eta)$ and $\beta < 0$ a.e.in Ω.*

Proof. h is proper, since $h(y^{\text{old}}) < \infty$. h is strictly convex and lower semi-continuous by summing the properties of corollary 4.2, propositions 4.5 and 4.7, and lemma 4.1. W.r.t. coercivity we have

$$h(y) \geq C\|y\|^2_{H^1(Y)} - C'\|y\| - C''$$

with positive constants C, C', C'' by equations (4.9b), (4.10b), (4.12) and (4.13). Consequently the claim holds by proposition 2.2 and $\beta < 0$ a.e. since $h(y)$ is finite. □

Theorem 4.3. *Problem 4.3 has a unique solution.*

Proof. Let y the unique minizer of h. Then

$$0 \in \partial h(y) = \partial(q+r)(y) + \partial\Pi(y)$$

where the sum-rule holds due to Ekeland and Témam 1999, Proposition 5.6 since $(-1, \mathbb{0}^N) \in \operatorname{dom}(q+r) \cap \operatorname{dom}\Pi$ and $q+r$ is continuous on $H^1(Y) \ni (-1, \mathbb{0}^N)$. Also, $q+r$

is Gâteaux-differentiable by propositions 4.6 and 4.8. Furthermore, by proposition 4.9, y in $\operatorname{dom}\partial\Pi$ and hence

$$0 = c(y,\cdot) + f_y + (\nabla r(y),\cdot) + (\nabla\hat{\pi}(y),\cdot) = h'(y,\cdot)$$

which shows existence.

Let $y_1, y_2 \in H^1(Y)$ solutions. Then for $y' = y_1 - y_2$ we have

$$\begin{aligned} 0 &= h'(y_1,y') - h'(y_2,y') \\ &= (\nabla\hat{\pi}(y_1) - \nabla\hat{\pi}(y_2), y') + (\nabla r(y_1) - \nabla r(y_2), y') + c(y',y') \\ &\geq c_v \int \beta'^2/(\beta_1\beta_2) + c_{\text{ell}}\|y'\|^2 \end{aligned}$$

using the monotonicity of ∇r and equation (4.9b). This shows that $\eta_1 = \eta_2$. Since $\beta_1\beta_2 > 0$ a.e. also $\beta' = 0 \Leftrightarrow \beta_1 = \beta_2$ almost everywhere in Ω from the first term. □

Corollary 4.3. *Problem 4.2 has a unique solution.*

4.1.4. Thermodynamical consistency

The proposed time discretization preserves the structural thermodynamical consistency in the way described by the following two propositions.

Proposition 4.10 (Nonnegative entropy production per time step)**.** *Let $z = (p,y)$ a solution to problem problem 4.2 with $\beta_{src} = 0$. Then*

$$F_\Psi(z) \geq F_\Psi(z^{old}) + \tau\Psi_\partial(z). \tag{4.14}$$

Proof. Test equation (4.8a) with $p' = p^{\text{old}}$ and equation (4.8b) with $y' = y$ to obtain

$$\begin{aligned} (p_{\text{kin}}\tfrac{\varepsilon}{\tau}(p^{\text{old}} - p), p^{\text{old}} - p) &\leq (-\nabla_1\hat{\psi}(p,y), p^{\text{old}} - p) + (\mathrm{G}', p^{\text{old}} - p)_{H^1} \\ (\tau \mathrm{m}\nabla y, \nabla y) &= (-\nabla_2\hat{\psi}(p,y) + \nabla_2\hat{\psi}(p^{\text{old}}, y^{\text{old}}), y) - (\tau\beta_{00}(\beta - \beta_\partial), \beta)_\partial \end{aligned}$$

where $\mathrm{G}' = \nabla\mathrm{G}_{\text{im}}(p) + \nabla\mathrm{G}_{\text{ex}}(p^{\text{old}})$ which implies that the sum of the r.h.s. terms is nonnegative. The difference in bulk entropy in terms of equation (3.11a) can be estimated pointwise almost everywhere according to lemma 2.1 yielding

$$\begin{aligned} S_\Psi(z) - S_\Psi(z^{\text{old}}) &= \int \hat{\psi}(z) - \hat{\psi}(z^{\text{old}}) - y\cdot\nabla_2\hat{\psi}(p,y) + y^{\text{old}}\cdot\nabla_2\hat{\psi}(p^{\text{old}}, y^{\text{old}}) \\ &\geq \int \nabla_1\hat{\psi}(p,y)\cdot(p - p^{\text{old}}) + y\cdot(\nabla_2\hat{\psi}(p^{\text{old}}, y^{\text{old}}) - \nabla_2\hat{\psi}(p,y)). \end{aligned}$$

With $p^{\text{old}}, p \in \mathcal{G}^M$ and assumption A4.1a this yields the claim. □

Proposition 4.11 (Conservation of mass and energy per time step)**.** *Let $z = (p, y)$ a solution to problem problem 4.2 with $\beta_{src} = 0$. Then*

$$E_\Psi(z) = E_\Psi(z^{old}) - \tau\Psi_\partial(z), \tag{4.15a}$$
$$C_\Psi(z) = C_\Psi(z^{old}). \tag{4.15b}$$

Proof. Test equation (4.8b) with $y' = (1, \mathbb{0}^N)$ and $y' = (0, (P_0^N e_i^N))$ for $i = 1, \dots, N$, respectively, like in the continuous proof to proposition 3.3 to obtain

$$0 = \int -\nabla_2\psi(p, \beta, \eta) + \nabla_2\psi(p^{\text{old}}, \beta^{\text{old}}, \eta^{\text{old}}) - \tau\Psi_\partial(z),$$
$$0 = \int (-\nabla_3\psi(p, \beta, \eta) + \nabla_3\psi(p^{\text{old}}, \beta^{\text{old}}\eta^{\text{old}})) \cdot e_i^N$$

which yields the claim. □

4.2. Multi-component problem in entropy form

Here we introduce an equivalent problem formulation in order to prepare for a straightforward spatial discretization that preserves the conservative properties of the model. Note that the additional coupling introduced for that matter is partially reverted when solving the arising discrete spatial problems afterwards.

The non-smoothness ψ couples the primal and dual problem in problem 4.2. We seek to reformulate the problem such that the coupling is merely linear. Previously, we have implicitly identified the tangent spaces $TY \cong Y$ with the original Euclidean subspace for convenience. From now on, for consistency with the interpretation of the conserved quantities and biconjugation, we generally identify the tangent spaces $D = TY \cong \mathbb{R} \times \Sigma_1^N$ and $Y \cong TD$ with appropriate affine subspaces in order to emphasize the respective sum constraints.

To that extent let $\psi^\star$ denote the convex conjugate of ψ for fixed p, i.e. $\psi^\star(p, d) = (\psi(p, \cdot))^*(d)$ as introduced in equation (2.1). Then

$$\psi^\star : \mathbb{R}^M \times D \to \overline{\mathbb{R}},$$
$$(p, d) \mapsto \sup\{d \cdot y - \psi(p, y) \mid y \in \operatorname{dom}\psi(p, \cdot)\}.$$

Note that for $d(p, y) = \nabla_2\psi(p, y)$, we have $\nabla_1\psi(p, \nabla_2\psi(p, \cdot)^{-1}(d)) = -\nabla_1\psi^\star(p, d(p, y))$ by equation (2.4a) and we add this relation in weak form with the additional variable d. We call the arising problem *in entropy form* to emphasize the incorporation of $\psi^\star$, which is an interpolation of the pure-phase negative entropies as explained in section 3.3.1.

Precisely, we denote the extended variables by

$$\begin{aligned} x &= (p, d), \text{ where } d = (e, c) \\ y &= (\beta, \eta), \end{aligned}$$

as well as $x^{\text{old}} = (p^{\text{old}}, d^{\text{old}})$, $d^{\text{old}} = (e^{\text{old}}, c^{\text{old}})$ and let the associated extended bi- and linear forms

$$\begin{aligned} a(x, x') &= a_p(p, p'), \\ b(x, y) &= -(d, y), \\ f_x(x) &= f_p(p), \\ f_y(y) &= -(d^{\text{old}}, y) - (\tau\beta_{src}, \beta) - (\tau\beta_{00}\beta_\partial, \beta). \end{aligned}$$

Note that f_y here does not differ from its earlier definition for all $y \in H^1(Y)$ at this point. However, in the finite dimensional setting of the following chapter 5, d^{old} and $\nabla_2\psi(p^{\text{old}}, y^{\text{old}})$ cannot be identified pointwise a.e. We stick to this definition for the entropy based formulation in order to allow maintaining the conserved quantities, see proposition 5.3.

We condense the non-smooth contribution to the primal problem in terms of

$$\begin{aligned} \phi(x) &= \chi_{G^M}(p) + \psi^\star(x), \\ \Phi(x) &= \chi_{\mathcal{G}^M}(p) + \int \hat{\psi}^\star(x), \end{aligned}$$

with the usual superposition operator induced by the pointwise convex conjugate parametrized by p

$$\hat{\psi}^\star(x)(\xi) = \psi^\star(p(\xi), d(\xi)) = \sup\{d(\xi) \cdot y - \psi(p(\xi), y) \mid y \in Y\}$$

for all $\xi \in \Omega$ and derivatives (if they exist). Note that $\Phi(x) = \infty$ iff $p \notin G^N$ or $d \notin \operatorname{range}\psi(p, \cdot)$ a.e.

Problem 4.4. *Find $x \in H^1(\mathbb{R}^M) \times L^2(D)$, $y \in H^1(Y)$ such that $\beta < 0$ a.e. and*

$$f_x(x' - x) \leq a(x, x' - x) + \Phi(x') - \Phi(x) + b(x' - x, y) \tag{4.16a}$$

$$f_y(y') = b(x, y') - c(y, y') \tag{4.16b}$$

for all test functions $x' \in H^1(\mathbb{R}^M) \times L^2(D)$, $y' \in H^1(Y)$.

Theorem 4.4. *(p, y) solves problem 4.2 iff (x, y) solves problem 4.4 where $x = (p, d)$ with $d = \nabla_2\psi(p, y) = \nabla\pi(y) + p \cdot \nabla\zeta(y)$ almost everywhere.*

We prepare the following result for the proof. Convex conjugation of the parametrized functional is equivalent to convex conjugating its parametrized integrand.

Lemma 4.2. *Let $p \in \mathcal{G}^M, d \in L^2(D)$ such that $\hat{\psi}^\star(p,d) \in L^1(\mathbb{R})$. Then*

$$(\int \hat{\psi}(p,\cdot))^*(d) = \int \hat{\psi}^\star(p,d).$$

Proof. $(\int \hat{\psi}(p,\cdot))^*(d) \leq \int \hat{\psi}^\star(p,d)$ follows straightforward from the pointwise convex conjugation. For the converse, let $\psi_n(p,y) = \psi(p,y) + \frac{1}{n}|y|^2, n > 0$. We show in sequence the (in-)equalities

$$(\int \hat{\psi}(p,\cdot))^*(d) \geq (\int \hat{\psi}_n(p,\cdot))^*(d), \tag{4.17a}$$

$$(\int \hat{\psi}_n(p,\cdot))^*(d) \geq \int \hat{\psi}_n^\star(p,d), \tag{4.17b}$$

$$\lim_{n\to\infty} \int \hat{\psi}_n^\star(p,d) = \int \hat{\psi}^\star(p,d) \tag{4.17c}$$

which completes the proof.

$\int \hat{\psi}(p,y) \leq \int \hat{\psi}_n(p,y)$ for all $y \in L^2(Y)$ follows from the pointwise definition and implies equation (4.17a) by convex conjugation. $\psi_n^\star(p,d) = \sup\{dy - \psi(p,y) - \frac{1}{n}|y|^2 \mid y \in Y\}$ is proper, strictly convex, coercive and has a unique minimizer $\tilde{y}$ pointwise a.e. We have the bound $\psi_n(p,\tilde{y}) - d\tilde{y} \leq \psi(p,\overline{y}) + \frac{1}{n}|\overline{y}|^2 - d\overline{y}$, for $\overline{y} = (-1, \mathbb{0}^N) \in Y$ a.e. Since we can linearly lower bound ψ on $G^M \times Y$ and $d \in L^2(Y)$ it follows from the pointwise bound with constant $\overline{y} \in L^2(Y)$ that $\tilde{y} \in L^2(D)$ and also $\psi(p,\tilde{y}) \in L^1(\mathbb{R})$. Then $\int \hat{\psi}_n(p,\cdot))^*(d) \geq (d,\tilde{y}) - \int \hat{\psi}_n(p,\tilde{y})$ which settles equation (4.17b). Finally, $\psi^\star(p,d)$ is finite and the limit of the non-decreasing sequence $(\psi_n^\star(p,d))_{n=1}^\infty$ pointwise almost everywhere. Now, by Beppo Levi's monotone convergence theorem, we have equation (4.17c). □

Proof of theorem 4.4. Let (x,y) solve problem 4.4. Then testing equation (4.16a) with (p,d') yields

$$0 \leq \int \hat{\psi}^\star(p,d') - \int \hat{\psi}^\star(p,d) - (d'-d,y),$$

i.e. $y \in \partial(\int \hat{\psi}^\star(p,\cdot))(d)$ and $y \in \partial(\int \hat{\psi}(p,\cdot))^*(d)$ by lemma 4.2. By proposition 2.7, $(\int \psi_n(p,\cdot))(y) + (\int \psi_n(p,\cdot))^*(d) = (d,y)$, i.e. $\int \psi_n(p,y) + \psi_n^\star(p,d) - dy = 0$. Since the integrand is necessarily nonnegative by the pointwise definition of $\psi^\star$, we deduce that it is zero almost everywhere and hence $y = \nabla_2\psi^\star(p,d), d = \nabla_2\psi(p,y)$ a.e. Plugging this into equation (4.16b) yields equation (4.8b). Testing equation (4.16a) with (p',d) yields

$$f_p(p'-p) \leq a_p(p,p'-p) + \chi_{\mathcal{G}^M}(p') - \chi_{\mathcal{G}^M}(p) + \int \psi^\star(p',d) - \psi^\star(p,d)$$

and pointwise we have $\psi^\star(p',d) - \psi^\star(p,d) \leq \nabla_1\psi^\star(p,d)(d'-d) = -\nabla_1\psi(p,y)(d'-d)$ by convexity of $\psi^\star$ and subsequent application of equation (2.4b), yielding equation (4.8a). Consequently, (p,y) solves problem 4.2.

For the converse, equation (4.16b) is immediate from equation (4.8b) and $d = \nabla_2\psi(p, y)$ a.e. This also implies $d \in L^2(D)$. Additionally we have

$$\int \hat{\psi}^\star(p', d') - \hat{\psi}^\star(p, d) - (d' - d, y) \geq \int \hat{\psi}(p, y) - \hat{\psi}(p', y) = (\hat{\zeta}(y), p - p')$$

for all $(p', d') \in H^1(\mathbb{R}^M) \times L^2(D)$ by application of equation (2.3b) and lower-bounding $\psi^\star(p', d') \geq y \cdot d' - \psi(p', y)$ pointwise a.e. Consequently equation (4.8a) implies equation (4.16a). □

4.2.1. Alternative convex conjugate splitting

By the decomposition of ψ w.r.t. π and ζ, another equivalent problem formulation can be obtained by only conjugating w.r.t. $\zeta(y) \cdot p$ a.e. Its advantages, predominantly the conservation of the strict barrier for β, are exploited in the subsequent section. To that extent let

$$\gamma(x) = \chi_{G^M}(p) + (p \cdot \zeta(\cdot))^*(d),$$
$$\Gamma(x) = \chi_{\mathcal{G}^M}(p) + \int \hat{\zeta}^\star(x),$$

where

$$\hat{\zeta}^\star(x)(\xi) = (p(\xi) \cdot \zeta(\cdot))^*(d(\xi)) = \sup\{d(\xi) \cdot y - p(\xi) \cdot \zeta(y) \mid y \in Y\} \text{ for all } \xi \in \Omega,$$

in slight abuse of the notation for parametrized convex conjugates in $\hat{\zeta}^\star$.

Problem 4.5. *Find $x \in H^1(\mathbb{R}^M) \times L^2(D)$, $y \in H^1(Y)$ such that $\beta < 0$ a.e. and*

$$f_x(x' - x) \leq a(x, x' - x) + \Gamma(x') - \Gamma(x) + b(x' - x, y) \tag{4.18a}$$
$$f_y(y') = b(x, y') - c(y, y') - (\nabla\hat{\pi}(y), y') \tag{4.18b}$$

for all test functions $x' \in H^1(\mathbb{R}^M) \times L^2(D)$, $y' \in H^1(Y)$.

Theorem 4.5. *(p, y) solves problem 4.2 iff (x, y) solves problem 4.5 where $x = (p, d)$ with $d = p \cdot \nabla\zeta(y)$ almost everywhere.*

The proof is virtually the same as for theorem 4.4.

4.3. Linearized Penrose–Fife type problem

The discretization and corresponding results above also apply to problem 3.2 in analogous manner. Additionally, for problem 3.2 consider the linearized semi-discretization obtained by approximating the time derivatives $\partial_t p, \partial_t \beta$ by backward finite differences and subsequent approximation of the non-smoothness by first-order Taylor expansion, cf. Deuflhard and Bornemann 2002, Section 6.4, i.e.

$$1/\beta \doteq 2/\beta^{\mathrm{old}} - \beta/{\beta^{\mathrm{old}}}^2, \tag{4.19a}$$

$$1/\beta^2 \doteq 3/{\beta^{\mathrm{old}}}^2 - 2\beta/{\beta^{\mathrm{old}}}^3. \tag{4.19b}$$

In particular this yields

$$\begin{aligned} \partial_t 1/\beta &= -1/\beta^2 \partial_t \beta && (4.20)\\ &\doteq -1/\beta^2(\beta - \beta^{\mathrm{old}})/\tau = (-1/\beta + \beta^{\mathrm{old}}/\beta^2)/\tau && (4.21)\\ &\doteq (1/\beta^{\mathrm{old}} - \beta/{\beta^{\mathrm{old}}}^2)/\tau. && (4.22) \end{aligned}$$

This (temporal) linearization in β along with the special structure of the continuous problem gives rise to the (bi-)linear forms

$$\begin{aligned} c_\beta(\beta, \beta) &= (c_v \beta/{\beta^{\mathrm{old}}}^2, \beta) + (\tau\kappa\nabla\beta, \nabla\beta) + (\tau\beta_{00}\beta, \beta)_\partial,\\ f_{p,\beta}(p) &= f_p(p) - (\widetilde{L}c, p),\\ f_\beta(\beta) &= -(c_v/\beta^{\mathrm{old}}, \beta) - (p^{\mathrm{old}}, \beta Lc) + (\tau\beta_{src}, \beta) - (\tau\beta_{00}\beta_\partial, \beta)_\partial. \end{aligned}$$

Note that the coupling between p and β is linear here in contrast to problem 4.2.

Problem 4.6. *Find $p \in H^1(\mathbb{R}^M)$, $\beta \in H^1(\mathbb{R})$ such that*

$$f_{p,\beta}(p' - p) \leq a_p(p, p' - p) + \chi_{\mathcal{G}^M}(p') - \chi_{\mathcal{G}^M}(p) + (p' - p, \beta Lc), \tag{4.23a}$$

$$f_\beta(\beta') = (p \cdot Lc, \beta') - c_\beta(\beta, \beta') \tag{4.23b}$$

for all $p \in H^1(\mathbb{R}^M)$, $\beta \in H^1(\mathbb{R})$.

Theorem 4.6. *Let $\beta_{src} = 0, p^{old} \in \mathcal{G}^M, \beta^{old} \in H^1(\mathbb{R}), \operatorname{esssup} \beta^{old} < 0$. Then problem 4.6 admits a unique solution.*

Proof. C.f. Gräser, Kahnt, and Kornhuber 2016, Theorem 3.1 up to scaling by τ. □

We refer to Klein 1997 for a more in-depth analysis of the non-smooth scalar case.

The linearization surely changes the total entropy production behaviour of the system. However, we can show that overall entropy production is still nonnegative in terms of

$$F_{\Psi,\rho}(p,\beta) = \int -c_v \log(-\beta) - p\widetilde{L}c + \text{const.} \tag{4.24}$$

Proposition 4.12 (Nonnegative entropy production per time step)**.** *Let (p, y) a solution to problem problem 4.6 with $\beta_{src} = 0$. Then*

$$F_{\Psi,\rho}(p,\beta) \geq F_{\Psi,\rho}(p^{old},\beta^{old}) + \tau\Psi_{\partial}(\beta). \tag{4.25}$$

Proof. Cf. Gräser, Kahnt, and Kornhuber 2016, Proposition 3.1 for the bulk and proposition 4.10 for the boundary contributions. □

Note that the conservation of energy is generally not maintained since e.g. testing equation (4.23b) with $\beta' = 1$ yields

$$\int e - e^{\text{old}} = c_v \int \beta - 2\beta^{\text{old}} + 1/{\beta^{\text{old}}}^2 + \int \ldots \mathrm{d}\partial\Omega.$$

5. Discrete non-isothermal multi-phase field systems

Let $\mathcal{T}$ a simplicial grid partitioning Ω and consider the linear finite element spaces

$$\mathcal{S} = \mathcal{S}(\mathcal{T}) = \{v \in C(\bar{\Omega}) \mid v_{|\tau} \text{ is affine } \forall \tau \in \mathcal{T}\} \subset H^1(\Omega). \tag{5.1}$$

We drop the argument of $\mathcal{S}$ in the remainder unless the triangulation it refers to is not obvious, i.e. if it does not refer to the *current one*. In the simplest case, we assume $\mathcal{T}$ to be conforming, i.e. nonempty intersections of simplices are faces of each of them

$$\tau_i \in \mathcal{T}, i = 1, \dots, i_{\max}, \emptyset \neq \bigcap_i \tau_i \Longrightarrow \bigcap_i \tau_i \text{ is a face of } \tau_j, j = 1, \dots, j_{\max}.$$

We incorporate an adaptive refinement strategy that locally refines the grid in order to reduce the spatial discretization error with an efficient allocation of the necessary degrees of freedom. To avoid stability issues resulting from degenerate triangles, we stick to the simplicial subdivision scheme known as *red* refinement, cf. Bey 2000; Bornemann, Erdmann, and Kornhuber 1993. With this choice, the assumption of $\mathcal{T}$ being conforming implies that our refinement is either uniform (and thereby non-local, opposing our adaptivity motivation) or requires closures, e.g. *green closures*, cf. Grande 2018. However, in this work we avoid such closures and allow for grids obtained from an initial conforming partitioning by red refinement with local hanging nodes on edge midpoints. Such a possibly non-conforming mesh hierarchy still induces a natural hierarchy of subspaces that can be used in geometric multigrid methods. For a detailed discussion of finite element spaces on hierarchies of non-conforming, locally refined grids, we refer to Gräser, Kornhuber, and Sack 2014; Gräser 2011.

Let $\mathcal{N}$ the set of non-hanging nodes of $\mathcal{S}$ and $\{\lambda_q \mid q \in \mathcal{N}\}$ the uniquely defined nodal basis with $\lambda_q(r) = \delta_{qr}, q, r \in \mathcal{N}$, linear on each element $\tau \in \mathcal{T}$. These basis functions equal the well-known hat functions in case of a conforming mesh (e.g. obtained by uniform refinement). They generalize to hat functions at non-hanging nodes augmented by linear terms to compensate for the hanging nodes such that inter-element continuity is ensured.

We consider the usual Cartesian product spaces of $\mathcal{S}$, e.g. $\mathcal{S}^M, M \in \mathbb{N}$. Additionally, we denote by

$$\mathcal{S}_c^N = \{(\eta_i)_{i=1}^N \in \mathcal{S}^N \mid \textstyle\sum_{i=1}^N \eta_i = c\}$$

the affine subspace with sum constraint $c \in \mathbb{R}$. The remainder makes use of the subspace $\mathcal{S}_0^N \cong \mathcal{S}^{N-1} \cong T\mathcal{S}_1^N$ and the affine subspace $\mathcal{S}_1^N \cong \mathcal{S}_0^N + \{\mathbb{1}^N/N\} \cong T\mathcal{S}_0^N$. We set

$$\mathcal{X} = \mathcal{S}^M \times \mathcal{S} \times S_1^N, \qquad \mathcal{Y} = \mathcal{S} \times \mathcal{S}_0^N$$

the primal and dual finite element subspaces of interest, respectively.

We choose the approximations to the inner products following the line of thought in Gräser 2011, section 3.4.3, i.e. we aim to lump the non-linear contributions imposed by superposition operators, we choose coinciding inner products for contributions originating from the same term in the time discretization process, we preserve the inherent saddle point structure, and preserve the conservation principles.

Let the linear nodal interpolation w.r.t. $\mathcal{T}$ given by

$$\mathcal{I}^{\mathcal{T}}(f) = \textstyle\sum_{n\in\mathcal{N}} f(n)\lambda_n$$

where $f(n)$ is the evaluation of f at the node $n \in \mathcal{N} \subset \Omega$.

5.1. Multi-component problem in entropy form

We define the lumped non-linear and non-smooth operator

$$\Phi^{\mathcal{T}}(x) = \textstyle\int \mathcal{I}^{\mathcal{T}}(\phi)(x) = \sum_{n\in\mathcal{N}} \phi(x(n)) \int \lambda_n$$

w.r.t. the non-hanging triangulation vertices. See Gräser 2011, Section 3.2 for a short discussion on the lumping of superposition operators preserving their locality. This definition gives rise to the following discretization of problem 4.4 with linear finite elements.

Problem 5.1. *Find $x \in \mathcal{X}$, $y \in \mathcal{Y}$ and*

$$f_x(x' - x) \leq a(x, x' - x) + \Phi^{\mathcal{T}}(x') - \Phi^{\mathcal{T}}(x) + b(x' - x, y) \tag{5.2a}$$
$$f_y(y') = b(x, y') - c(y, y') \tag{5.2b}$$

for all test functions $x' \in \mathcal{X}$, $y' \in \mathcal{Y}$.

We define the subset

$$\mathcal{Y} \subset \mathcal{Y}^- = \{y = (\beta, \eta) \in \mathcal{Y} \mid (\lambda_n, \beta) < 0 \text{ for all } n \in \mathcal{N}\}$$

which determines the dual domain. Note that this is an open set. Let

$$\begin{aligned}\mathcal{L}(x,y) &= J(x) + b(x,y) - \tfrac{1}{2}c(y,y) - f_x(x) - f_y(y),\\ J(x) &= \tfrac{1}{2}a(x,x) + \Phi^{\mathcal{T}}(x)\end{aligned}$$

the Lagrangian associated with equation (5.2). Then we can state the following saddle point problem.

Problem 5.2. *Find $x \in \mathcal{X}$, $y \in \mathcal{Y}$ such that*

$$\mathcal{L}(x,y') \le \mathcal{L}(x,y) \le \mathcal{L}(x',y) \tag{5.3}$$

for all $x' \in \mathcal{X}$, $y' \in \mathcal{Y}$.

5.1.1. Existence and uniqueness

Both problems are equivalent and exhibit a unique solution.

Theorem 5.1. *Problem 5.2 admits a unique solution.*

Proof. Let $g(y) = J^*(f_x - b(\cdot,y))$ and $h(y) = g(y) + \frac{1}{2}c(y,y) + f_y(y)$. At first we show that h has a unique minimizer. Obviously g, h are proper. $c(\cdot,\cdot) + f_y$ is continuous and strictly convex. g is lower semi-continuous and convex by convex conjugation of J and linearity of $f_x - b(\cdot,y)$ in y. Consequently h is lower semi-continuous and strictly convex. We have the lower bound $g(y) \ge f_x(x^{\mathrm{old}}) - b(x^{\mathrm{old}},y) - J(x^{\mathrm{old}})$ and c is an elliptic bilinear form, hence, h is coercive. h admits a unique minimizer $\hat{y}$ by proposition 2.2. Also,

$$\begin{aligned}g(y) &\ge \mathrm{const} + \sup\{(d,y) - \textstyle\sum_{n\in\mathcal{N}} \psi^\star(p,d(n))W_n \mid d \in \mathcal{S}\times\mathcal{S}_1^N\}\\ &= \mathrm{const} + \textstyle\sum_{n\in\mathcal{N}} W_n \sup\{W_n^{-1}d\cdot(\lambda_n,y) - \psi^\star(p,d) \mid d \in \mathbb{R}\times\Sigma_1^N\}\\ &= \mathrm{const} + \textstyle\sum_{n\in\mathcal{N}} W_n \psi(p, W_n^{-1}(\lambda_n,y))\end{aligned}$$

for all $p \in G^M$ where $W_n = \int \lambda_n > 0$, $\mathrm{const} = -\frac{1}{2}a(p,p) + f_p(p)$ and (λ_n, y) to be understood componentwise, i.e. $(\lambda_n,y) = ((\lambda_n,\beta),(\lambda_n,\eta_j)_{j=1}^N) \in \mathbb{R}\times\Sigma_0^N$. Then for $y \notin \mathcal{Y}^-$ we have that $g(y) = \infty$ since $W_n^{-1}(\lambda_n,y) \notin \operatorname{dom}\psi(p,\cdot)$ for some $n \in \mathcal{N}$ and consequently $\hat{y} \in \mathcal{Y}^-$.

$b(\cdot,y) - f_x$ is a bounded linear functional. J is strictly convex and lower semi-continuous on $\mathcal{X}$. For $y \in \mathcal{Y}^-$, $p \in \mathcal{G}^M$, we have that $W_n^{-1}(\lambda_n,y) \in \operatorname{dom}(p(n),\cdot)$ for all $n \in$

$\mathcal{N}$, i.e. there is $\tilde{d} \in \mathcal{S} \times \mathcal{S}_1^N$ such that $\tilde{d}(n) \in \operatorname{dom} \psi^\star(p(n), \cdot)$ and $W_n^{-1}(\lambda_n, y) = \nabla_2 \psi^\star(p(n), \tilde{d}(n))$. Then

$$\begin{aligned}
\mathcal{L}(x,y) &= \tfrac{1}{2}a(x,x) + \Phi^{\mathcal{T}}(x) + b(x,y) - f_x(x) + \operatorname{const}(y) \\
&\geq a_{\text{ell}}\|p\|^2 - \operatorname{const}\|p\| + \textstyle\sum_{n\in\mathcal{N}} W_n(\psi^\star(x(n)) - W_n^{-1} d(n) \cdot (\lambda_n, y)) \\
&= a_{\text{ell}}\|p\|^2 - \operatorname{const}\|p\| + \textstyle\sum_{n\in\mathcal{N}} W_n(\psi^\star(p(n), d(n)) - d(n) \cdot \nabla_2 \psi^\star(p(n), \tilde{d}(n)) \\
&\geq a_{\text{ell}}\|p\|^2 - \operatorname{const}\|p\| + \textstyle\sum_{n\in\mathcal{N}} W_n(c_{0,n} + c_{1,n}|d(n) - \tilde{d}(n)|) \\
&\geq c_p\|p\|^2 + c_d\|d\| + \operatorname{const}
\end{aligned}$$

by application of proposition 2.9 for all $n \in \mathcal{N}$ with positive constants $c_p, c_d > 0$ and hence $\mathcal{L}(\cdot, y)$ is coercive for $y \in \mathcal{Y}^-$. Consequently $\hat{x}(y) = \operatorname{argmin}\{\mathcal{L}(x,y) \mid x \in \mathcal{S}^M \times \mathcal{S} \times S_1^N\}$ is well-defined by proposition 2.2 for $y \in \mathcal{Y}^-$.

$\hat{x}(\hat{y})$ minimizes $\mathcal{L}(\cdot, \hat{y})$ by the previous argument and $\hat{y}$ maximizes $\mathcal{L}(\hat{x}(\hat{y}), \cdot)$ since $\mathcal{L}(\hat{x}(y), y) = -h(y)$ for $y \in \mathcal{Y}^-$. Consequently $(\hat{x}(\hat{y}), \hat{y})$ is a solution to problem 5.2. It is unique since for two saddlepoint candidates $(x_1, y_1) \neq (x_2, y_2)$ the strict convexity above implies the contradiction

$$\mathcal{L}(x_1, y_2) < \mathcal{L}(x_1, y_1) < \mathcal{L}(x_2, y_1) < \mathcal{L}(x_2, y_2) < \mathcal{L}(x_1, y_2).$$

□

Just like for the semi-discrete problems, problem 5.1 holds just the optimality conditions for the Lagrangian $\mathcal{L}$.

Proposition 5.1. *Problem 5.1 and problem 5.2 are equivalent.*

Proof. C.f. Ekeland and Témam 1999, Proposition 1.7 wherein the closedness of the domain is not essential for our usage. The equality in equation (5.2b) is obtained from the inequality by choosing appropriate test directions. □

5.1.2. Thermodynamic consistency

The lumped non-linearity $\Phi^{\mathcal{T}}$ disallows for a straightforward entropy growth preservation in terms of F_Ψ or any of its conjugate relatives from the continuous modeling without additional assumptions or approximations. Instead we consider the following discrete variant.

Proposition 5.2 (Nonnegative discrete entropy production per time step)**.** *Let $x^{old}{}_{|\tau}$ affine for all $\tau \in \mathcal{T}$ and (x, y) the solution to problem problem 5.1 with $\beta_{src} = 0$. Then*

$$\int \mathcal{I}^{\mathcal{T}}(-\psi^\star)(x) \geq \int \mathcal{I}^{\mathcal{T}}(-\psi^\star)(x^{old}) + \tau \Psi_\partial(p, y).$$

Proof. Test equation (5.2a) with x^{old} and equation (5.2b) with y, cf. proposition 4.10. □

Note that the elementwise affinity condition in proposition 5.2 holds e.g. for the case that $\mathcal{T}$ is a refinement of $\mathcal{T}^{\mathrm{old}}$; however the adaptive scheme in section 5.3.2 does not guarantee such a trait in our approach. Regarding upperbounding the discrete entropy difference above with a entropy difference in the sense of F_Ψ from the continuous modeling, note that it is straighforward to upperbound $\int \mathcal{I}^{\mathcal{T}}(-\psi^\star)(x) \leq \int -\psi^\star(x)$ by elementwise linearity of x and convexity of $\psi^\star$, but we cannot generally lowerbound it with parameter x^{old} for basically the same reason.

By the choice of scalar products in the discrete formulation, the conservative properties prevail trivially.

Proposition 5.3 (Conservation of mass and energy per time step)**.** *Let (x, y) the solution to problem 5.1 with $\beta_{src} = 0$ and $x = (p, e, c)$. Then*

$$\int e = \int e^{old} - \tau \Psi_\partial(p, y),$$
$$\int c = \int c^{old}.$$

Proof. Test equation (5.2b) with $y' = (1, \mathbb{0}^N)$ and $y' = (0, P_0^N e_i^N)$ for $i = 1, \ldots, N$, respectively. □

5.1.3. Alternative convex conjugate splitting

Note that in problem 5.1 and 5.2 we do not require the strict negativity of the approximated negative inverse temperature β. This is due to the fact that we shifted the logarithmic barrier in π to the primal problem in the *entropy form*.

By virtue of the splitting exploited in the formulation of **??**, let

$$\Gamma^{\mathcal{T}}(x) = \int \mathcal{I}^{\mathcal{T}}(\gamma(x)) = \textstyle\sum_{n\in\mathcal{N}} \gamma(x(n)) \int \lambda_n,$$
$$\Pi^{\mathcal{T}}(y) = \int \mathcal{I}^{\mathcal{T}}(\pi(y)) = \textstyle\sum_{n\in\mathcal{N}} \pi(y(n)) \int \lambda_n$$

which leads to the following discretization of **??**.

Problem 5.3. *Find $x \in \mathcal{X}$, $y \in S \times S_0^N$ and*

$$f_x(x' - x) \leq a(x, x' - x) + \Gamma^{\mathcal{T}}(x') - \Gamma^{\mathcal{T}}(x) + b(x' - x, y) \tag{5.4a}$$
$$-f_y(y' - y) \leq -b(x, y' - y) + \Pi^{\mathcal{T}}(y') - \Pi^{\mathcal{T}}(y) + c(y, y' - y) \tag{5.4b}$$

for all test functions $x' \in \mathcal{X}$, $y' \in S \times S_0^N$.

Existence and uniqueness of solutions to problem 5.3 can be shown in analogy to problem 5.1, additionally exploiting the strict convexity and lower semi-continuity of Π, as well as coercivity of the dual problem by the quadratic contributions from c eventually dominating any decreasing contribution from $\Pi^{\mathcal{T}}(y)$. Solutions to problem 5.3 naturally fulfill the strict negativity constraint $\beta < 0$ nodewise due to the logarithmic barrier and by linear interpolation everywhere. However, the nodal interpolation of Π with triangulations that differ with the progression of time steps makes it difficult to conserve the overall internal energy (which would be e augmented by appropriate contributions from $\Pi^{\mathcal{T}}$), which is why we neglect this approach in favor of problem 5.1. Despite the interpretational deficiency of locally nonnegative β for approximations of the negative inverse temperature field, its role in problem 5.1 is merely that of a mediating flow variable for the conserved quantities.

5.2. Linearized Penrose–Fife type problem

The discretization of problem 4.6 with linear finite elements is analoguous. The lumping of the non-linearity here is significantly less intrusive in the sense that the nodal interpolation of the Gibbs simplex constraint implies conservation of the Gibbs simplex constraint locally everywhere by linearity of the ansatz functions.

Problem 5.4. *Find $p \in \mathcal{S}^M$, $\beta \in \mathcal{S}$ such that*

$$f_{p,\beta}(p' - p) \leq a_p(p, p' - p) + (p' - p, \beta Lc) + \chi_{\mathcal{G}^M}(p') - \chi_{\mathcal{G}^M}(p) \tag{5.5a}$$

$$f_\beta(\beta') = (p \cdot Lc, \beta') - c_\beta(\beta, \beta') \tag{5.5b}$$

for all test functions $p' \in \mathcal{S}^M$, $\beta' \in \mathcal{S}$.

Existence and uniqueness as well as thermodynamic consistency in terms of nonnegative entropy production carry over from section 4.3.

5.3. Adaptive finite elements

As the phase field p is expected to strongly vary across the phase boundaries, spatial adaptivity based on a posteriori error estimates is mandatory.

The initial grid for the adaptive refinement should be sufficiently fine to detect basic features of the unknown spatial approximation and sufficiently coarse for efficiency of the overall adaptive procedure. In the first time step, we select a suitable, uniformly

refined grid $\mathcal{T}^{\text{old}}$. For successive time steps, the construction of such a grid starts with the grid $\mathcal{T}^{\text{old}}$ from the preceding time step. We begin by coarsening $\mathcal{T}^{\text{old}}$. To this end, we keep all simplices from the grid $\mathcal{T}^{\text{old}}$ from the preceding time step that were obtained by at most $j_{\min}$ refinements. In addition, we keep all simplices τ such that p^{old} exhibits a strong local variation on τ that is not visible after coarsening, i.e., such that

$$\|\nabla(I_\tau p^{\text{old}})\|_{L^\infty(\tau)} \geq \text{Tol}_{\text{derefine}} \qquad \text{and} \qquad \|\nabla(I_{\tau'} p^{\text{old}})\|_{L^\infty(\tau')} < \text{Tol}_{\text{derefine}}$$

hold with τ' denoting the simplex resulting from coarsening of τ. Here, I_τ and $I_{\tau'}$ are the linear interpolation operators to τ and τ', respectively. This set of simplices is completed by additional local refinements. Possible additional refinement is used to uniformly bound the ratio of diameters of adjacent simplices.

5.3.1. Hierarchical a posteriori error estimation

Hierarchical error estimates rely on the solution of local defect problems. While originally introduced for linear elliptic problems (cf. Bornemann, Erdmann, and Kornhuber 1993; Deuflhard, Leinen, and Yserentant 1989; Holst, Ovall, and Szypowski 2011; Zienkiewicz, Gago, and Kelly 1983) this technique was successfully extended to nonlinear problems (cf. Bank and Smith 1993), constrained minimization (cf. Hoppe and Kornhuber 1994; Kornhuber 1996; Kornhuber, Krause, et al. 2007; Siebert and Veeser 2007; Zou et al. 2011) and non-smooth saddle point problems (cf. Gräser, Kornhuber, and Sack 2010; Gräser and Sander 2014b; Gräser 2011). We now derive an a posteriori error estimate by a suitable approximation of the defect problem associated with the defect Lagrangian

$$\mathcal{D}(e_x, e_y) = \mathcal{L}(x + e_x, y + e_y).$$

Consider a uniform refinement $\mathcal{T}'$ of the grid $\mathcal{T}$. Let $\mathcal{N}'$ denote its set of non-hanging nodes and $\mathcal{Q} = \mathcal{S}(\mathcal{T}')$ defined analogously to (5.1) with nodal basis $\{\lambda'_n \mid n \in \mathcal{N}'\}$. Additionally, let $\mathcal{E} = \mathcal{N}' \setminus \mathcal{N}$ the set of all edge mid points in $\mathcal{T}$ that are non-hanging in $\mathcal{T}'$. Note that we have $\mathcal{Q} = \mathcal{S} \oplus \mathcal{V}$ with $\mathcal{V}$ denoting the incremental space

$$\mathcal{V} = \text{span}\{\lambda'_n \mid n \in \mathcal{E}\} \subset \mathcal{Q}.$$

In the first step the defect problem is discretized with respect to the larger finite element space

$$(\mathcal{Q}^M \times \mathcal{Q} \times \mathcal{Q}_1^N) \times (\mathcal{Q} \times \mathcal{Q}_0^N),$$

where $\mathcal{Q}_c^N = \{(\eta_i)_{i=1}^N \in \mathcal{Q}^N \mid \sum_{i=1}^N \eta_i = c\}$. In the second step, the discrete defect problem is localized by ignoring the coupling between $\mathcal{S}$ and $\mathcal{V}$ and also the coupling between λ'_n for all $n \in \mathcal{E}$. We obtain the following local saddle point problems in algebraic notation.

Problem 5.5. *For all $n \in \mathcal{E}$ find $e_{x,n} \in \mathbb{R}^M \times \mathbb{R} \times \Sigma_1^M$, $e_{y,n} \in \mathbb{R} \times \Sigma_0^N$ such that*

$$\mathcal{D}_n(e_{x,n}, y') \leq \mathcal{D}_n(e_{x,n}, e_{y,n}) \leq \mathcal{D}_n(x', e_{y,n})$$

for all $x' \in \mathbb{R}^M \times \mathbb{R} \times \Sigma_1^M$, $y' \in \mathbb{R} \times \Sigma_0^N$.

Here the local defect problems are given by

$$\begin{aligned}
\mathcal{D}_n(e_x, e_y) &= J_n(e_x) + b(e_x, e_y) - \tfrac{1}{2}c(e_y, e_y) - f_{x,n}(e_x) - f_{y,n}(e_y),\\
J_n(e_x) &= \tfrac{1}{2}a(e_x, e_x) + \Phi_{x,n}^{\mathcal{T}}(x + e_x),\\
f_{x,n}(e_x) &= f_x(e_x\lambda_n') - a(x, e_x\lambda_n') - b(e_x\lambda_n', y),\\
f_{y,n}(e_y) &= f_y(e_y\lambda_n') - b(x, e_y\lambda_n') + c(y, e_y\lambda_n').
\end{aligned}$$

We define the hierarchical a posteriori error estimate

$$\begin{aligned}
e_{\mathcal{T}}^{\mathrm{est}} &= (\textstyle\sum_{n\in\mathcal{E}} e_n^2)^{\frac{1}{2}},\\
e_n^2 &= \|e_{x,n}\lambda_n'\|_a^2 + \|e_{y,n}\lambda_n'\|_c^2
\end{aligned}$$

for all $n \in \mathcal{E}$ and with the problem-dependent norms $\|x\|_a^2 = a(x,x)$, $\|y\|_c^2 = c(y,y)$.

5.3.2. Adaptive mesh refinement

The adaptive mesh refinement of the initial grid $\mathcal{T}$ resulting from our coarsening procedure is based on the local error indicators e_n. In each step, the indicators e_{n_i}, $i = 1, \ldots, |\mathcal{E}|$, are arranged with decreasing value, to determine the minimal number i_0 of indicators such that

$$\textstyle\sum_{i=1}^{i_0} e_{n_i}^2 \geqslant \rho e_{\mathcal{T}}^2$$

holds with a given parameter $\rho \in [0,1]$. Then all simplices $\tau \in \mathcal{T}$ with the property $n_i \in \tau$ for some n_i with $i \leq i_0$ are marked for refinement, cf. Dörfler 1996. Each marked simplex is partitioned by red refinement. Again, possible additional refinement is used to uniformly bound the ratio of diameters of adjacent simplices. The refinement process is stopped when the estimated relative error is less than a given tolerance, i.e., if

$$e_{\mathcal{T}}^2 < \mathrm{Tol}_{\mathrm{adapt}}(\|x\|_a^2 + \|y\|_c^2)$$

with $\mathrm{Tol}_{\mathrm{adapt}} > 0$.

6. Algebraic solutions

6.1. Algebraic formulation

Let $K = \dim \mathcal{S} = |\mathcal{N}|$ the dimension of the scalar linear finite element ansatz space, therefore coinciding with the number of non-hanging vertices $\mathcal{N}$ of the grid $\mathcal{T}$. We use the abbreviated notation λ_k for the nodal basis function associated with non-hanging vertex $v_k \in \mathcal{N}$ for $k = 1, \dots, K$ and given enumeration of the vertices in $\mathcal{N}$. For a product space $\mathcal{S}^M$ we construct a convenient numbering of its basis by

$$\lambda_i^M = \lambda_k e_j^K, \quad k = \lfloor \tfrac{i-1}{M} \rfloor + 1, j = (i - 1 \bmod M) + 1$$

for $i = 1, \dots, KM$. This allows for convenient nodal blocking since all degrees of freedom associated with the same node exhibit consecutive indices within the product space.

We identify elements of product spaces of S with their coefficient representation w.r.t. the associated basis above, e.g. $S^M \ni x \cong X \in \mathbb{R}^{KM}$ via the bijection induced by

$$x = \textstyle\sum_{i=1}^{KM} X_i \lambda_i^M.$$

We consider the coefficient spaces

$$\mathcal{X} = (\mathbb{R}^M \times \mathbb{R} \times \Sigma_1^N)^K \subset \mathbb{R}^{K(M+1+N)}, \qquad \mathcal{Y} = (\mathbb{R} \times \Sigma_0^N)^K \subset \mathbb{R}^{K(1+N)},$$

and assume that the disambiguation w.r.t. the respective linear finite element function spaces of the same name is formally obvious from the respective context. Correspondingly, the effective domain for the dual coefficient subset is

$$\mathcal{Y}^- = \{Y \in \mathcal{Y} \mid ((BY)_{M+1+(M+1+N)(k-1)} > 0 \text{ for all } k = 1, \dots, K\}.$$

We introduce a blockwise notation using brackets to conveniently account for the node-wise clustering, i.e. e.g. for $X \in R^{K(M+1+N)}$

$$X[k] = (X_i)_{i=(k-1)(M+1+N)+1}^{k(M+1+N)}$$

and $X = (X[k])_{k=1}^K$. This allows e.g. to identify $\mathcal{Y}^- = \{Y \in \mathcal{Y} \mid ((BY)[k])_{M+1} > 0 \text{ for all } k = 1, \dots, K\}$.

6.1.1. Multi-component problem in entropy form

The bi- and linear forms give rise to the matrices and vectors

$$\begin{aligned}
A_{ij} &= a(\lambda_j^{M+1+N}, \lambda_i^{M+1+N}), && i,j = 1,\dots,K(M+1+N),\\
B_{ij} &= b(\lambda_j^{M+1+N}, \lambda_i^{1+N}), && i = 1,\dots,K(1+N), j = 1,\dots,K(M+1+N),\\
C_{ij} &= -c(\lambda_i^{1+N}, \lambda_j^{1+N}), && i,j = 1,\dots,K(1+N),\\
(F_x)_i &= f_x(\lambda_i^{M+1+N}), && i = 1,\dots,K(M+1+N),\\
(F_y)_i &= f_y(\lambda_i^{1+N}), && i = 1,\dots,K(1+N)
\end{aligned}$$

and B^T the transpose of B. Let W denote the nodal weights

$$W = (\textstyle\int \lambda_k)_{k=1}^K.$$

We introduce evaluation of the lumped non-smoothness $\Phi^{\mathcal{T}}$ in terms of a coefficient vector $X \in \mathbb{R}^{K(M+1+N)}$ via its associated linear finite element function

$$\Phi^{\mathrm{cf}}(X) = \Phi^{\mathcal{T}}(\textstyle\sum_{i=1}^{K(M+1+N)} X_i \lambda_i^{K(M+1+N)}) = \sum_{k=1}^K \phi(X[k]) W_k.$$

Using these definitions, problem 5.1 can be written in algebraic form.

Problem 6.1. *Find $X \in \mathcal{X}$, $Y \in \mathcal{Y}$ such that*

$$AX \cdot (X' - X) + \Phi^{cf}(X') - \Phi^{cf}(X) + B^T Y \cdot (X' - X) \geq F_x \cdot (X' - X) \tag{6.1}$$

$$BX \cdot Y' + CY \cdot Y' = F_y \cdot Y' \tag{6.2}$$

for all $X' \in \mathcal{X}$, $Y' \in \mathcal{Y}$.

Quadrature Note that for the right hand side contributions, an exact quadrature rule can be obtained w.r.t. the grid $\mathcal{T}^{\mathrm{old}}$ while assembling for $\mathcal{T}$. As a consequence, exact conservation of energy and mass can be expected for practical algebraic solutions up to the projection of the initial conditions onto an arbitrarily chosen initial grid, despite the coarsening and refinement procedures.

6.1.2. Linearized Penrose–Fife type problem

In analogous manner, for problem 5.4 we define the matrices and vectors

$$\begin{aligned}
(A_p)_{ij} &= a_p(\lambda_j^M, \lambda_i^M), && i,j = 1,\dots,KM,\\
(B_\beta)_{ij} &= (\lambda_j^M, \lambda_i Lc), && i = 1,\dots,K, j = 1,\dots,K(M+1+N),\\
(C_\beta)_{ij} &= -c_\beta(\lambda_j, \lambda_i), && i,j = 1,\dots,K,\\
(F_{p,\beta})_i &= f_{p,\beta}(\lambda_i^M), && i = 1,\dots,K,\\
(F_\beta)_i &= f_\beta(\lambda_i), && i = 1,\dots,K,
\end{aligned}$$

and capture the (lumped) non-smoothness in terms of a node-wise Gibbs obstacle

$$G^{M,K} = \{P \in \mathbb{R}^{KM} \mid \textstyle\sum_{i=1}^{KM} P_i \lambda_i^{MK} \in \mathcal{G}^M\}$$

giving rise to

$$\chi_{G^{M,K}}(P) = \begin{cases} 0 & \text{if } P[k] \in G^M \text{ for all } k = 1,\dots,K \\ \infty & \text{else.} \end{cases}$$

We write an equivalent formulation of problem 5.4 in algebraic form as follows.

Problem 6.2. *Find $P \in \mathbb{R}^{KM}$, $B \in \mathbb{R}^K$ such that*

$$A_p P \cdot (P' - P) + \chi_{G^{M,K}}(P') - \chi_{G^{M,K}}(P) + B_\beta^T B \cdot (P' - P) \geq F_{p,\beta} \cdot (P' - P), \tag{6.3a}$$

$$B_\beta P \cdot B' + C_\beta B \cdot B' = F_\beta \cdot B' \tag{6.3b}$$

for all $P' \in \mathbb{R}^{KM}$, $B' \in \mathbb{R}^K$.

6.2. Non-smooth Newton method for saddle point problem

In order to solve the algebraic system in problem 6.1, we use a non-smooth Schur–Newton method as proposed in Gräser and Kornhuber 2009.

Notable differences to the assumptions made therein are notationally the sign of the matrix C, our restriction of the dual space to the affine subspace $\mathcal{Y}$, the fact that we cannot assume global Lipschitz-continuity of the subdifferential of the primal convex functional in a straightforward manner, and the implicit definition of our primal non-smoothness Φ^{cf} due to the incorporation of $\psi^\star$.

A similar approach is taken for problem 6.2. For details, we refer to Gräser, Kahnt, and Kornhuber 2016. Here we confine ourselves to a presentation of the more general setting.

6.2.1. The primal problem - decoupled

We consider the primal problem, that is finding a solution X in equation (6.1), for fixed $Y \in \mathcal{Y}^-$ in terms of

$$G_Y^{\mathrm{cf}}(X) = J^{\mathrm{cf}}(X) + (B^T Y - F_x) \cdot X,$$
$$J^{\mathrm{cf}}(X) = \tfrac{1}{2} AX \cdot X + \Phi^{\mathrm{cf}}(X).$$

By the very arguments as in the proof to theorem 5.1, we conclude that

$$\hat{X} = \hat{X}(Y) = \operatorname{argmin} G_Y^{\mathrm{cf}}(X) = (\partial J^{\mathrm{cf}})^{-1}(F_x - B^T Y)$$

is well-defined and omit the dependency on Y for convenience wherever unambiguous.

The coefficients for the primal problem for given potentials, i.e. fixed dual variable Y, can be obtained by exploiting the special structure that was introduced artificially when the problem was constructed in section 4.2. There the primal part of the model problem was built to incorporate the phases, internal energy, and chemical components by weakly coupling the respective transformations from their dual potentials via the underlying reduced grand canonical potential ψ. In the discrete case we can partition the retrieval of the node-wise blocked coefficients into chunks dealing with the phases and the conserved thermodynamical local quantities separately by explicitly making use of this. In particular, the non-smooth and implicit contributions to the primal non-smoothness ϕ, which pose the main difficulties to the algebraic solution of the primal problem, are separated again.

To this extent, let $X \in \mathcal{X}$, then we deinterlace the contributions of X in terms of

$$P[k] = (X[k]_i)_{i=1}^{M}, \tag{6.4a}$$
$$D[k] = (X[k]_i)_{i=M+1}^{M+1+N} \tag{6.4b}$$

for $k = 1, \ldots, K$ and $P = (P[k])_{k=1}^{K}$, $D = (D[k])_{k=1}^{K}$ the phase field respectively energy and chemical concentration coefficient (block) vectors. Note that we do not denote the dependency on X explicitly and treat P, D as the respective parts of X implicitly from here on out. We use $\hat{X} \cong (\hat{P}, \hat{D})$ in the interlaced sense of equation (6.4) for the respective optimizer as well.

Accordingly, we have the relevant operator representations split up again. As the primal quadratic operator A and the linear contribution F_x only act on the phase contribution P, we incorporate A_p as introduced in problem 6.2 and define the separate phase and conserved right hand side contribution as

$$(F_p)_i = f_p(\lambda_i^M), \qquad i = 1, \ldots, KM; \qquad (F_d)_i = 0, \qquad i = 1, \ldots, K(1+N).$$

Similarly, B only acts on the D-part and we define the additional bilinear contribution associated with the algebraic primal problem

$$(B_d)_{ij} = -(\lambda_j^{1+N}, \lambda_i^{1+N}), \qquad i,j = 1,\dots,K(1+N).$$

We introduce algebraic equivalents for the non-smooth thermodynamical contributions indicated by the superscript 'cf' as

$$\begin{aligned}\Psi^{\mathrm{cf}}(P,Y) &= \textstyle\sum_{k=1}^K \psi(P[k],Y[k])W_k,\\ \Psi^{\star,\mathrm{cf}}(P,D) &= \textstyle\sum_{k=1}^K \psi^\star(P[k],D[k])W_k.\end{aligned}$$

Note that $\nabla_1\Psi^{\mathrm{cf}}$ does not depend on its first argument since $\psi(\cdot,y)$ is (affine) linear. We exploit this fact in the following and emphasize the independence by writing $\nabla_1\Psi^{\mathrm{cf}}(\not{P},Y)$. This independence allows to simplify the primal problem significantly by computationally separating the non-smooth thermodynamical contribution from the Gibbs obstacle again. To that extent let

$$\varphi^{\mathrm{cf}}(P) = \tfrac{1}{2}A_pP\cdot P + \chi_{G^{M,K}}(P).$$

Proposition 6.1. *φ^{cf} is proper, strongly convex, and lower semi-continuous. Its subdifferential is single-valued. The subdifferential's inverse is single-valued and Lipschitz continuous.*

Proof. A_P is positive definite. $G^{M,K}$ is a closed convex set. Then $\partial\varphi^{-1}(Q) = P$ is the unique solution to finding $P \in G^{M,K}$ such that $(A_PP - Q)\cdot(P' - P) \geq 0$ for all $P' \in G^{M,K}$. Furthermore $(\partial\varphi^{\mathrm{cf}})^{-1} : (\mathbb{R}^{KM}, \|\cdot\|_{A_p^{-1}}) \to (\mathbb{R}^{KM}, \|\cdot\|_{A_p})$ has Lipschitz constant $L \leq 1$, cf. Kinderlehrer and Stampacchia 2000, Theorem 2.1. □

Let

$$\begin{aligned}M &= -(\operatorname{diag} W)^{-1}B_d,\\ \hat{V} &= \hat{V}(Y) = (\operatorname{diag} W^{-1})(F_d - B_dY)\end{aligned}$$

where $F_d \in (\mathbb{R}\times\Sigma_0^N)^K$. By the choice of sign M is a symmetric positive definite matrix embodying the difference between lumped contributions and pure linear finite element mass matrix. Note that in the algebraic formulation for problem 6.1, we have $F_d = \mathbb{0}^{(1+N)K}$. Then $\hat{V} = MY$ and $(\hat{V})[k]_1 < 0$ for all $k = 1,\dots,K$ iff $Y \in \mathcal{Y}^-$.

For the defect problems, the contribution $F_d \in (\mathbb{R}\times\Sigma_0^N)^K$ is potentially nonzero, which is why we include it in the following deductions.

For given potentials we can compute the phase configuration (and subsequently the conserved quantities) as follows.

Theorem 6.1. *Let $Y \in \mathcal{Y}^-$. Then*

$$\hat{P} = (\partial\varphi^{cf})^{-1}(F_p + \nabla_1\Psi^{cf}(\hat{P}, \hat{V})), \tag{6.5a}$$

$$\hat{D} = (\operatorname{diag} W)^{-1}\nabla_2\Psi^{cf}(\hat{P}, \hat{V}). \tag{6.5b}$$

Proof. The first order optimality conditions for G_Y^{cf} are

$$-A\hat{X} - B^T Y + F_X \in \partial\Phi^{\mathrm{cf}}(\hat{X})$$

which can be written equivalently in decomposed form

$$F_P - A_p\hat{P} - \nabla_1\Psi^{\star,\mathrm{cf}}(\hat{P}, \hat{D}) \in \partial\chi_{G^{M,K}}(\hat{P}) \tag{6.6a}$$

$$F_d - B_d Y - \nabla_2\Psi^{\star,\mathrm{cf}}(\hat{P}, \hat{D}) = 0. \tag{6.6b}$$

By parametrized convex conjugate definition of $\psi^\star$, continuous differentiability of ψ and equation (2.2) we have

$$\nabla_2\psi^\star(\hat{P}[k], \hat{D}[k]) = \hat{V}[k] \quad \Leftrightarrow \quad \nabla_2\psi(\hat{P}[k], \hat{V}[k]) = \hat{D}[k] \tag{6.7}$$

for all $k = 1, \ldots, K$. Hence, (6.6b) $\Leftrightarrow$ (6.5b).

The representation of $\hat{D}$ in equation (6.7) implies

$$-\nabla_1\Psi^{\star,\mathrm{cf}}(\hat{P}, \hat{D}) = \nabla_1\Psi^{\mathrm{cf}}(\hat{P}, \hat{V})$$

by applying equation (2.4b) for each $k = 1, \ldots, K$. Plugging this into equation (6.6a) yields

$$F_p + \nabla_1\Psi^{\mathrm{cf}}(\hat{P}, \hat{V}) \in A_p\hat{P} + \partial\chi_{G^{M,K}}(\hat{P}) = \partial\varphi^{\mathrm{cf}}(\hat{P}) \tag{6.8}$$

which is equivalent to the claim (6.5a). □

By convex conjugation and (6.7), we have the identities

$$\begin{aligned}\Psi^{\star,\mathrm{cf}}(\hat{X}) &= (F_d - B_d Y)\cdot\hat{D} - \Psi^{\mathrm{cf}}(\hat{P}, \hat{V}),\\ \Phi^{\mathrm{cf}}(\hat{X}) &= F_d\cdot\hat{D} - B\hat{X}\cdot Y - \Psi^{\mathrm{cf}}(\hat{P}, \hat{V}) + \chi_{G^{M,K}}(\hat{P}).\end{aligned} \tag{6.9}$$

Note that the primal solution not only is unique for each fixed $Y \in \mathcal{Y}^-$, but the mapping $\hat{X} : \mathcal{Y}^- \to \mathcal{X}$ is injective.

Lemma 6.1. *Let $Y_1 \neq Y_2 \in \mathcal{Y}$. Then $\hat{X}(Y_1) \neq \hat{X}(Y_2)$.*

Proof. If $\hat{X}(Y_1) = \hat{X}(Y_2)$, then equation (6.6b) implies $B_d Y_1 = B_d Y_2$. Since $-B_d = \mathbb{M} \otimes \mathrm{Id}^{1+N}$ the Kronecker tensor product of $\mathbb{M}_{ij} = (\lambda_j, \lambda_i)$ the common s.p.d. mass matrix and the identity matrix, this implies $Y_1 = Y_2$ which is a contradiction. □

6.2.2. Dual Schur complement formulation

For (X, Y) the solution of problem 6.1, we have $Y \in \mathcal{Y}^-$ by the arguments in the proof for theorem 5.1. Hence, with $\hat{X}$ the unique solution to the primal problem we can apply straightforward block elimination to obtain the equivalent dual problem.

Problem 6.3. *Find Y such that*

$$-B\hat{X} - CY + F_y = 0.$$

The associated optimization potential is an algebraic derivate of the Lagrangian $\mathcal{L}$. To that extent let

$$\begin{aligned} H^{\mathrm{cf}}(Y) &= -L^{\mathrm{cf}}(\hat{V}, Y), \\ L^{\mathrm{cf}}(X, Y) &= J^{\mathrm{cf}}(X) - F_x \cdot X + (BX - F_y) \cdot Y + \tfrac{1}{2} CY \cdot Y \end{aligned}$$

denote the dual convex functional with the identities

$$\begin{aligned} H^{\mathrm{cf}}(Y) &= (J^{\mathrm{cf}})^*(F_x - B^T Y) + F_y \cdot Y - \tfrac{1}{2} CY \cdot Y && (6.10) \\ &= -\varphi^{\mathrm{cf}}(\hat{P}) + \Psi^{\mathrm{cf}}(\hat{P}, \hat{V}) + F_p \cdot \hat{P} - \tfrac{1}{2} CY \cdot Y + F_y \cdot Y. && (6.11) \end{aligned}$$

by convex conjugation for the primal problem functional and identity (6.9).

In direct adoption of the results from theorem 5.1 we have the following results.

Proposition 6.2. *H^{cf} is proper, strictly convex and lower semi-continuous.*

Theorem 6.2. *Problem 6.3 admits a unique solution $\hat{Y} \in \mathcal{Y}^-$.*

In this finite-dimensional setting, locally Lipschitz continuous differentiability is readily obtained.

Theorem 6.3. *H^{cf} is Fréchet-differentiable and $\nabla H^{cf}(Y) = -B\hat{X} - CY + F_y$.*

Proof. $\hat{P} \in G^{M,K}$ single-valued as of equation (6.5a). Hence, H^{cf} is Gâteaux-differentiable by equation (6.11). Futhermore, $\hat{P}$ is continuous by proposition 6.1. Proposition 2.5 implies Fréchet-differentiability of H^{cf}. The gradient identity follows from application of the chain rule to equation (6.10). □

As a consequence of identity (6.5b) we have

$$\nabla H^{\mathrm{cf}}(Y) = M^T \nabla_2 \Psi^{\mathrm{cf}}(\hat{P}, \hat{V}) - CY + F_y.$$

Proposition 6.3. *∇H^{cf} is locally Lipschitz.*

6.2.3. Minimization of the dual problem

We apply gradient-related descent methods of the form

$$Y_{\nu+1} = Y_\nu + \rho_\nu \delta Y_\nu, \qquad \nu = 0, 1, \ldots, \tag{6.12}$$

with step size ρ_ν and descent direction δY_ν. The non-smooth Schur–Newton method as introduced in Gräser and Kornhuber 2009 is such a descent method where

$$\delta Y_\nu = -\mathcal{H}_\nu^{-1} \nabla H^{\mathrm{cf}}(Y_\nu). \tag{6.13}$$

$\mathcal{H}_\nu = \mathcal{H}(Y_\nu)$ is a generalized linearization of the non-smooth, non-linear but locally Lipschitz-continuous Schur complement operator $-\nabla H^{\mathrm{cf}}$ at Y_ν playing the role of the Lagrangian's Hessian. In Gräser and Kornhuber 2009, Section 4, an explicit generalized linearization is obtained for a primal quadratic functional with componentwise obstacle. Our non-linearity Φ^{cf} does not fall into that category. However, by virtue of the splitting equation (6.4), the non-smoothness is constrained to the phase variable and similar concepts can be exploited. In order to cope with the simplex constraints as they occur in our setting for $\hat{P}$, we follow the construction in Gräser, Kornhuber, and Sack 2014. The idea is to restrict the primal operator to the maximal subspace $\mathcal{W}$ such that it is locally smooth.

Consider the identity equation (6.11), allowing for a separation of the simplex obstacle from the smooth thermodynamical potential contribution. Due to the product structure of the feasible set $G^{M,K}$ we can determine the subspace in each block individually using the node-wise blocked notation for $\hat{P}$ induced by equation (6.4). To that extent let

$$\begin{aligned}
\mathbb{W}(p) &= \operatorname{span}\{e_i^M - e_j^M \in \mathbb{R}^M \mid 1 \le i < j \le M,\, p_i > 0,\, p_j > 0\},\\
\mathcal{W}(P) &= \{\tilde{P} \in \mathbb{R}^{MK} \mid \tilde{P}[k] \in \mathbb{W}(P[k]) \text{ for all } k = 1, \ldots, K\}
\end{aligned}$$

for $p \in \mathbb{R}^M$, $P \in \mathbb{R}^{MK}$. Here $\mathbb{W}(\hat{P}[k])$ is the maximal subspace where χ_{G^M} is locally smooth near $\hat{P}[k]$. Since $\mathcal{W}(P)$ is a product space the orthogonal projection $\mathcal{P}_{\mathcal{W}(P)} : \mathbb{R}^{MK} \to \mathcal{W}(P)$ is given by a block diagonal matrix where the k-th diagonal block is the orthogonal projection $\mathcal{P}_{\mathbb{W}(P[k])} : \mathbb{R}^M \to \mathbb{W}(P[k])$. For an explicit representation of $\mathcal{P}_{\mathbb{W}(P[k])} \in \mathbb{R}^{M,M}$ we refer to Gräser, Kornhuber, and Sack 2014. We set

$$\hat{A} = \mathcal{P}_{\mathcal{W}(\hat{P})} A_p \mathcal{P}_{\mathcal{W}(\hat{P})} : \mathcal{W}(\hat{P}) \to \mathcal{W}(\hat{P}).$$

Although the chain rule does not hold in general for generalized Jacobians in the sense of Clarke (see, e.g. Gräser 2011), we define a generalized linearization of the non-linear negated Schur complement operator ∇H^{cf} at Y in an analogous manner by

$$\begin{aligned}\nabla^2 H^{\mathrm{cf}}(Y) \approx \mathcal{H}(Y) &= M^T \nabla_{21}\Psi^{\mathrm{cf}}(\hat{P},\hat{V})\cdot\hat{P}' + M^T\nabla_{22}\Psi^{\mathrm{cf}}(\hat{P},\hat{V})M - C,\\ \hat{P}' &= \hat{A}^+\nabla_{12}\Psi^{\mathrm{cf}}(\hat{P},\hat{V})M\end{aligned}$$

where $(\cdot)^+$ is the Moore–Penrose pseudoinverse of $\hat{A}$ and $\hat{P}'$ a generalized linearization of equation (6.5a).

The step sizes are chosen to be *efficient*, i.e. for any sequence Y_ν

$$H^{\mathrm{cf}}(Y_\nu + \rho_\nu \delta Y_\nu) \leq H^{\mathrm{cf}}(Y_\nu) - \mathrm{const}(\nabla H^{\mathrm{cf}}(Y_\nu)\cdot\delta Y_\nu/|\delta Y_\nu|)^2$$

for all $\nu \in \mathcal{N}$ with $\nabla H^{\mathrm{cf}}(Y_\nu) \neq 0$ and the constant positive and independent of ν, cf. Ortega and Rheinboldt 1970; Gräser and Kornhuber 2009.

As a consequence we can show global convergence.

Theorem 6.4. *Let Y_ν the iterates obtained by the descent method* (6.12) *with Schur–Newton directions* (6.13) *($\mathcal{H}_\nu = \mathcal{H}(Y_\nu)$) and efficient step size ρ_ν for any initial $Y_0 \in \mathcal{Y}^-$. Then $Y_\nu \to \hat{Y}$ of problem 6.3.*

Proof. The claim is implied by Gräser and Kornhuber 2009, Theorem 3.1, if we can show that the descent directions δY_ν are gradient-related. H_ν is s.p.d. This implies $H_\nu Y \cdot Y \geq c|Y|^2$ with $c > 0$. Furthermore, $\{\hat{A} \mid$ there exists $P \in G^{M,K}$ such that $\hat{A} = \mathcal{P}_{\mathcal{W}(\hat{P})} A_p \mathcal{P}_{\mathcal{W}(\hat{P})}\}$ is finite and $H_\nu \in \{Y \mid H^{\mathrm{cf}}(Y) \leq H^{\mathrm{cf}}(Y_0)\}$ compact for all $\nu \in \mathcal{N}$. Hence, there exists $C > 0$ such that $|H_\nu| \leq C$ for all $\nu \in \mathcal{N}$. Consequently,

$$-\nabla H^{\mathrm{cf}}(Y_\nu)\cdot\delta Y_\nu \geq c|\mathcal{H}_\nu^- 1 \nabla H^{\mathrm{cf}}(Y_\nu)| \geq \tfrac{c}{C}|\nabla H^{\mathrm{cf}}(Y_\nu)||\delta Y_\nu|$$

with a constant independent of ν. □

6.3. Determining algebraic approximations

By the discretization approach taken in this work, we subsequently compute approximations of solutions associated with times t_n for $n = 1, \ldots, n_{\max}$, cf. chapter 4. Each of these stationary problems is again approximated by computing a sequence of solutions on nested grids, cf. section 5.3.2. Finally, each such nested approximation itself is approximated by iterating equation (6.12) until any of the stopping criteria

$$\nu \geq \nu_{\mathrm{stop}}, \qquad \|Y_{\nu+1} - Y_\nu\|_c \leq \mathrm{Tol}_{\mathrm{abs}}, \qquad \tfrac{\mathrm{Tol}_{\mathrm{abs}}}{\|Y_\nu\|_c} \leq \mathrm{Tol}_{\mathrm{rel}} \tag{6.14}$$

is satisfied, where $\mathrm{Tol}_{\mathrm{abs}}$ is a a mere tool to capture machine precision inaccuracies. Any initial iterate $Y_0 \in \mathcal{Y}^-$ would do as our approach is globally convergent. Note however that the nested adaptive grids in each time step allow to use *nested iteration*, i.e. the initial iterate on each refinement level is obtained by nodal interpolation of the final iterate from the preceding one. On the first refinement level, the initial iterate is obtained by nodal interpolation of the final approximation in the preceding time step or the initial conditions respectively.

During each iteration of the algorithm the following types of subproblems have to be solved: The primal variable $\hat{P}(Y_\nu)$ needs to be computed, which allows to evaluate ∇H^{cf} and determine $\hat{A}$; the descent direction δY_ν needs to be approximated; and a step size ρ_ν has to be chosen. Note that it is not necessary to evaluate $\mathcal{H}_\nu^{-1}$ exactly in (6.13) because global convergence is preserved as long as the approximation of $\mathcal{H}_\nu^{-1}$ is sufficiently accurate. Since the dual functional H^{cf} is strongly convex, one can also show global linear convergence with a rate depending on the bounds for $\mathcal{H}_\nu$ and the step size rule. For further details we refer to Gräser and Kornhuber 2009.

6.3.1. Truncated non-smooth Newton multigrid method

Computing $\hat{P}(Y)$ is equivalent to minimizing $\varphi^{\mathrm{cf}}(\cdot)+\Psi^{\mathrm{cf}}(\cdot,\hat{V})-F_p\cdot(\cdot)$, cf. theorem 6.1 i.e., a convex minimization problem for a quadratic functional with local simplex constraints with linear contribution depending non-linearly on Y. Solutions to these convex minimization problems can efficiently be approximated using non-linear multigrid methods, cf. Kornhuber and Krause 2006; Gräser, Kornhuber, and Sack 2014. More precisely the truncated non-smooth Newton multigrid (TNNMG) method for simplex-constrained problems as proposed in Gräser, Kornhuber, and Sack 2014 allows to solve these problems with an effective complexity of $O(M^2K)$. It is an iterative scheme

$$\begin{aligned} P_{l+0.5} &= P_l + \mathcal{F}(P_l),\\ P_{l+1} &= P_{l+0.5} + \mathcal{C}(P_{l+0.5}). \end{aligned}$$

Its convergence properties mainly stem from a non-smooth smoother instance $\mathcal{F}$ that is best described as a simplicial Gauss–Seidel method, i.e. successive subspace correction along the Gibbs simplex' edges for each node, and was shown to converge in Gräser and Sander 2014a. Its convergence is accelerated using linear corrections $\mathcal{C}(P_{l+0.5})$ that are the solutions to the following linear problem.

Problem 6.4. *Find $\delta P_{l+0.5} \in \mathcal{W}(P_{l+0.5})$ such that*

$$\hat{A}\delta P_{l+0.5} = F_p - \nabla_1 \Psi^{cf}(P, \hat{V})$$

where $\hat{A} = \mathcal{P}_{\mathcal{W}(P_{l+0.5})} A_p \mathcal{P}_{\mathcal{W}(P_{l+0.5})}$.

Approximations $\delta P'_{l+0.5}$ to problem 6.4 can be determined by means of a geometric multigrid method using the existing nested grid structure. To ensure convergence of the TNNMG method, $\mathcal{C}(P_{l+0.5})$ is obtained from $\delta P'_{l+0.5}$ by projection to the admissible set and subsequent damping ensuring that the linear correction does not increase the system's energy. This method was used in all subsequent numerical examples.

6.3.2. Schur–Newton descent linear multigrid solver

Another type of subproblems are the linear problems (6.13) for the symmetric positive definite operators $\mathcal{H}_\nu$. $\mathcal{H}_\nu$ is hard to obtain explicitly but is a linear Schur complement. Hence, it is equivalent to solving the following linear saddle point problem.

Problem 6.5. *Find $\delta Y \in (\mathbb{R} \times \Sigma_0^N)^K$ such that*

$$\begin{pmatrix} -\hat{A} & \nabla_{12}\Psi^{cf}(\hat{P}, \hat{V})M \\ M^T\nabla_{21}\Psi^{cf}(\hat{P}, \hat{V}) & M^T\nabla_{22}\Psi^{cf}(\hat{P}, \hat{V})M - C \end{pmatrix} \begin{pmatrix} \sim \\ \delta Y \end{pmatrix} = \begin{pmatrix} 0 \\ -\nabla H^{cf}(Y) \end{pmatrix}$$

with indifferent primal variable $\sim$.

Its solution is unique in $(\ker \mathcal{P}_{\mathcal{W}(\hat{P}(Y_\nu))})^\perp \times (\mathbb{R} \times \Sigma_0^N)$. Again, these can be approximated efficiently using a geometric linear multigrid method. We use a Vanka-type smoother by applying a Gauss-Seidel scheme on the $|\mathcal{N}| = K$ blocks (of the multigrid hierarchy level respectively). The local $M + (1 + N)$-dimensional symmetric indefinite subproblems are then directly solved using a regularized LDL^t-decomposition. For this the truncated diagonal entries are set to one and the corresponding right hand side values to zero. All other diagonal entries are multiplied by $1 + \rho$ with $\rho = 10^{-8}$.

In all our experiments, we used this vertex-based Vanka-approach as pre-smoother, post-smoother and as iterative base solver. We are not aware of any convergence proof for the linear iterative method resulting from this approach. To increase its robustness we use it as preconditioner for a GMRes iteration.

Sparser dual operator Note that the dual operator exhibits the sparsity pattern of M^TM where M is essentially a mass matrix causing a significantly less sparse dual descent linear operator compared to the original problem. As Gräser and Kornhuber 2009 extended their analysis to inexact versions, in order to reduce the computational effort, we tested simplifying problem 6.5 by replacing M with Id^{1+N}. This effectively ignores the coupling for the non-smooth contributions. As a result, the extended sparsity pattern for the lower right block becomes significantly simpler, i.e. essentially that of a mass matrix again and thereby reduces the computational complexity for

both, the assembly of the operator as well as the solution of the linear problem in all our numerical examples. This approached seemed to be detrimental to the overall convergence of the dual descent method and we did not investigate it further in this work.

Explicit sub-problem kernels The regularization of the local sub-problems can be avoided as the respective kernels are known explicitly. They result from the affine subspaces and the truncation only. This can be used to compute an explicit transformation such that the transformed indefinite sub-problems exhibit a regular saddle point matrix, e.g. using Householder transformations. For the primal variable, this amounts to omitting the truncated degrees of freedom and subsequently transforming the remaining M_{sub} degrees of freedom to a symmetric negative definite $(M_{\text{sub}} - 1)$-dimensional operator by exploiting the local Gibbs-constraint where $M_{\text{sub}} \leq M$. More simply, for the dual variable, this amounts to transforming the $1 + N$ degrees of freedom to a $1 + (N - 1)$-dimensional symmetric positive definite operator by exploiting the local kernel $(0, \mathbb{1}^N)$. The local symmetric indefinite regular sub-problems may then be solved by an LDL^t-decomposition. In our experiments the computational overhead of this method compared to problem-agnostic regularization showed to be disfavourable.

6.3.3. Stepsize rule

Efficient step sizes ρ_ν as required in Theorem 6.4 can be obtained by classical step size rules like, e.g., bisection or the Armijo rule. We use the latter, i.e. we iterate

$$\rho_{\nu,i} = \rho_{\nu,i-1} \cdot \text{Step}_{\text{reduce}}, \quad i = 1, \dots$$

until the criterion

$$f_\nu(0) - f_\nu(\rho_{\nu,i}) \leq \text{Step}_{\text{accept}} \cdot \rho_{\nu,i} \cdot \nabla f_\nu(0)$$

is met, where $f_\nu(\rho) = H^{\text{cf}}(Y_\nu + \rho \delta Y_\nu)$ and $\nabla f_\nu(0) = \delta Y_\nu \cdot \nabla H^{\text{cf}}(Y_\nu)$.

In order to reduce the computational effort in terms of evaluating the primal variable when testing for different step sizes, we incorporate the heuristic criterion of setting step size $\rho_\nu = 1$ if

$$|\delta Y_\nu| \leq \text{Descent}_{\text{reduce}} |\delta Y_{\nu-1}|$$

with $|\delta Y_{-1}| = 0$.

7. Numerical experiments

Implementation Our implementation is based on the finite element assemblers and solvers of DUNE (Distributed and Unified Numerics Environment) framework written in C++, cf. Bastian, Blatt, Dedner, Engwer, Klöfkorn, Ohlberger, et al. 2008; Bastian, Blatt, Dedner, Engwer, Klöfkorn, Kornhuber, et al. 2008. It depends on the functionality of several other modules:

- managing the grid using *dune-alugrid*, cf. Alkämper et al. 2016;
- handling adaptive grids using *dune-subgrid*, cf. Gräser, Sack, and Sander 2009;
- writing data for visualization using *dune-vtk*[1];
- function space bases and functions using *dune-functions*, cf. Engwer et al. 2017; Engwer et al. 2018;
- finite element assemblers and solvers developed and hosted at Freie Universität Berlin using *dune-fufem*, *dune-solvers*, *dune-matrix-vector*, and *dune-tnnmg*[2].

The implementation is available as a separate DUNE module *dune-phasefield*[3].

Machine specifications The computations are performed on a machine with 4 cores at 3.30GHz and 8GB RAM.

[1] `https://gitlab.dune-project.org/simon.praetorius/dune-vtk`
[2] `https://git.imp.fu-berlin.de/agnumpde`
[3] `https://git.imp.fu-berlin.de/maxka-dune`

Model parameters Unless specifically denoted otherwise, we consider the following setting.

$$\begin{aligned} \varepsilon &= 5 \cdot 10^{-2}, & \tau &= 5 \cdot 10^{-2}, & & \\ c_m &= 1.0, & c_v &= 1.0, & \nu &= 1 \cdot 10^{-4}, \\ \kappa &= 1.0, & \mathrm{m} &= P_0^N \mathrm{Id}^N P_0^N, & T &= \mathbb{1}^{N,M}, \\ \beta_{00} &= 0.0, & \beta_\partial &= -1.0, & & \end{aligned}$$

Solver parameters In all experiments, we parametrize our mesh adaptivity (section 5.3) with

$$j_{\min} = 1, \qquad \mathrm{Tol}_{\mathrm{adapt}} = 8 \cdot 10^{-3}, \qquad \mathrm{Tol}_{\mathrm{derefine}} = 1 \cdot 10^{-6},$$

our newton descent (section 6.3) with

$$\mathrm{Tol}_{\mathrm{abs}} = 1 \cdot 10^{-11}, \qquad \mathrm{Tol}_{\mathrm{rel}} = 1 \cdot 10^{-11},$$

and our multigrid methods in sections 6.3.1 and 6.3.2 are W(2,2)-cycles with a base solver consisting of 2 smoother iterations.

The Armijo step rule in section 6.3.3 starts with an initial step size $\rho_{\nu,0} = 1$ and uses the parameters $\mathrm{Step}_{\mathrm{accept}} = 0.05$ and $\mathrm{Step}_{\mathrm{reduce}} = 0.9$. We use $\mathrm{Descent}_{\mathrm{reduce}} = 0.7$ for the heuristic step size rule.

We write ν_r^k for the Schur–Newton iteration count on the r-th adaptive nested grid level in time step k. By $\nu_{\max} = (\nu_{\max})_{n=1}^{n_{\max}}$ we denote the sequence of maximal number of Schur–Newton iterations needed to satisfy any of the criteria 6.14 for the algebraic problem of the stationary problem on the respective finest adaptive grid $\mathcal{T}^{\max}$. In addition, let $\nu_{\mathrm{any}} = (\nu_{\mathrm{any}})_{n=1}^{n_{\max}}$ denote the sequence of maximal number of Schur–Newton iterations needed to solve the spatial problem in time step k, i.e. on any of the nested adaptive grids.

7.1. Thermal feedback

In order to illustrate the equilibration of energy in terms of latent heat and temperature as well as the evolution of entropy, we consider the multi-phase, single-component case as of problem 3.2. For results concerning the linearized discretization problem 4.6, we refer to Gräser, Kahnt, and Kornhuber 2016. Here, we sequentally solve the nonsmooth problem 5.1 with $M = 4$, and $N = 1$. We choose $\mathrm{m} = 0$

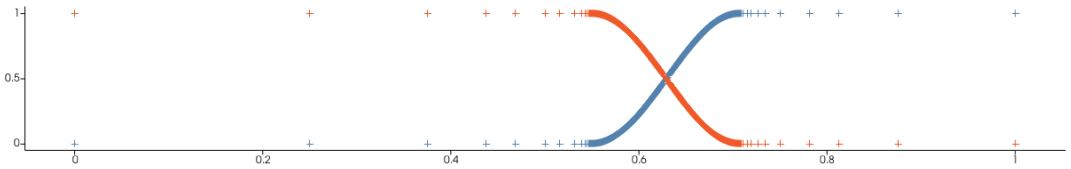

Figure 7.1.: Shrink experiment in 1d: depicting the phases p_1^n (blue, liquid) and p_2^n (red, solid) at the grid vertices resulting from adaptive refinement at time step $n = 100$.

and $\beta_\partial = 0$ for a thermally isolated system. This allows to assess the thermodynamical quantities without further ado. Note that this does not conform with our general (semi-)discrete existence analysis and has $\|\cdot\|_c$ not being a proper norm in the continuous case. Due to the finite-dimensional nature of the fully discrete problems this does not pose a significant problem for the numerical experiments, though. We choose the latent heats $Lc_1 = 0$ and $Lc_i = 2$ for $i = 2, 3, 4$, a constant initial temperature $\check{\beta}$ and an initial binary phase field $\check{p}$ exhibiting a linear interface generated via $p_1^*(x_1, \ldots, x_{\dim}) = \min\{1, \max\{0, (x_1 - x_1^*)/0.15\}\}$. Precisely, let $\mathcal{T}_0$ a regular conforming initial triangulation of Ω and $\mathcal{T}_4$ its fourth uniform refinement. Then $\check{p}_1(x) = \mathcal{I}^{\mathcal{T}_4} p_1^*(x)$, $\check{p}_2 = 1 - \check{p}_0$, and $\check{p}_3 = \check{p}_4 = 0$. We have $\check{c} = c_1 = 1$ and $\check{e} = \mathcal{I}^{\mathcal{T}_4} \nabla_2 \rho(\check{p}, \check{\beta})$ as initial conserved quantity densities.

Model property: Shrink We set $x_1^* = 0.75$ and $\check{\beta} = -0.5$. For $\dim = 1$ we choose $\Omega = [0, 1]$, $\mathcal{T}_0 = \{[0, 1]\}$, and $\mathrm{Tol}_{\mathrm{adapt}} = 5 \cdot 10^{-4}$. For $\dim = 2$ we choose $\Omega = [0, 1] \times [0, 0.2]$, $\mathcal{T}_0$ a conforming triangulation from 5 squares of size $[0, 0.2]^2$ each subdivided into two triangles, and $\mathrm{Tol}_{\mathrm{adapt}} = 1 \cdot 10^{-2}$. The phase configurations in time step 100 and the respective adaptive grids are depicted in figure 7.1 and figure 7.2.

We observe a shrinking of the initial grain. Furthermore, this shrinking process is slowing down as time increases due to the intrinsic cooling by melting, cf. figure 7.3. The absorption of latent heat is driving the approximate temperature $-1/\beta^n$ towards the melting temperature $T = 1$ at equilibrium.

Model property: Growth We alter $x_1^* = 0.15$ and $\check{\beta} = -5$. Additionally, we set $\kappa = 0.2$, decelerating the diffusive thermal leveling. The spatial setup is as before. The phase configurations in time step $n = 100$ and the respective adaptive grids are depicted in figure 7.4 and figure 7.5.

We observe a growth of the initial grain. Analogously to before, this growth process slows down with the time advancing due to the intrinsic heating by solidification, cf. figure 7.6. The absorption of latent heat is driving the approximate temperature

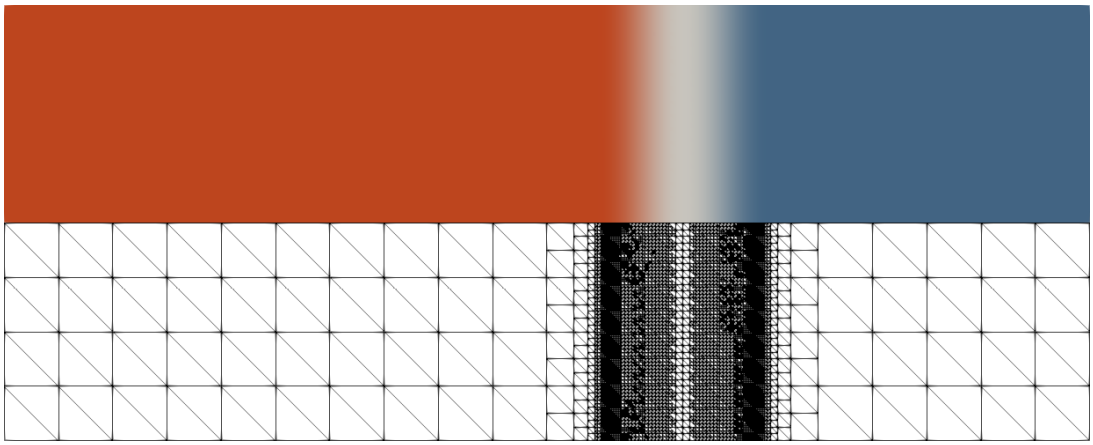

Figure 7.2.: Shrink experiment in 2d: depicting the phases p_1^n (blue, liquid) and p_2^n (red, solid) and the grid resulting from adaptive refinement at time step $n = 100$ in 2d.

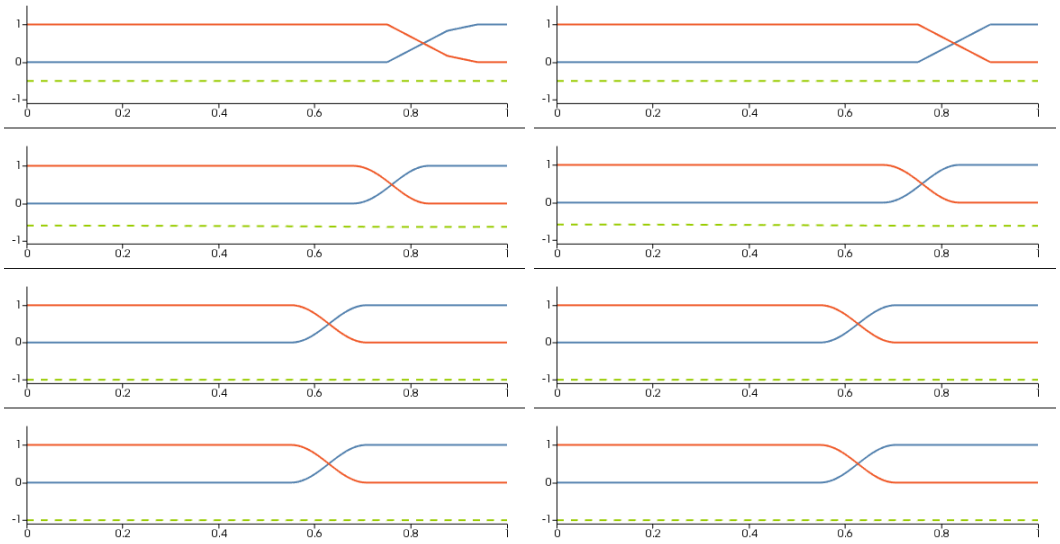

Figure 7.3.: Shrink experiment in 1d (left) and 2d (right); depicting the phase variables p_1^n, p_2^n (blue, red) and negative inverse temperature β^n (green, dashed) over the first spatial coordinate x_1 (at $x_2 = 0.1$ in 2d); time steps $n = 0, 10, 100, 200$ from top to bottom. The phase interface is moving to the left with decreasing velocity as the negative inverse temperature profile approaches -1 (from above).

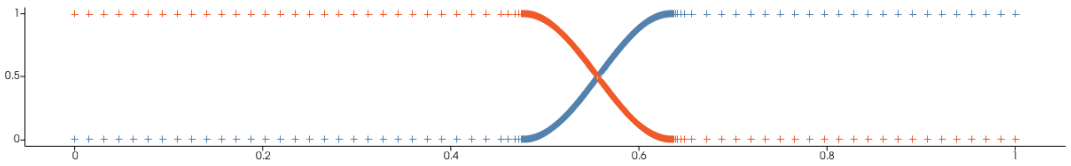

Figure 7.4.: Growth experiment in 1d: depicting the phases p_1^n (blue, liquid) and p_2^n (red, solid) at the grid vertices resulting from adaptive refinement at time step $n = 100$.

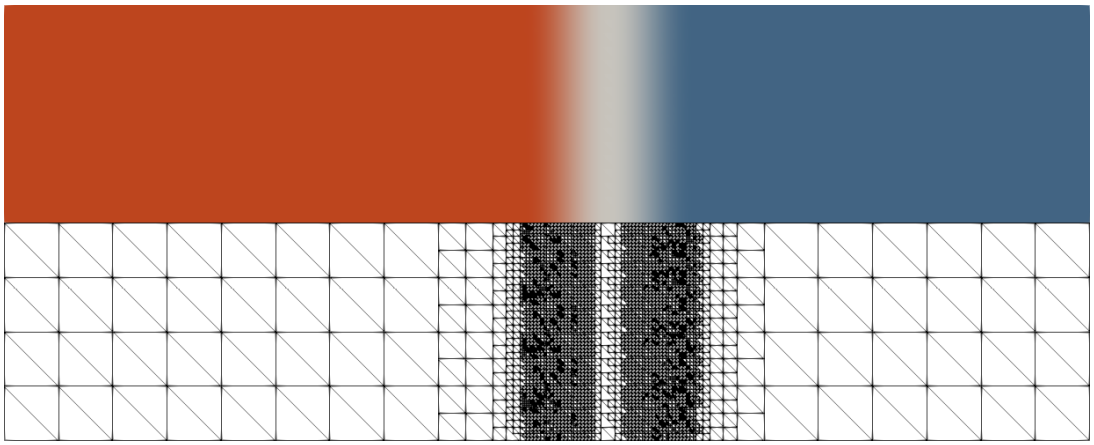

Figure 7.5.: Growth experiment in 2d: depicting the phases p_1^n (blue, liquid) and p_2^n (red, solid) and the grid resulting from adaptive refinement at time step $n = 100$ in 2d.

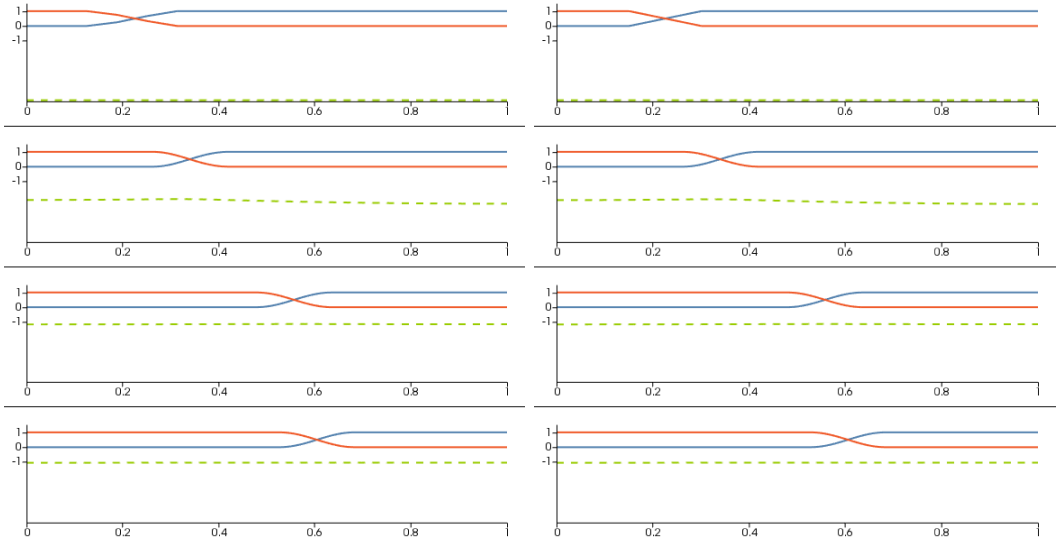

Figure 7.6.: Growth experiment in 1d (left) and 2d (right); depicting the phase variables p_1^n, p_2^n (blue, red) and negative inverse temperature β^n (dashed, green) over the first spatial coordinate x_1 (at $x_2 = 0.1$ in 2d); time steps $n = 0, 10, 100, 200$ from top to bottom. The phase interface is moving to the right with decreasing velocity as the negative inverse temperature profile approaches -1 (from below).

$-1/\beta^n$ towards the melting temperature $T = 1$ at equilibrium.

Numerical thermodynamic consistency The conserved quantities $E = \int e$, $C = \int c$ are maintained numerically as depicted in figures 7.7 and 7.8. In both experiments, the total approximated discrete entropy $S^{\mathrm{cf}} = \int \psi(p, y) - \nabla_2 \psi(p, y) - g(p)$ is monotonically increasing over time up to an observable kink in the entropy curve for the *growth* experiment in 2D. Here, our solver fails to solve the linear subproblems with high accuracy leading to insufficient resolution of the approximated entropy density. Additionally, we plot $\beta_{\mathrm{med}} = (\max\{\beta(\xi) \mid \xi \in \Omega\} + \min\{\beta(\xi) \mid \xi \in \Omega\})/2$.

Spatial discretization: order of convergence and hierarchical error estimation We experimentally investigate the spatial order of convergence for the *growth* setup on Ω pruned to the phase-relevant region $[0, 0.5]$ and $[0, 0.5] \times [0, 0.2]$ for $\mathrm{dim} = 1, 2$, respectively. In the two-dimensional case, $\mathcal{T}_0$ is built from 10 squares of size $[0, 0.1]^2$. In each case we consider the stationary problem at time step 5.

We approximate the exact error by $e^{\mathrm{app}}_{x,\mathcal{T}} = x_{\mathcal{T}} - x_*$, $e^{\mathrm{app}}_{y,\mathcal{T}} = y_{\mathcal{T}} - y_*$, with linear finite element solutions $x_{\mathcal{T}}, y_{\mathcal{T}}$ for successively uniformly refined grids $\mathcal{T} = \mathcal{T}_2, \dots \mathcal{T}_{\mathrm{max}-1}$

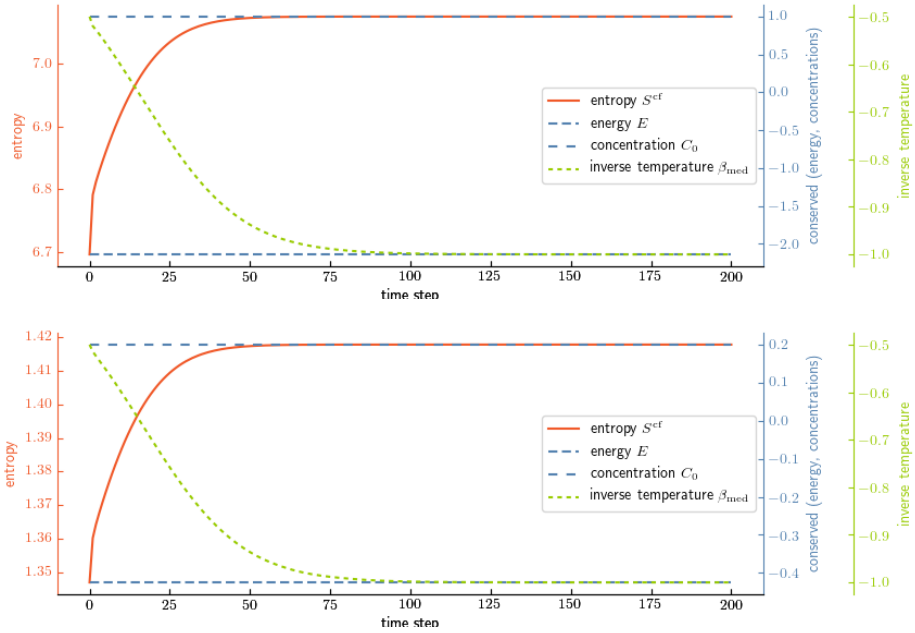

Figure 7.7.: Entropy, internal energy, and mass over time steps $n = 0, \ldots, 200$ for the *shrink* experiment with dim = 1 (top) and dim = 2 (bot).

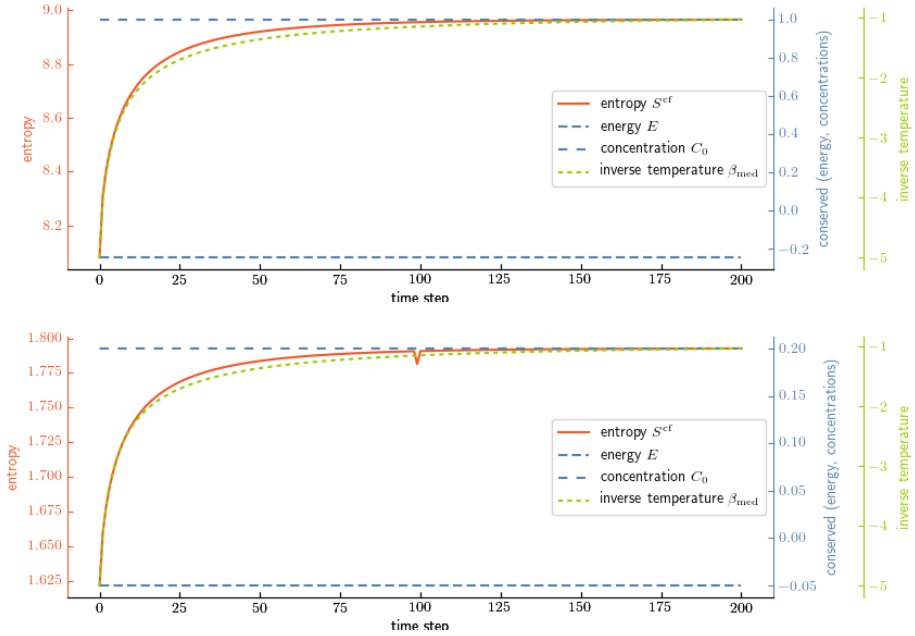

Figure 7.8.: Entropy, internal energy, and mass over time steps $n = 0, \ldots, 200$ for the *growth* experiment with dim = 1 (top) and dim = 2 (bot).

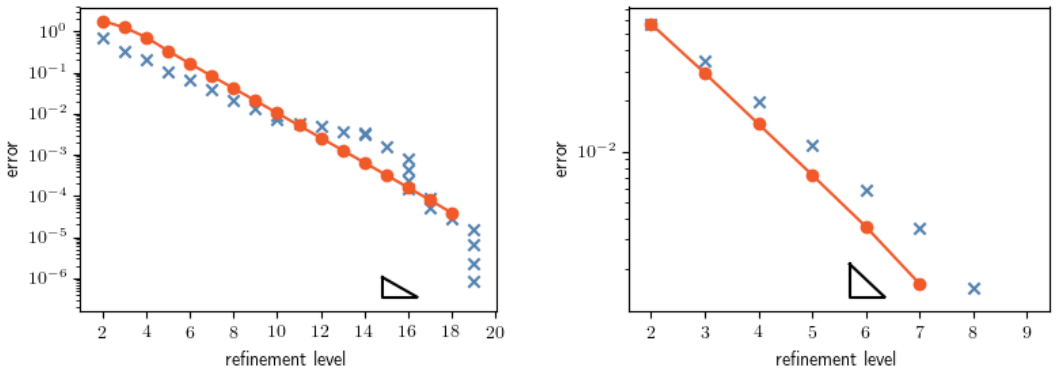

Figure 7.9.: Numerical assessment of spatial order of convergence in 1d (left) and 2d (right) for the *growth* experiment at time step 5: $e_{\mathcal{T}}^{\mathrm{app}}$ (red) over uniform grid refinement level suggests asymptotic order $O(h)$. An equilateral triangle for comparison. Red curves exhibit approximated slopes 1.00 and 1.04 to base 2, respectively. The estimated hierarchical error e^{est} (blue) over respective maximal grid refinement level exhibits analogous values.

and $x_* = x_{\mathcal{T}_{\max}}, y_* = y_{\mathcal{T}_{\max}}$ the approximations for the respective finest grid $\mathcal{T}_{\max}$ in lieu of the exact solution. Our results suggest optimal order $O(h)$ of the discretization error in terms of the approximations

$$e_{\mathcal{T}}^{\mathrm{app}} = \|e_{x,\mathcal{T}}^{\mathrm{app}}\|_a + \|e_{y,\mathcal{T}}^{\mathrm{app}}\|_c,$$

cf. Hardering 2017, as depicted in figure 7.9. Additionally, we depict the estimated error $e_{\mathcal{T}}^{\mathrm{est}}$ (see section 5.3.1) for the adaptive refinement scheme with hierarchical error estimation in a scatter plot over the respective maximal grid refinement level for comparison. Note that the maximal adaptive grid refinement level does not necessarily increase with each refinement step for the grid adaptivity based on Dörfler marking from the hierarchical a-posteriori error estimation.

Solver performance For the *shrink* and *growth* experiments we investigate the maximal number of iterations of the Schur–Newton solver in figures 7.10 and 7.11. Note that the maximal number of Schur–Newton iterations remains bounded below 9 with the exception of the spike in time step 99 for the *growth* experiment in 2D. Here, the linear solver used to approximate the solution to section 6.3.2 yields non-descent directions, i.e. $\nabla H^{\mathrm{cf}}(Y_\nu) \cdot \delta Y_\nu > 0$. On detection of these cases, we resort to a simple gradient descent algorithm, leading to bad convergence rates. We cut off the iterative solver at $\nu_{\mathrm{stop}} = 30$. This coincides with the kink observed in the respective entropy plot in figure 7.8. The boundedness of the iteration steps of the Schur–Newton method indicates mesh independence and is in accordance with previous computations with multi-component Cahn–Hilliard systems, cf. Gräser and Sander 2014b.

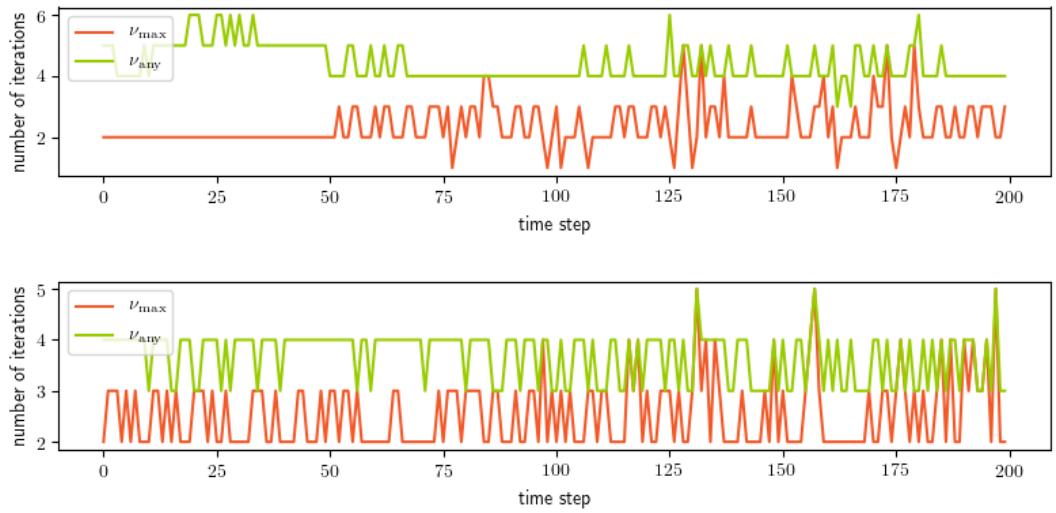

Figure 7.10.: Schur–Newton iterations over time step for the *shrink* experiment with dim = 1 (top) and dim = 2 (bottom).

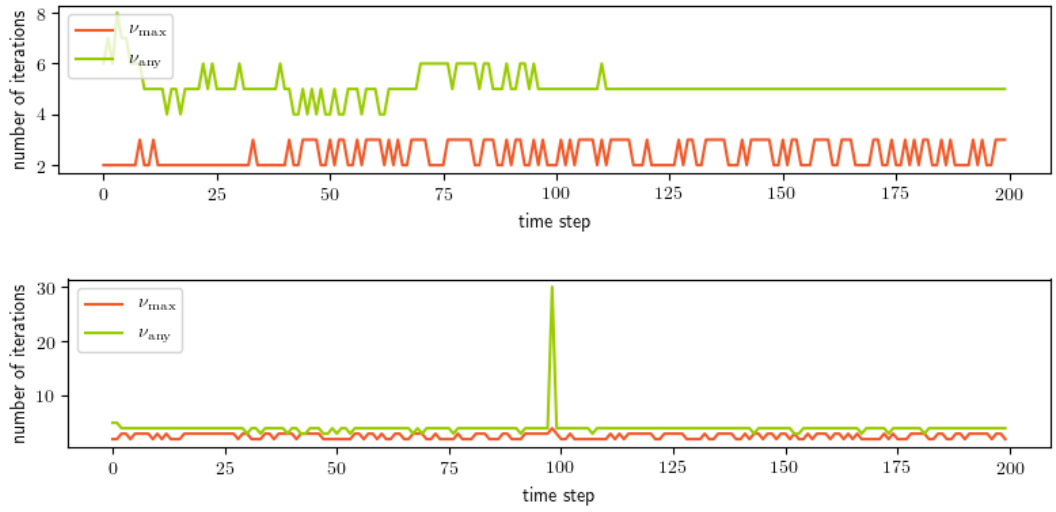

Figure 7.11.: Schur–Newton iterations over time step for the *growth* experiment with dim = 1 (top) and dim = 2 (bottom).

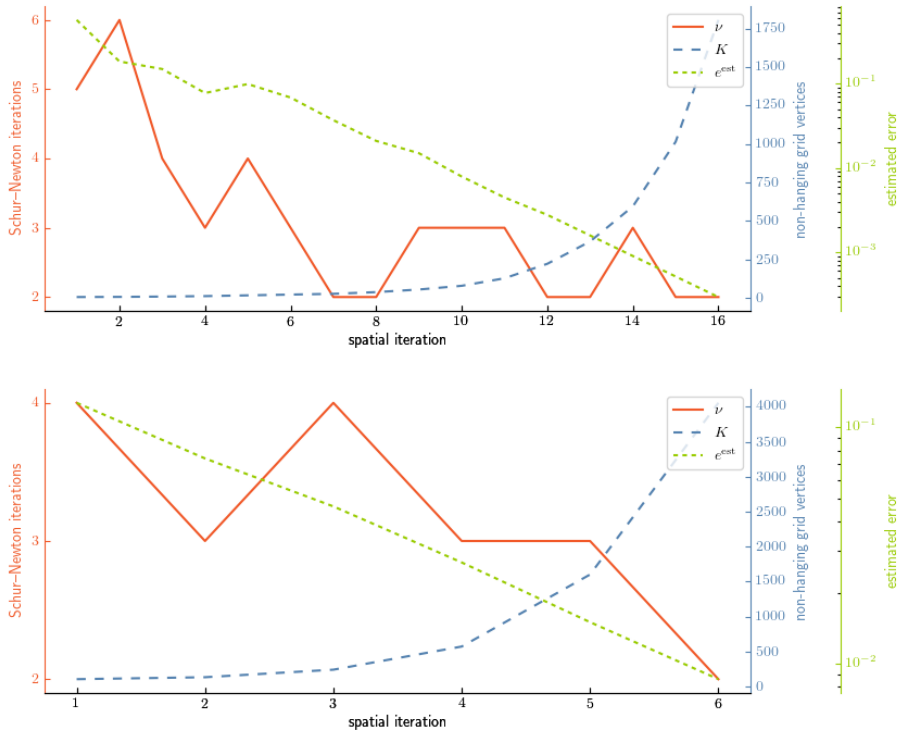

Figure 7.12.: Schur–Newton iterations, degrees of freedom and estimated error over spatial iterations (adaptive grid refinement steps) for *shrink* experiment at time step $n = 20$ with $\dim = 1$ (top) and $\dim = 2$ (bottom).

Finally, we illustrate the behavior of our solver for the adaptive sequence of algebraic problems tackled to obtain a spatial approximation for exemplary time step 20, cf. figures 7.12 and 7.13. The number of degrees of freedom is monotonically increasing by construction. Accordingly, the estimated error is (mostly) decreasing. The number of Schur–Newton iterations stays bounded.

7.2. Multicomponent growth

To illustrate approximations of the multi-component case, we consider two following two settings: $\dim = 1$, $M = 3$, and $N = 2$; $\dim = 2$, $M = 4$, and $N = 3$ for time steps $k = 1, \ldots, 200$.

In both settings we choose thermal coefficients

$$\kappa = 5 \cdot 10^1, \qquad \beta_{00} = 5 \cdot 10^1, \qquad \beta_{\partial} = -1.2,$$

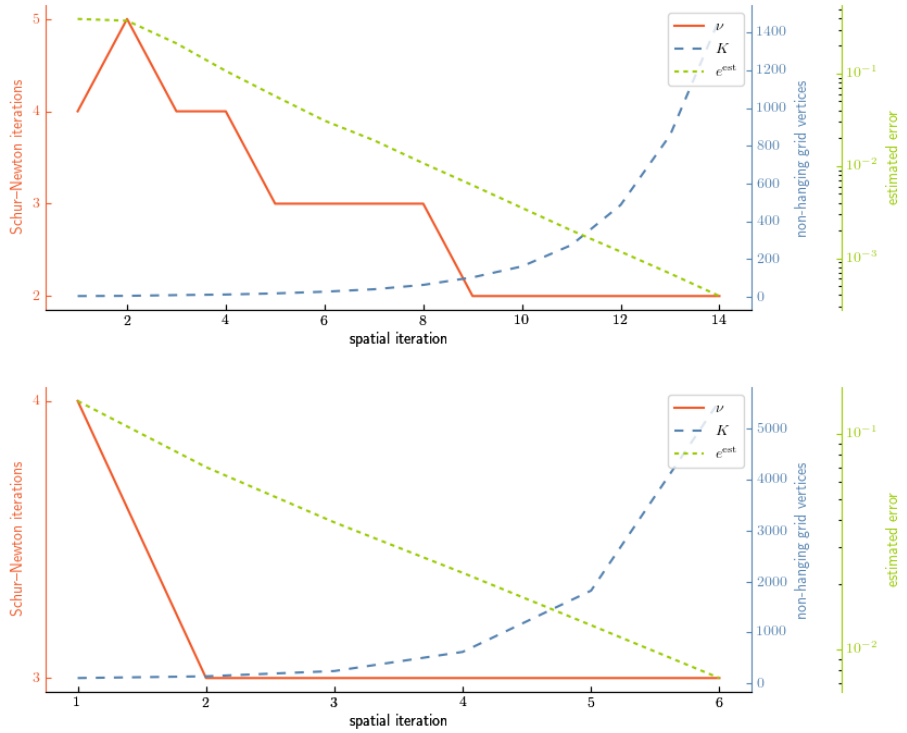

Figure 7.13.: Schur–Newton iterations, degrees of freedom and estimated error over spatial iterations (adaptive grid refinement steps) for *growth* experiment at time step $n = 20$ with $\dim = 1$ (top) and $\dim = 2$ (bottom).

with (frozen in time) component mobilities

$$\mathrm{m} = \mathrm{m}(p) = p_1 \cdot 5 \cdot 10^{-2} \cdot (\tfrac{N}{N-1}\mathrm{Id}^N - \tfrac{1}{N-1}\mathbb{1}^{N,N}).$$

Note that these parameter dependent diffusivities are formally not covered by the infinite-dimensional analysis in this work. We consider latent heats $L_{1j} = 0$ and $L_{ij} = 2+6\cdot\delta_{i-1,j}$ for $i = 2,\dots,M$, $j = 1,\dots,N$ and melting temperatures $T_{i,j} = 1$ for all i, j. The initial values are obtained as follows: $\check{p}_1 = \mathcal{I}^{\mathcal{T}_6} \min\{1, \max\{0, (x_1 - 0.15)/0.1\}\}$, $\check{p}_2 = 1-\check{p}_1, \check{p}_i = 0$ for $i = 3,\dots,M$. We chose $\check{\beta} = -1.2$ and $\check{\eta}_j = 0$ for $j = 1,\dots,N$. As of problem 4.4, the initial values are in terms of internal energy density and chemical concentration (instead of their potentials), i.e. precisely we have $\check{e} = \mathcal{I}^{\mathcal{T}_6}\nabla_2\psi(\check{p}, \check{\beta}, \check{\eta})$ and $\check{c} = \mathcal{I}^{\mathcal{T}_6}\nabla_3\psi(\check{p}, \check{\beta}, \check{\eta})$.

Numerical thermodynamic consistency The thermal permeability of the boundary shows in the numerical evaluation of the thermodynamic quantities. The chemical components are conserved numerically as their total remains unchanged by design, cf. figure 7.14. Again, we observe kinks which we attribute to cases where the linear subproblems are not solved with sufficient accuracy.

Spatial discretization: order of convergence and hierarchical error estimation We experimentally investigate the spatial order of convergence at time step 5 on Ω pruned to the phase-relevant region $[0, 0.5]$ and $[0, 0.5] \times [0, 0.2]$ for $(\dim, M, N) = (1, 3, 2)$ or $(2, 4, 3)$, respectively. With approximated exact errors as before, cf. section 7.1, our results also suggest optimal order $O(h)$ in the multi-component setting as depicted in figure 7.15.

Solver performance For both settings we investigate the maximal number of iterations $\nu_{\max}$ of the Schur–Newton solver for the stationary problem on the respective finest adaptive grid $\mathcal{T}_{\max}$ for each time step n in figure 7.16.

The maximal number of Schur–Newton iterations remains bounded below 25 in both with the exception of the spikes in time steps 114 and 164 for the experiment with $(\dim, M, N) = (2, 4, 3)$. Here again, the linear solver used to approximate the solution to section 6.3.2 yields non-descent directions, i.e. $\nabla H^{\mathrm{cf}}(Y_\nu) \cdot \delta Y_\nu > 0$. On detection of these cases, we resort to a simple gradient descent algorithm, leading to bad convergence rates. We cut off the iterative solver at $\nu_{\mathrm{stop}} = 100$, but in both cases the iterative processes is stopped earlier as the problem energy $h(\cdot)$ is detected to not be decreasing with the computed updated iterate. The relative increase at these points is in the order of 10^{-8}. Disregarding these problems originating from a subsolver deficiency, the boundedness of the iteration steps of the Schur–Newton method indicates mesh independence for our multi-component setting. Again, this is in accordance

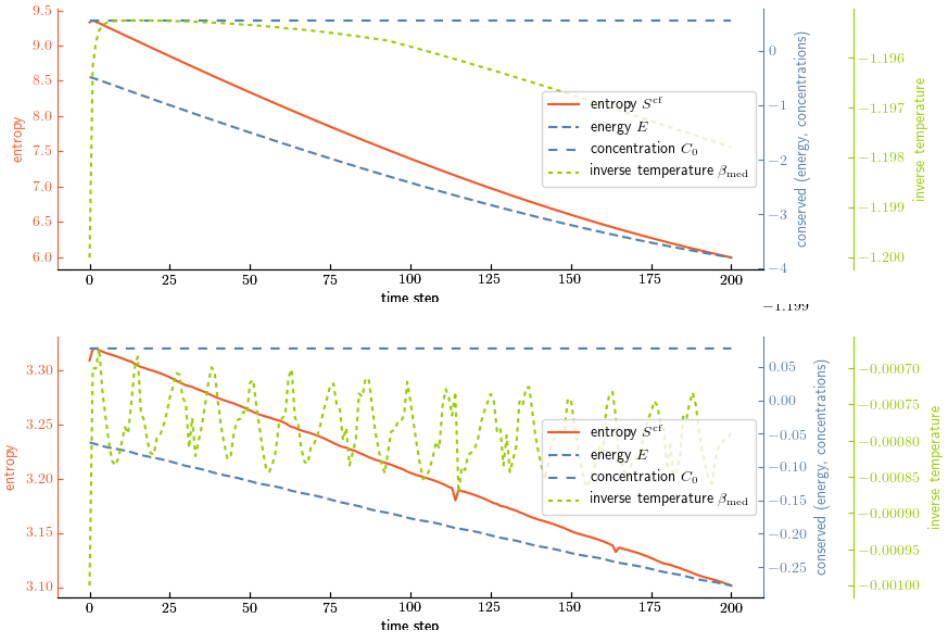

Figure 7.14.: Entropy, internal energy, and mass over time steps $n = 0, \ldots, 200$ for (dim, M, N) set to $(1, 3, 2)$ (top) and $(2, 4, 3)$ (bottom). The components are conserved while the other thermodynamical quantities are impacted by the thermal boundary conditions. The kinks in the bottom entropy plot can be attributed to insufficiencies of the linear subsolver.

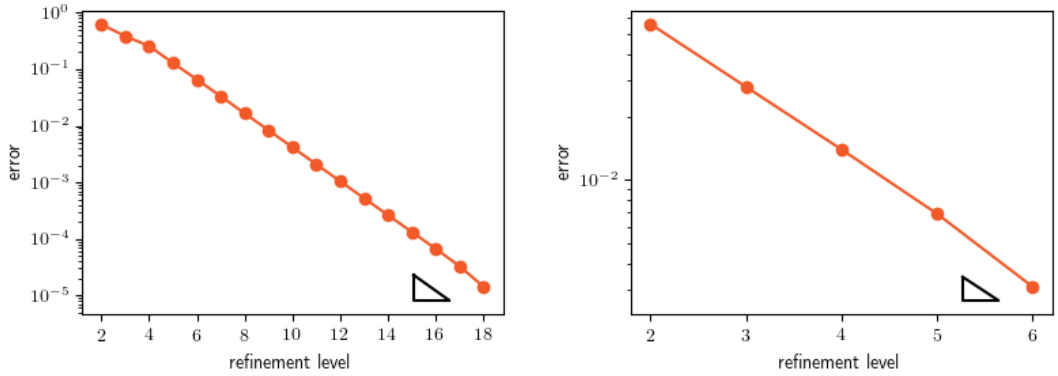

Figure 7.15.: Numerical assessment of spatial order of convergence: e^{app} over uniform grid refinement level suggests asymptotic order $O(h)$. An equilateral triangle for comparison and the approximated slope to base 2 denoted in the legend. $(\mathrm{dim}, M, N) = (1, 3, 2), (2, 4, 3)$ for top and bottom figure, respectively.

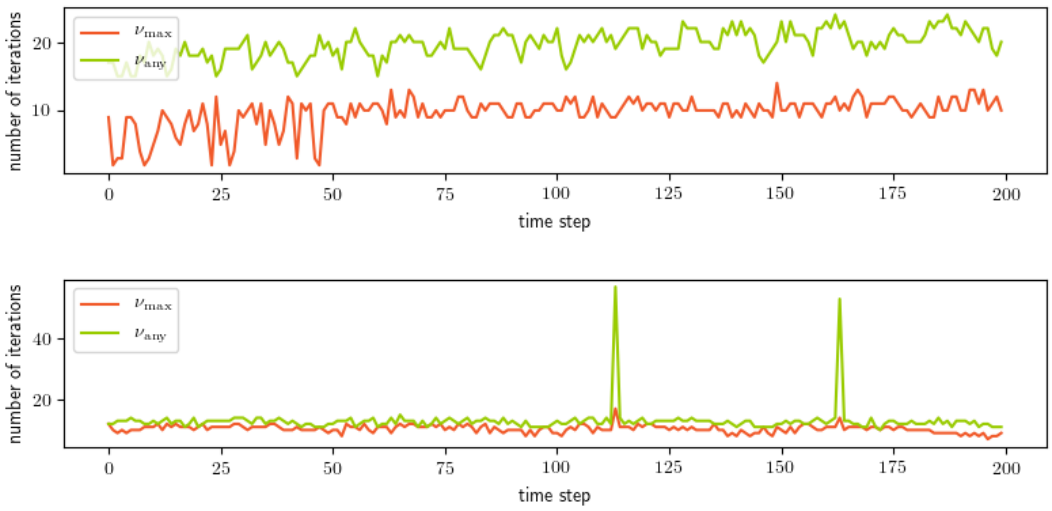

Figure 7.16.: Schur–Newton iterations over time step for $(\dim, M, N) = (1, 3, 2)$ (top) and $(2, 4, 3)$ (bottom), respectively.

with previous computations with multi-component Cahn–Hilliard systems, Gräser and Sander 2014b.

Finally, we illustrate the behavior of our solver for the adaptive sequence of algebraic problems tackled to obtain a spatial approximation for exemplary time step 20, cf. figure 7.17. The number of degrees of freedom $((M-1+1+N-1)+(1+N-1))\cdot K$ is monotonically increasing by design due to the nested grids originating from adaptive refinement. Accordingly, the estimated error is decreasing. The number of Schur–Newton iterations stays bounded.

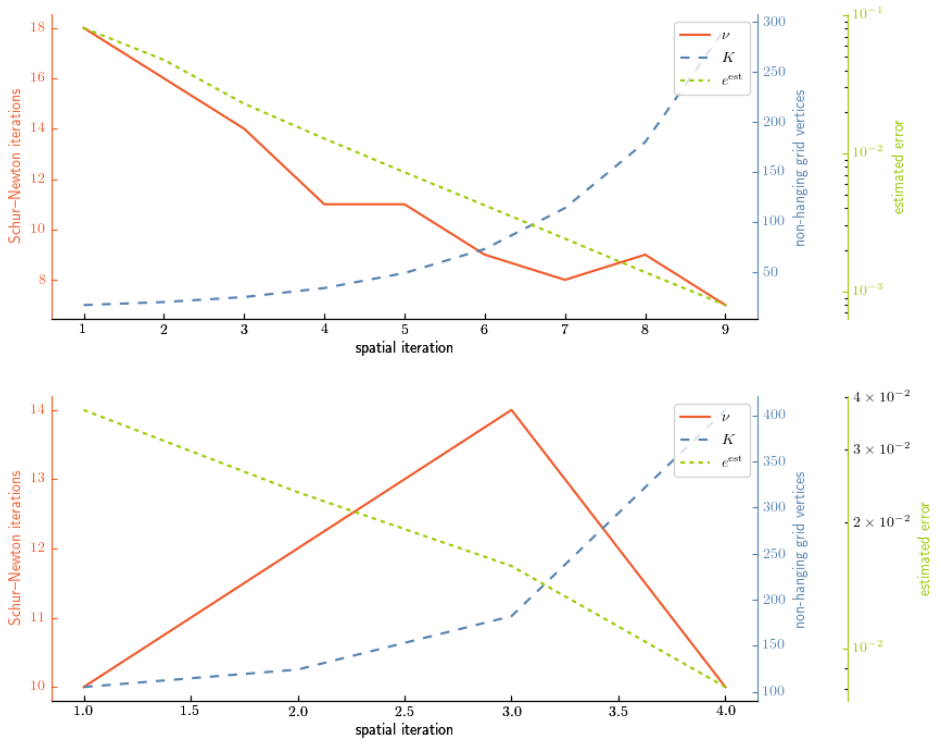

Figure 7.17.: Schur–Newton iterations, degrees of freedom and estimated error over spatial iterations (adaptive grid refinement steps) for the multicomponent problem with $(\dim, M, N) = (1, 3, 2)$ (top) and$(2, 4, 3)$ (bottom), respectively.

A. Reduced grand potential computations

We consider

$$\begin{aligned}\psi : \mathbb{R}^M \times \mathbb{R} \times \Sigma_0^N &\to \overline{\mathbb{R}},\\ (p, \beta, \eta) &\mapsto \pi(\beta) + p \cdot \zeta(\beta, \eta) + \tfrac{\nu}{2}|\eta|^2\end{aligned}$$

for $M, N \in \mathbb{N}$ with $\nu > 0$ as introduced in section 3.3.1 where

$$\begin{aligned}\pi : \mathbb{R} &\to \overline{\mathbb{R}},\\ \beta &\mapsto \begin{cases} -c_v \log(-\beta) & \text{if } \beta < 0,\\ \infty & \text{else,}\end{cases}\\ \zeta_i : \mathbb{R} \times \Sigma_0^N &\to \mathbb{R},\\ y = (\beta, \eta) &\mapsto c_m \log \sigma_{0,i}(\beta, \eta),\end{aligned}$$

with

$$\begin{aligned}\sigma_{k,i} : \mathbb{R} \times \Sigma_0^N &\to \mathbb{R},\\ (\beta, \eta) &\mapsto \textstyle\sum_{j=1}^N L_{i,j}^k \tilde{\eta}_{i,j},\\ \tilde{\eta}_{i,j} : \mathbb{R} \times \Sigma_0^N &\to \mathbb{R},\\ (\beta, \eta) &= \exp((\eta_j - \widetilde{L}_{i,j} - \beta L_{i,j})/c_m),\end{aligned}$$

for $k \in \mathbb{N}$, $i = 1, \dots, M$, $j = 1, \dots, N$ and $c_v, c_m > 0$, $L, \widetilde{L} \in \mathbb{R}^{M,N}$. We write $\sigma = (\sigma_i)_{i=1}^M$ and $\zeta = (\zeta_i)_{i=1}^M$.

Functions of the type of ζ_i are also known in recent machine learning literature as *LogSumExp* or *RealSoftMax* functions where they provide a smooth approximation to the maximum function.

A.1. Derivatives

In order to simplify the notation for the derivatives, this section uses formal partial derivatives as if all variables were independent despite the constrained definition with $\eta \in \Sigma_0^N$.

A. Reduced grand potential computations

Note the following identities for the partial derivatives of our helper functions

$$\begin{aligned}\partial_\beta \sigma_{k,i} &= -\sigma_{k+1,i}/c_m,\\ \partial_{\eta_j} \sigma_{k,i} &= L^k_{i,j}\tilde{\eta}_{i,j}/c_m,\end{aligned}$$

for $k \in \mathbb{N}$, $j = 1, \ldots, N$.

The first order derivatives are

$$\begin{aligned}\nabla_p \psi(p,\beta,\eta) &= \zeta(\beta,\eta),\\ \nabla_\beta \psi(p,\beta,\eta) &= \nabla\pi(\beta) + \textstyle\sum_{i=1}^M p_i \nabla_\beta \zeta_i(\beta,\eta),\\ \nabla_\eta \psi(p,\beta,\eta) &= \textstyle\sum_{i=1}^M p_i \nabla_\eta \zeta_i(\beta,\eta) + \nu\eta,\end{aligned}$$

where

$$\begin{aligned}\nabla\pi(\beta) &= -c_v/\beta,\\ \nabla_\beta \zeta_i(\beta,\eta) &= -\sigma_{1,i}/\sigma_{0,i},\end{aligned}$$

and

$$\begin{aligned}\nabla_\eta \zeta_i(\beta,\eta) &= P_0^N(\partial_{\eta_j}\zeta_i(\beta,\eta))_{j=1}^N,\\ \partial_{\eta_j}\zeta_i(\beta,\eta) &= \tilde{\eta}_{i,j}/\sigma_{0,i}.\end{aligned}$$

The second order partial derivatives are

$$\begin{aligned}\nabla_p\nabla_p \psi(p,\beta,\eta) &= 0,\\ \nabla_p\nabla_\beta \psi(p,\beta,\eta) &= \nabla_\beta \zeta(\beta,\eta),\\ \nabla_p\nabla_\eta \psi(p,\beta,\eta) &= \nabla_\eta \zeta(\beta,\eta),\\ \nabla_\beta\nabla_\beta \psi(p,\beta,\eta) &= \nabla\nabla\pi(\beta) + \textstyle\sum_{i=1}^M p_i \nabla_\beta\nabla_\beta \zeta_i(\beta,\eta),\\ \nabla_\beta\nabla_\eta \psi(p,\beta,\eta) &= \textstyle\sum_{i=1}^M p_i \nabla_\beta\nabla_\eta \zeta_i(\beta,\eta),\\ \nabla_\eta\nabla_\eta \psi(p,\beta,\eta) &= \operatorname{diag}\nu + \textstyle\sum_{i=1}^M p_i \nabla_\eta\nabla_\eta \zeta(\beta,\eta),\end{aligned}$$

where $\nabla_\beta\zeta = (\nabla_\beta\zeta_i)_{i=1}^N$, $\nabla_\eta\zeta = (\nabla_\eta\zeta_i)_{i=1}^N$, and

$$\begin{aligned}\nabla\nabla\pi(\beta) &= c_v/\beta^2,\\ \nabla_\beta\nabla_\beta\zeta_i(\beta,\eta) &= (\sigma_{2,i}\sigma_{0,i} - \sigma_{1,i}^2)/(c_m\sigma_{0,i}^2),\\ \nabla_\beta\nabla_\eta\zeta_i(\beta,\eta) &= P_0^N(\partial_\beta\partial_{\eta_j}\zeta_i(\beta,\eta))_{j=1}^N,\\ \partial_\beta\partial_{\eta_j}\zeta_i(\beta,\eta) &= \tilde{\eta}_{i,j}(\sigma_{1,i} - L_{i,j}\sigma_{0,i})/(c_m\sigma_{0,i}^2),\\ \nabla_\eta\nabla_\eta\zeta_i(\beta,\eta) &= P_0^N(\partial_{\eta_k}\partial_{\eta_j}\zeta_i(\beta,\eta))_{k,j=1}^N P_0^N,\\ \partial_{\eta_k}\partial_{\eta_j}\zeta_i(\beta,\eta) &= \tilde{\eta}_{i,j}(\delta_{jk}\sigma_{0,i} - \tilde{\eta}_{i,k})/(c_m\sigma_{0,i}^2),\end{aligned}$$

with δ_{jk} denoting the Kronecker delta.

A.2. Convexity

Let $N \in \mathbb{N}$ and

$$\begin{aligned} r(x,y) &= r_1(x,y) - r_2(x,y), \\ r_1(x,y) &= \textstyle\sum_{j=1}^N x_j y_j^2 \sum_{k=1}^N x_k, \\ r_2(x,y) &= (\textstyle\sum_{j=1}^N x_j y_j)^2. \end{aligned}$$

Lemma A.1. *Let $x, y \in \mathbb{R}^N$. Then $r(x,y) \geq 0$. For $x > 0$ the inequality is strict iff $y \notin \operatorname{span}\{\mathbb{1}^N\}$.*

Proof. We manipulate the sum indices to find an equivalent form with non-negative terms, using notably $\sum_{j=1}^N \sum_{k=j+1}^N a_{jk} = \sum_{k=1}^N \sum_{j=1}^{k-1} a_{jk}$.

$$\begin{aligned} r_1(x,y) &= \textstyle\sum_{k=1}^N \sum_{j=1}^N x_k x_j y_j^2 \\ &= \textstyle\sum_{k=1}^N (\sum_{j=1}^{k-1} x_k x_j y_j^2 + x_k^2 y_k^2 + \sum_{j=k+1}^N x_k x_j y_j^2) \\ &= \textstyle\sum_{k=1}^N \sum_{j=1}^{k-1} x_k x_j y_j^2 + \sum_{k=1}^N x_k^2 y_k^2 + \sum_{k=1}^N \sum_{j=k+1}^N x_k x_j y_j^2 \\ &= \textstyle\sum_{k=1}^N \sum_{j=1}^{k-1} x_k x_j y_j^2 + \sum_{k=1}^N x_k^2 y_k^2 + \sum_{j=1}^N \sum_{k=j+1}^N x_j x_k y_k^2 \\ &= \textstyle\sum_{k=1}^N \sum_{j=1}^{k-1} x_k x_j y_j^2 + \sum_{k=1}^N x_k^2 y_k^2 + \sum_{k=1}^N \sum_{j=1}^{k-1} x_j x_k y_k^2 \\ &= \textstyle\sum_{k=1}^N \sum_{j=1}^{k-1} x_k x_j (y_j^2 + y_k^2) + \sum_{k=1}^N x_k^2 y_k^2 \\ r_2(x,y) &= (\textstyle\sum_{j=1}^N x_j y_j)^2 \\ &= \textstyle\sum_{k=1}^N x_k y_k (\sum_{j=1}^{k-1} x_j y_j + x_k y_k + \sum_{j=k+1}^N x_j y_j) \\ &= \textstyle\sum_{k=1}^N \sum_{j=1}^{k-1} x_k y_k x_j y_j + \sum_{k=1}^N x_k^2 y_k^2 + \sum_{k=1}^N \sum_{j=k+1}^N x_k y_k x_j y_j \\ &= \textstyle\sum_{k=1}^N \sum_{j=1}^{k-1} x_k y_k x_j y_j + \sum_{k=1}^N x_k^2 y_k^2 + \sum_{j=1}^N \sum_{k=j+1}^N x_j y_j x_k y_k \\ &= \textstyle\sum_{k=1}^N \sum_{j=1}^{k-1} x_k y_k x_j y_j + \sum_{k=1}^N x_k^2 y_k^2 + \sum_{k=1}^N \sum_{j=1}^{k-1} x_j y_j x_k y_k \\ &= 2 \textstyle\sum_{k=1}^N \sum_{j=1}^{k-1} x_j y_j x_k y_k + \sum_{k=1}^N x_k^2 y_k^2 \\ r(x,y) &= r_1(x,y) - r_2(x,y) \\ &= \textstyle\sum_{k=1}^N \sum_{j=1}^{k-1} x_k x_j (y_k^2 - 2 y_k y_j + y_j^2) \\ &= \textstyle\sum_{k=1}^N \sum_{j=1}^{k-1} x_k x_j (y_k - y_j)^2 \geq 0 \end{aligned}$$

□

Proposition A.1. *ζ_i is convex.*

Proof. The Hessian H of $\zeta_i \in C^\infty(\mathbb{R} \times \mathbb{R}^N)$ satisfies

$$\begin{aligned}(\beta', \eta')^T H(\beta, \eta)(\beta', \eta') &= \beta'^2(\sigma_2\sigma_0 - \sigma_1^2) + \textstyle\sum_{k=1}^N 2\beta'\eta_k'(\tilde{\eta}_k\sigma_1 - L_k\tilde{\eta}_k\sigma_0) \\ &\quad + \textstyle\sum_{j,k=1}^N \eta_j'\eta_k'(\delta_{jk}\tilde{\eta}_k\sigma_0 - \tilde{\eta}_j\tilde{\eta}_k) \\ &= \textstyle\sum_{j,k=1}^N \tilde{\eta}_j\tilde{\eta}_k(\eta_j'^2 - 2\eta_j'L_j\beta' + L_j^2\beta'^2 - \eta_j'\eta_k' \\ &\quad + 2\eta_j'L_k\beta' - L_jL_k\beta'^2) \\ &= \textstyle\sum_{j=1}^N \tilde{\eta}_j(\eta_j'^2 - 2\eta_j'L_j\beta' + L_j^2\beta'^2)\sum_{k=1}^N \tilde{\eta}_k \\ &\quad - (\textstyle\sum_{j=1}^N \tilde{\eta}_j(\eta_j' - L_j\beta'))^2 \\ &= r(\tilde{\eta}, \eta' - L\beta') \geq 0\end{aligned}$$

for all $(\beta', \eta') \in \mathbb{R} \times \mathbb{R}^N$, using lemma A.1. □

For fixed but arbitrary L the directions of non-strict convexity of ζ_i on $\mathbb{R}^- \times \Sigma_0^N$ are those in the 1-dimensional subspace $\{(\beta, \eta) \mid \eta - L\beta \in \operatorname{span}\{\mathbb{1}^M\}\}$.

A.3. Bounds

Proposition A.2. *For $i = 1, \ldots, M$ there are $c_{0,i}, c_{1,i}, c_{2,i}, c_{3,i} > 0$ such that*

$$|\zeta_i(y)| \leq c_{0,i} + c_{1,i}|y|_n, \tag{A.1a}$$

$$|\nabla\zeta_i(y)|_n \leq c_{2,i}, \tag{A.1b}$$

$$|\zeta_i(y) - \zeta_i(y')|_n \leq c_{2,i}|y - y'|_n, \tag{A.1c}$$

for all $y, y' \in \mathbb{R} \times \mathbb{R}^N$, $n = 2, \infty$.

Proof. The Euclidean norm and the maximum norm are equivalent by

$$(N+1)^{-\frac{1}{2}}|y|_2 \leq |y|_\infty \leq |y|_2.$$

We drop the index i as well as the constant $c_m > 0$ for the remainder of this proof to shorten the notation. Note the corresponding incorporation of the respective columns of $L, \widetilde{L}$ in lieu of the full matrices. Equation (A.1a) holds by

$$\begin{aligned}\pm\zeta(\beta, \eta) &= \log \textstyle\sum_{j=1}^N \exp(\eta_j)\exp(-\beta L_j)/\exp(\widetilde{L}_j) \\ &\leq |\widetilde{L}|_\infty \pm \log\left(\exp(|\beta|)^{\pm}|L|_\infty \textstyle\sum_{j=1}^N \exp(\eta_j)\right) \\ &\leq |\widetilde{L}|_\infty + |L|_\infty|\beta| \pm \log\left(N\exp(\pm|\eta|_\infty)\right) \\ &\leq |\widetilde{L}|_\infty + \log(N) + 2\max\{|L|_\infty, 1\}|(\beta, \eta)|_\infty.\end{aligned}$$

Equation (A.1b) holds by

$$\partial_\beta \zeta(y) = -\sigma_1(y)/\sigma_0(y) \leq |L|_\infty,$$
$$\partial_{\eta_j} \zeta(y) = \tilde{\eta}_j(y)/\sigma_0(y) \leq 1.$$

Equation (A.1c) holds by application of equation (A.1b);

$$|\zeta(y) - \zeta(y')|_n \leq \int_0^1 |\nabla \zeta(y' + t(y - y'))t(y - y')|_n \, \mathrm{d}t \leq c_2 |y - y'|_n \int_0^1 t \, \mathrm{d}t.$$

□

A.4. Numerical evaluation

The numerical evaluation of ζ_i can be stabilized using by the following identity:

$$\zeta_i(\beta, \eta) = V_i + c_m \log \tilde{\sigma}_{0,i}(\beta, \eta, V_i)$$

for any $V_i \in \mathbb{R}$ where

$$\tilde{\sigma}_{k,i}(\beta, \eta, V_i) = \textstyle\sum_j L^k_{i,j} \tilde{\eta}_{i,j}(\beta, \eta, V_i),$$
$$\tilde{\eta}_{i,j}(\beta, \eta, V_i) = \exp((\eta_j - \widetilde{L}_{i,j} - \beta L_{i,j} - V_i)/c_m).$$

We choose $V_i = \max\{\tilde{\eta}_{i,j} \mid j = 1, \ldots, N\}$ for each $i = 1, \ldots, M$. This can also be applied to the derivatives. As

$$\partial_\beta \tilde{\eta}_{i,j}(\beta, \eta, V_i) = -L_{i,j} \tilde{\eta}_{i,j}(\beta, \eta, V_i)/c_m,$$
$$\partial_{\eta_k} \tilde{\eta}_{i,j}(\beta, \eta, V_i) = \delta_{jk} \tilde{\eta}_{i,j}(\beta, \eta, V_i)/c_m,$$

and

$$\partial_\beta \tilde{\sigma}_{k,i}(\beta, \eta, V_i) = -\tilde{\sigma}_{k+1,i}(\beta, \eta, V_i)/c_m,$$
$$\partial_{\eta_j} \tilde{\sigma}_{k,j}(\beta, \eta, V_i) = L^k_{i,j} \tilde{\eta}_{i,j}(\beta, \eta, V_i)/c_m,$$

we have the identities

$$\nabla_\beta \zeta_i(\beta, \eta) = -\tilde{\sigma}_{1,i}/\tilde{\sigma}_{0,i},$$
$$\nabla_{\eta_j} \zeta_i(\beta, \eta) = \tilde{\eta}_{i,j}/\tilde{\sigma}_{0,i}$$

and correspondingly for the second derivatives.

B. Zusammenfassung

Die vorliegende Arbeit beschäftigt sich mit einem thermodynamisch konsistenten Modell zur Beschreibung von Legierungen unter Einbezug mehrerer chemischer Komponenten sowie im Sinne von Phasenfeldmodellen über den physikalischen Begriff hinaus verallgemeinerten Phasen. Aktuelle Simulationen von z.B. Erstarrungsprozessen mittels solcher Modelle mit anwendungsnahen Parametern sind vorranging expliziter Natur im Sinne der Zeitdiskretisierung und zuverlässige Ergebnisse erfordern hierbei bekanntermaßen die Berechnung vieler Zwischenschritte. Implizite Methoden hingegen bergen einige numerische Herausforderungen insbesondere auch aufgrund der nicht-Glattheit der zugrundeliegenden Energien.

Ziel dieser Arbeit ist die konsistente Herleitung sowie effiziente und robuste Berechnung von impliziten numerischen Annäherungen an kontinuierliche Lösungen solcher temperaturgekoppelten Mehrphasen- und Mehrkomponenten-Modelle unter Berücksichtigung der modellinhärenten Invarianten bei gleichzeitiger Ausnutzung der zugrundeliegenden physikalischen Strukturen, insbesondere bezüglich bestimmter Dualitäten.

Aufbauend auf den Grundlagen für Mehrphasen- und -komponenten-Modelle in Kapitel 2 wird in Kapitel 3 ein flexibles thermodynamisch konsistentes Modell vorgestellt. Davon ausgehend werden in den darauffolgenden Kapiteln 4 und 5 schrittweise Diskretisierungen hergeleitet, Existenz und Eindeutigkeit von Lösungen der resultierenden Systeme bewiesen und die Erhaltungseigenschaften der dadurch erzeugten Annäherungen diskutiert. Hierbei ermöglichen adaptive Gitter eine problemangepasste Verteilung der räumlichen Freiheitsgrade auf Basis eines hierarchischen Fehlerschätzers. Die numerische Lösung dieser Systeme durch algebraische Umformulierungen und Anwendung von nicht-glatten Mehrgittermethoden wird in Kapitel 6 vorgestellt. Das entstehende zentrale nicht-lineare Sattelpunktproblem kann äquivalent durch Auswertung eines nicht-glatten Teilproblems in ein Minimierungsproblem überführt werden, für das ein effizientes Abstiegsverfahren bekannt ist. Zuletzt werden in Kapitel 7 rechnerische Experimente durchgeführt um die angestrebte thermodynamische Konsistenz sowie die numerische Effizienz zu belegen.

Bibliography

Alkämper, M. et al. (2016). "The Dune-alugrid Module." en. In: *Archive of Numerical Software* 4.1, pp. 1–28. DOI: 10.11588/ANS.2016.1.23252.

Bank, R. E. and R. K. Smith (1993). "A Posteriori Error Estimates Based on Hierarchical Bases". In: *SIAM Journal on Numerical Analysis* 30.4, pp. 921–935. DOI: 10.1137/0730048.

Bartels, S. (2015). *Numerical Methods for Nonlinear Partial Differential Equations*. Springer International Publishing. DOI: 10.1007/978-3-319-13797-1.

Bastian, P., M. Blatt, A. Dedner, C. Engwer, R. Klöfkorn, R. Kornhuber, et al. (2008). "A Generic Grid Interface for Parallel and Adaptive Scientific Computing. Part Ii: Implementation and Tests in Dune". In: *Computing* 82.2-3, pp. 121–138. DOI: 10.1007/s00607-008-0004-9.

Bastian, P., M. Blatt, A. Dedner, C. Engwer, R. Klöfkorn, M. Ohlberger, et al. (2008). "A Generic Grid Interface for Parallel and Adaptive Scientific Computing. Part I: Abstract Framework". In: *Computing* 82.2-3, pp. 103–119. DOI: 10.1007/s00607-008-0003-x.

Bey, J. (2000). "Simplicial Grid Refinement: On Freudenthal's Algorithm and the Optimal Number of Congruence Classes". In: *Numerische Mathematik* 85.1, pp. 1–29. DOI: 10.1007/s002110050475.

Blank, L. et al. (2012). "Primal-dual Active Set Methods for Allen-Cahn Variational Inequalities with Nonlocal Constraints". In: *Numerical Methods for Partial Differential Equations* 29.3, pp. 999–1030. DOI: 10.1002/num.21742.

Bornemann, F. A. (1990). "An adaptive multilevel approach to parabolic equations I. General theory and 1D implementation". In: *IMPACT of Computing in Science and Engineering* 2.4, pp. 279–317. DOI: 10.1016/0899-8248(90)90016-4.

Bornemann, F. A., B. Erdmann, and R. Kornhuber (1993). "Adaptive Multivlevel Methods in Three Space Dimensions". In: *International Journal for Numerical Methods in Engineering* 36.18, pp. 3187–3203. DOI: 10.1002/nme.1620361808.

Brézis, H. (1971). "Monotonicity Methods in Hilbert Spaces and Some Applications to Nonlinear Partial Differential Equations". In: *Contributions to Nonlinear Functional Analysis*. Elsevier, pp. 101–156. DOI: 10.1016/b978-0-12-775850-3.50009-1.

Brokate, M. and J. Sprekels (1996). "Hysteresis Operators". In: *Hysteresis and Phase Transitions*. Springer New York, pp. 22–121. DOI: 10.1007/978-1-4612-4048-8_3.

Caginalp, G. (1989). "Stefan and Hele-shaw Type Models As Asymptotic Limits of the Phase-field Equations". In: *Physical Review A* 39.11, pp. 5887–5896. DOI: 10.1103/physreva.39.5887.

Cahn, J. W. and J. E. Hilliard (1958). "Free Energy of a Nonuniform System. I. Interfacial Free Energy". In: *The Journal of chemical physics* 28.2, pp. 258–267. DOI: 10.1063/1.1744102.

Choudhury, A. and B. Nestler (2012). "Grand-potential Formulation for Multicomponent Phase Transformations Combined with Thin-interface Asymptotics of the Double-obstacle Potential". In: *Physical Review E* 85.2, p. 021602. ISSN: 1539-3755. DOI: 10.1103/physreve.85.021602.

Crank, J. (1987). *Free and Moving Boundary Problems*. Oxford University Press.

Deimling, K. (2010). *Nonlinear Functional Analysis*. Courier Corporation.

Deuflhard, P. and F. A. Bornemann (2002). *Scientific Computing with Ordinary Differential Equations*. Vol. 42. Springer New York. DOI: 10.1007/978-0-387-21582-2.

Deuflhard, P., P. Leinen, and H. Yserentant (1989). "Concepts of an adaptive hierarchical finite element code". In: *IMPACT of Computing in Science and Engineering* 1.1, pp. 3–35. DOI: 10.1016/0899-8248(89)90018-9.

Deuflhard, P. and M. Weiser (2011). *Adaptive Lösung partieller Differentialgleichungen*. Numerische Mathematik. De Gruyter. DOI: 10.1515/9783110218039.

Dörfler, W. (1996). "A Convergent Adaptive Algorithm for Poisson's Equation". In: *SIAM Journal on Numerical Analysis* 33.3, pp. 1106–1124. DOI: 10.1137/0733054.

Eiken, J., B. Böttger, and I. Steinbach (2006). "Multiphase-field approach for multicomponent alloys with extrapolation scheme for numerical application". In: *Physical Review E* 73.6. DOI: 10.1103/physreve.73.066122.

Ekeland, I. and R. Témam (1999). *Convex Analysis and Variational Problems*. Society for Industrial and Applied Mathematics. DOI: 10.1137/1.9781611971088.

Engwer, C. et al. (2017). "The Interface for Functions in the Dune-functions Module". en. In: *Archive of Numerical Software* Vol 5, No 1 (2017). DOI: 10.11588/ANS.2017.1.27683.

Engwer, C. et al. (2018). "Function Space Bases in the Dune-functions Module". In: *arXiv*, arXiv–1806. arXiv: 1806.09545 [cs.MS].

Garcke, H. (2000). "On Mathematical Models for Phase Separation in Elastically Stressed Solids". PhD thesis. Math. Inst. der Univ.

Goebel, R. and R. T. Rockafellar (2008). "Local Strong Convexity and Local Lipschitz Continuity of the Gradient of Convex Functions". In: *Journal of Convex Analysis* 15.2, pp. 263–270.

Grande, J. (2018). "Red–green Refinement of Simplicial Meshes in D Dimensions". In: *Mathematics of Computation* 88.316, pp. 751–782. DOI: 10.1090/mcom/3383.

Gräser, C. (2011). "Convex Minimization and Phase Field Models". PhD thesis. DOI: 10.17169/REFUBIUM-11584.

Gräser, C. (2015). "A Note on Poincaré- and Friedrichs-type Inequalities". In: arXiv: 1512.02842 [math.AP].

Gräser, C., M. Kahnt, and R. Kornhuber (2016). "Numerical Approximation of Multiphase Penrose–fife Systems". In: *Computational Methods in Applied Mathematics* 16.4, pp. 523–542. ISSN: 1609-9389. DOI: 10.1515/cmam-2016-0020.

Gräser, C. and R. Kornhuber (2009). "Nonsmooth Newton Methods for Set-valued Saddle Point Problems". In: *SIAM Journal on Numerical Analysis* 47.2, pp. 1251–1273. DOI: 10.1137/060671012.

Gräser, C., R. Kornhuber, and U. Sack (2010). "On Hierarchical Error Estimators for Time-discretized Phase Field Models". In: *Numerical Mathematics and Advanced Applications 2009*. Springer, pp. 397–405.

Gräser, C., R. Kornhuber, and U. Sack (2013). "Time Discretizations of Anisotropic Allen-cahn Equations". In: *IMA Journal of Numerical Analysis* 33.4, pp. 1226–1244. ISSN: 0272-4979. DOI: 10.1093/imanum/drs043.

Gräser, C., R. Kornhuber, and U. Sack (2014). "Numerical simulation of coarsening in binary solder alloys". In: *Computational Materials Science* 93, pp. 221–233. ISSN: 0927-0256. DOI: 10.1016/j.commatsci.2014.06.010.

Gräser, C., U. Sack, and O. Sander (2009). "Truncated Nonsmooth Newton Multigrid Methods for Convex Minimization Problems". In: *Lecture Notes in Computational Science and Engineering*. Ed. by M. Bercovier et al. Vol. 70. . Lecture Notes in Computational Science and Engineering. Berlin, Heidelberg: Springer Berlin Heidelberg, pp. 129–136. ISBN: 9783642026775. DOI: 10.1007/978-3-642-02677-5_12.

Gräser, C. and O. Sander (2014a). "Polyhedral Gauß–seidel Converges". In: *Journal of Numerical Mathematics* 22.3, pp. 221–254. DOI: 10.1515/jnma-2014-0010.

Gräser, C. and O. Sander (2014b). "Truncated Nonsmooth Newton Multigrid Methods for Simplex-constrained Minimization Problems". In: *preprint*.

Haasen, P. (1994). *Physikalische Metallkunde*. Springer Berlin Heidelberg. DOI: 10.1007/978-3-642-87849-7.

Hardering, H. (2017). "The Aubin–nitsche Trick for Semilinear Problems". In: *arXiv preprint arXiv:1707.00963*. arXiv: 1707.00963 [math.NA].

Holst, M., J. S. Ovall, and R. Szypowski (2011). "An Efficient, Reliable and Robust Error Estimator for Elliptic Problems in R3". In: *Applied Numerical Mathematics* 61.5, pp. 675–695. DOI: 10.1016/j.apnum.2011.01.002.

Hoppe, R. H. W. and R. Kornhuber (1994). "Adaptive Multilevel Methods for Obstacle Problems". In: *SIAM Journal on Numerical Analysis* 31.2, pp. 301–323. DOI: 10.1137/0731016.

Kim, S. G., W. T. Kim, and T. Suzuki (1998). "Interfacial Compositions of Solid and Liquid in a Phase-field Model with Finite Interface Thickness for Isothermal Solidification in Binary Alloys". In: *Physical Review E* 58.3, pp. 3316–3323. DOI: 10.1103/physreve.58.3316.

Kinderlehrer, D. and G. Stampacchia (2000). *An Introduction to Variational Inequalities and Their Applications*. Society for Industrial and Applied Mathematics. DOI: 10.1137/1.9780898719451.

Klein, W. O. (1997). *Existence and Approximation Results for Phase-field Systems of Penrose-fife Type and Stefan Problems*. Shaker.

Kornhuber, R. (1996). "A Posteriori Error Estimates for Elliptic Variational Inequalities". In: *Computers & Mathematics with Applications* 31.8, pp. 49–60. DOI: 10.1016/0898-1221(96)00030-2.

Kornhuber, R. (1997). *Adaptive Monotone Multigrid Methods for Nonlinear Variational Problems*. B.G. Teubner. ISBN: 3519027224.

Kornhuber, R. and R. Krause (2006). "Robust Multigrid Methods for Vector-valued Allen–cahn Equations with Logarithmic Free Energy". In: *Computing and Visualization in Science* 9.2, pp. 103–116. DOI: 10.1007/s00791-006-0020-2.

Kornhuber, R., R. Krause, et al. (2007). "A Monotone Multigrid Solver for Two Body Contact Problems in Biomechanics". In: *Computing and Visualization in Science* 11.1, pp. 3–15. DOI: 10.1007/s00791-006-0053-6.

Lagerstrom, P. A. (1988). *Matched Asymptotic Expansions*. Springer New York. DOI: 10.1007/978-1-4757-1990-1.

Mielke, A. (2011). "A Gradient Structure for Reaction–diffusion Systems and for Energy-drift-diffusion Systems". In: *Nonlinearity* 24.4, pp. 1329–1346. ISSN: 0951-7715. DOI: 10.1088/0951-7715/24/4/016.

Nestler, B. and A. Choudhury (2011). "Phase-field Modeling of Multi-component Systems". In: *Current Opinion in Solid State and Materials Science* 15.3, pp. 93–105. DOI: 10.1016/j.cossms.2011.01.003.

Nestler, B., H. Garcke, and B. Stinner (2005). "Multicomponent Alloy Solidification: Phase-field Modeling and Simulations". In: *Physical Review E* 71.4, p. 041609. DOI: 10.1103/physreve.71.041609.

Onsager, L. (1931). "Reciprocal Relations in Irreversible Processes. I." In: *Physical Review* 37.4 (4), pp. 405–426. ISSN: 0031-899X. DOI: 10.1103/physrev.37.405.

Ortega, J. M. and W. C. Rheinboldt (1970). *Iterative Solution of Nonlinear Equations in Several Variables*. Elsevier. DOI: 10.1016/c2013-0-11263-9.

Peletier, M. A. (2012). "Variational Modelling: Energies, Gradient Flows, and Large Deviations". In: arXiv: 1402.1990 [math-ph].

Penrose, O. and P. C. Fife (1990). "Thermodynamically Consistent Models of Phase-field Type for the Kinetic of Phase Transitions". In: *Physica D: Nonlinear Phenomena* 43.1, pp. 44–62. DOI: 10.1016/0167-2789(90)90015-h.

Plapp, M. (2011). "Unified Derivation of Phase-field Models for Alloy Solidification from a Grand-potential Functional". In: *Physical Review E* 84.3, p. 031601. ISSN: 1539-3755. DOI: 10.1103/physreve.84.031601.

Rockafellar, R. T. (1970a). *Convex Analysis*. 28. Princeton university press.

Rockafellar, R. T. (1970b). "On the Maximal Monotonicity of Subdifferential Mappings". In: *Pacific Journal of Mathematics* 33.1, pp. 209–216.

Schiela, A. (2009). "Barrier Methods for Optimal Control Problems with State Constraints". In: *SIAM Journal on Optimization* 20.2, pp. 1002–1031. DOI: 10.1137/070692789.

Siebert, K. and A. Veeser (2007). "A Unilaterally Constrained Quadratic Minimization with Adaptive Finite Elements". In: *SIAM Journal on Optimization* 18.1, pp. 260–289. DOI: 10.1137/05064597x.

Steinbach, I. (2013). "Phase-Field Model for Microstructure Evolution at the Mesoscopic Scale". In: *Annual Review of Materials Research* 43.1, pp. 89–107. DOI: 10.1146/annurev-matsci-071312-121703.

Steinbach, I. et al. (1996). "A Phase Field Concept for Multiphase Systems". In: *Physica D: Nonlinear Phenomena* 94.3, pp. 135–147. DOI: 10.1016/0167-2789(95)00298-7.

Stinner, B. (2007). *Weak Solutions to a Multi-phase Field System of Parabolic Equations Related to Alloy Solidification*. Vol. 17. 2. Universität Regensburg, pp. 589–638. DOI: 10.5283/EPUB.13826.

Stinner, B., B. Nestler, and H. Garcke (2004). "A Diffuse Interface Model for Alloys with Multiple Components and Phases". In: *SIAM Journal on Applied Mathematics* 64.3, pp. 775–799. DOI: 10.1137/s0036139902413143.

Visintin, A. (2012). *Models of Phase Transitions*. Vol. 26. Springer Science & Business Media.

Wheeler, A. A., W. J. Boettinger, and G. B. McFadden (1992). "Phase-field Model for Isothermal Phase Transitions in Binary Alloys". In: *Physical Review A* 45.10, pp. 7424–7439. ISSN: 1050-2947. DOI: 10.1103/physreva.45.7424.

Wheeler, A. A., G. B. McFadden, and W. J. Boettinger (1996). "Phase-field Model for Solidification of a Eutectic Alloy". In: *Proceedings of the Royal Society of London. Series A: Mathematical, Physical and Engineering Sciences* 452.1946, pp. 495–525. DOI: 10.1098/rspa.1996.0026.

Zeidler, E. (1990). *Nonlinear Functional Analysis and Its Applications: Ii/b: Nonlinear Monotone Operators*. Springer New York. DOI: 10.1007/978-1-4612-0981-2.

Zienkiewicz, O. C., J. P. D. S. R. Gago, and D. W. Kelly (1983). "The Hierarchical Concept in Finite Element Analysis". In: *Computers & Structures* 16.1-4, pp. 53–65. ISSN: 0045-7949. DOI: 10.1016/0045-7949(83)90147-5.

Zorn, M. A. (1946). "Derivatives and Fréchet Differentials". In: *Bulletin of the American Mathematical Society* 52.2, pp. 133–138. ISSN: 0002-9904. DOI: 10.1090/s0002-9904-1946-08524-9.

Zou, Q. et al. (2011). "Hierarchical Error Estimates for the Energy Functional in Obstacle Problems". In: *Numerische Mathematik* 117.4, pp. 653–677. ISSN: 0029-599X. DOI: 10.1007/s00211-011-0364-5.